REMARKS

Claims 20, 22-24, 26, 31, and 34 were pending in the subject application. Claim 39 has been added, while two finally rejected claims have been canceled (claims 26 and 34) without prejudice to applicant's right to pursue the subject matter of these claims in another application. Support for the newly added claims may be found, *inter alia*, in originally-filed claim 19. In addition, applicant respectfully notes that independent claims 20 and 31 have been amended. Support for this amendment may be found, *inter alia*, on page 2, lines 7-11 of the originally-filed specification. This amendment does not involve any issue of new matter. Applicant respectfully requests entry of the subject amendment such that claims 20, 22-24, 31 and 39 will be pending.

Applicant notes that if this amendment does not place the claims in condition for allowance, it does place the claims in better condition for appeal according to MPEP 714.13 (III). Accordingly, applicant respectfully requests that this amendment be entered.

Applicant also notes that, as will be detailed in the subsection below titled "Claim Rejections- 35 USC §102", the Examiner has raised a new ground of rejection not necessitated by applicant's amendment or by applicant's untimely filing of an IDS, and therefore the finality of the present office action is premature and thus improper pursuant to MPEP 706.07(a). Accordingly, applicant requests that the finality of the present office action be withdrawn.

Obviousness-Type Double Patenting

The Examiner rejects claims 20, 22-24, 26, 31, and 34 under the judicially created doctrine of obviousness-type double patenting over claims 1-4, 19, and 20 of U.S. Patent No. 6,498,142 B1 ("the '142 patent"). The Examiner alleges that the '142 patent teaches a method of treating chronic renal failure or a renal condition in claims 1-4, 19 and 20, and these claims fall within the scope of instant claims 20, 22-24, 26, 31 and 34, *i.e.* the claims of the '142 patent anticipate the instant claims.

Applicants traverse the Examiner's rejection. The Examiner alleges that the claims of the '142 patent anticipate the instant claims. Without commenting on whether the '142 claims do or do not anticipate the instant claims, anticipation is not a proper basis for an obviousness-type

double patenting pursuant to MPEP 804 (II). Specifically, MPEP 804 (II) recites as follows:

> Domination and double patenting should not be confused. They are two separate issues. One patent or application "dominates" a second patent or application when the first patent or application has a broad or generic claim which fully encompasses or reads on an invention defined in a narrower or more specific claim in another patent or application. Domination by itself, *i.e.*, in the absence of statutory or nonstatutory double patenting grounds, cannot support a double patenting rejection. In re Kaplan, 789 F.2d 1574, 1577-78, 229 USPQ 678, 681 (Fed. Cir.1986); and In re Sarrett, 327 F.2d 1005, 1014-15, 140 USPQ 474, 482(CCPA 1964).

Since the Examiner is basing his rejection on the alleged dominance of the the claims from the subject application over the claims of the '142, such rejection is not proper. Applicants respectfully request reconsideration and withdrawal of this ground of rejection.

Claim Rejections- 35 USC §112, 1st paragraph, Enablement

Claims 20, 22-24, 26, 31, and 34 are rejected under 35 U.S.C. 112 1st paragraph because the specification allegedly does not enable the full scope of the invention. Applicant notes the following with respect to the office action:

(a) The Examiner alleges that "applicant's argument has been fully considered, but is not deemed to be persuasive because claims 21, 27 and 38 were previously rejected (see pages 6-8) and recitation of the limitations of these claims do not overcome the scope of enablement rejection set forth in the previous office action. While limiting to certain cell-types, the scope of the invention is unusually broad."

(b) The Examiner contends that the claims recite the allegedly generic term "restoring the cellular phenotype".

(c) The Examiner alleges that that the scope of pathways is broad.

(d) The Examiner alleges that applicants "have not fully addressed the issues raised in the previous office action (the middle of page 7)".

(e) The Examiner alleges that the genus of morphogens with 60% or 70% amino acid sequence identity to the C-terminal seven-cysteine domain of human OP-1 without a specific functional limitation, and that the instant specification fails to disclose the conservative regions that are critical to the structure and function of the genus claimed and the sites at which variability can be tolerated or sufficient guidance and working examples on the genus of morphogens.

In response, applicants first submit that although the Examiner correctly cited, on the top paragraph of page 7 of the previous office action, the eight factors that an Examiner must be consider when determining whether a disclosure is enabling, as listed on MPEP2164.01(a), the Examiner did not take these factors into consideration when assessing the enablement of the disclosure in the previous and the present office action. Moreover, the Examiner provides little, if any, analysis of how she applied these factors when examining the application. Instead, the Examiner merely recites elements of the claims and alleges that they are "too broad", failing to meet the standard required by MPEP 2164. Further MPEP 2164.04 states that "[i]n order to make a rejection the Examiner has the initial burden to establish a reasonable basis to question the enablement provided for the claimed invention. *In re Wright*, 999 F.2d 1557, 1562, 27 USPQ2d 1510, 1513 (Fed. Cir. 1993)". Since the Examiner has merely listed the eight factors but has not applied them, the Examiner has failed to establish a lack of enablement.

With respect to (a) above, the Examiner again fails to describe why she considered the amended claims as "too broad" in light of the specification. The Examiner merely alleges that incorporating the features previously recited in dependent claims 21, 27 and 38 into claims 20 and 31 does not enable claims 20 and 31 since the Examiner previously held each of the dependent claims as also being not enabled. Applicants submit that the logic in this reasoning is incorrect, because while a claim reciting elements ABX, ABY and ABX may each not be

enabled (where "A', "B", "X", "Y" and "Z" each represent an element), a claim reciting each of the elements ABXYZ might very well be. In summary, the Examiner has not provided valid reasoning as to why claims 20 and 31 are not enabled, when in fact the disclosure, combined with the state of the art at the time the application was filed, allowed one skilled in the art to carry out the claimed invention without excessive experimentation..

With respect to (b) ("restoring the cellular phenotype") and (c) (pathways) above, again, the Examiner fails to explain why the claims containing these terms are not enabled in light of the specification. Merely stating that the claims are "too broad", or that a certain term is "too broad" is not sufficient basis for alleging that a claim fails the enablement requirement. Applicants note that the pathways of the claimed invention do not refer to just any pathway, but only to pathways that "induce intracellular formation of a Smad complex" and that are "activated by specific binding of a morphogen to its transmembrane receptor", in accordance with the guidance provided by the specification. Similarly, "restoring the cellular phenotype", rather than being "too broad" (as characterized by the Examiner) refers to the phenotypes of the seven cell types recited in the claims (lung, heart, blood vessel, stomach, a muscle, renal and intestinal). Accordingly, when one skilled in the art contemplates restoring the cellular phenotype of one of these seven cell types, there is <u>one</u> cellular phenotype that is being restored. Thus, the term "cellular phenotype" is well within the teachings of the specification in light of what was known at the time the application was filed.

With respect to (d), applicants submit that applicants fully addressed the issues raised on page 7, middle paragraph in the previous office action. This section of the prior office action states that every element of the claims is "too broad", again failing to carry out the detailed enablement analysis required by MPEP 2164. In response applicants amended claims 20 and 31 in the amendment dated March 15, 2004 to more clearly describe the cells, the pathways, the smad complex and the morphogens. The Examiner further alleged that the claims were directed to curing cancer and reviving a dead cell; in response, applicants redirected the Examiner to the language of the claims and provided an example of what the claims recite. Accordingly, applicants were responsive to the general allegations the Examiner set forth.

With respect to (e), applicants note that the claims have been amended to recite functional features of the morphogens *i.e.* wherein the morphogen (a) stimulates endochondral bone formation in an *in vivo* bone assay; or (b) stimulates N_CAM or L1 isoform production in an NG108-15 neuronal cell line; or (c) both, so as to more clearly set forth the claimed invention. Further, applicants submit that one skilled in the art at the time the invention could have easily generated an amino acid sequence alignment of the morphogens disclosed in the application, and from such alignment determined which residues tend to be conserved and which tend to be substituted between the morphogens, the later being residues which could more easily be mutated without a concomitant loss in morphogen function. Thus, given the degree of homology between the morphogens described in the specification, one skilled in the art could have quickly determined structure-function relationships between amino acid residues in the morphogen and biological function. Applicants also note that dependent claims 39 has been added, which specifically recites OP-1 as the morphogen. Accordingly, the amended claims are enabled by the specification.

Finally, applicants submit that based on the teachings of the specification, subsequent research groups have published additional examples of the use of morphogens to restore a cellular phenotype to a cell affected by disease, damage, or age by using morphogens to activate an intracellular pathway induces expression of a phenotype-specific gene as claimed in the subject application. Applicants submit the following six examples, each directed to one of the six cell types recited in the claims:

Cell Type	Reference	Expression/Phenotype
Lung	Buckley S, Shi W, Driscoll B, Ferrario A, Anderson K, Warburton D. BMP4 signaling induces senescence and modulates the oncogenic phenotype of A549 lung adenocarcinoma cells. Am J Physiol Lung Cell Mol Physiol. **2004**;286(1):L81-6. Epub 2003 Sep 05. **(Exhibit A)**	Teaches that when A549 lung cancer cells are treated continuously with 100 ng/ml of BMP4, a senescent phenotype is observed. The BMP-treated cells appeared larger than untreated cells, grew more slowly, had more senescence-associated beta-galactosidase activity (the phenotype specific gene), and had less telomerase

		activity. (See abstract)
Cardiac	Izumi M, Fujio Y, Kunisada K, Negoro S, Tone E, Funamoto M, Osugi T, Oshima Y, Nakaoka Y, Kishimoto T, Yamauchi-Takihara K, Hirota H. Bone morphogenetic protein-2 inhibits serum deprivation-induced apoptosis of neonatal cardiac myocytes through activation of the Smad1 pathway. J Biol Chem. **2001** ;276(33):31133-41. **(Exhibit B)**	BMP-2 promoted survival and inhibited apoptosis of serum-deprived myocytes. Moreover, BMP-2 and Smad1 enhanced the expression of the anti-apoptotic molecule Bcl-x(L), (the phenotype specific gene). (See abstract)
Blood vessel	Dorai H, Sampath TK.; Bone morphogenetic protein-7 modulates genes that maintain the vascular smooth muscle cell phenotype in culture. J Bone Joint Surg Am. **2001**;83-A Suppl 1(Pt 1):S70-8. **(Exhibit C)**	BMP-7 stimulated the expression of developmentally regulated as well as SMC-specific markers, namely, Id-1 and Id-2, alpha-actin, and SMC-specific heavy-chain myosin (the phenotype specific genes), in vascular smooth muscle cells, a cell type of blood vessels. (See abstract)
Stomach	Wen XZ, Miyake S, Akiyama Y, Yuasa Y; BMP-2 modulates the proliferation and differentiation of normal and cancerous gastric cells. Biochem Biophys Res Commun. **2004** ;316(1):100-6. **(Exhibit D)**	BMP-2 increased the expression of pepsinogen II, a differentiation marker of the stomach (the phenotype-specific gene), in MKN74 cell (gastric epithelial cells). (See abstract)
Muscle	Nakajima Y, Yamagishi T, Ando K, Nakamura H Significance of bone morphogenetic protein-4 function in the initial myofibrillogenesis of chick cardiogenesis. Dev Biol. **2002** May 15;245(2):291-303. **(Exhibit E)**	BMP-2 and BMP-4 induced the expressions of sarcomeric alpha-actinin and titin (the phenotype specific genes), which are two muscle genes. (See abstract)
Intestine	Haramis AP, Begthel H, van den Born M, van Es J, Jonkheer S, Offerhaus GJ, Clevers H.; De novo crypt formation and juvenile polyposis on BMP inhibition in	BMP genes inhibit the de novo crypt formation and polyp growth of intestinal epithelial cells. (See abstract)

	mouse intestine. Science. **2004** ;303(5664):1684-6. **(Exhibit F)**	

Contrary to the allegations by the Examiner that the scope of the claimed invention is too broad, the above-cited articles confirm the utility, enablement and proper scope of the claimed invention. Accordingly, applicants respectfully request reconsideration and withdrawal of this ground of rejection.

Claim Rejections- 35 USC §102

Claims 20, 22-24, 26, 31, and 34 are rejected under 35 U.S.C. 102 as allegedly anticipated by Kuberasampath et al. (WO 94/06449, the "'449 publication"). The Examiner alleged in the previous office action (mailed December 17, 2003) that the '449 publication taught the use of morphogens to maintain liver function in a mammal, and therefore anticipated the claimed invention. In response. Applicants amended claims 21 and 31, from which all other rejected claims dependent, to recite specific cell types (*i.e.* lung cell, a heart cell, a blood vessel cell, a stomach cell, a muscle cell, a renal cell or an intestinal cell) in the amendment filed on March 15, 2004. Since hepatocytes were not included among the recited cell types, the alleged hepatocyte teachings of the '449 publication would fail to anticipate the claimed invention.

In the present Office Action, the Examiner alleges that applicants prior amendment of March 15, 2004 has been considered but is not deemed persuasive. However, the examiner concedes that applicant's claim amendment did overcome the hepatocyte rejection previously raised, and proceeds to set forth a new ground for rejection *i.e.* the Examiner, for the first time, alleges that the '449 publication "also teach(s) treatment of transplant tissues *e.g.* liver, lung, kidney, pancrease, heart, etc. to provide a cryoprotective effect to the tissue (line 17-23 of page 18)" (See page 7, 1st paragraph of Office Action).

Since the Examiner has raised a new ground of rejection, the finality of the present office

action is premature and thus improper. MPEP 706.07(a) states as follows:

> Under present practice, second or any subsequent actions on the merits shall be final, except where the examiner introduces a new ground of rejection that is neither necessitated by applicant's amendment of the claims nor based on information submitted in an information disclosure statement filed during the period set forth in **37 CFR 1.97(c)** with the fee set forth in **37 CFR 1.17(p)**.

Since the examiner's new ground of rejection was not necessitated by Applicants amendment and instead could have been raised in the previous Office Action, and because the new ground of rejection was not based on information submitted in an information disclosure statement filed during the above-stated period, the Examiner has made a premature final rejection according to MPEP 706.07(a). Applicants respectfully request withdrawal of the finality of the present Final Rejection.

With respect to the substance of the new ground of rejection, applicants submit that, pursuant to MPEP 2131.01, "a claim is anticipated only if each and every element as set forth in the claim is found, either expressly or inherently described, in a single prior art reference." Applicants submit that claims 20 and 31, from which all other claims depend, recite the use of a morphogen to treat a cell "affected by disease, damage, or age." This feature of the claimed invention is not taught by the '449 publication, and therefore the '449 publication cannot anticipate the claimed invention. More specifically, if an organ is to be transplanted from one subject to another, one skilled in the art would select a donor organ that is not "affected by disease, damage or age". For instance, one skilled in the art would not select a heart diseased with dilated cardiomyopathy to transplant into a subject afflicted with cardiac hypertrophy (or vice versa). Likewise, one skilled in the art would not select a lung damaged by years of smoking to treat a subject afflicted with cystic fibrosis. Instead, one skilled in the art would select an organ that is neither diseased nor damaged for transplantation into a subject in need thereof. Therefore, since the '449 publication does not teach the use of morphogens to treat diseased, damaged or age-afflicted organs with a morphogens, it does not anticipate the claimed invention. Accordingly, applicants request reconsideration and withdrawal of this ground of rejection.

Claim Objections- Minor Informalities

The Examiner objects to claims 20, 22-24, 26, 31 and 34 as allegedly reciting non-elected subject matter (non-elected species). In response, applicants note that generic linking claims are pending (i.e. claims 20 and 31). Applicants are entitled to examination of a reasonable number of species upon the allowance of the elected species. Accordingly, the above-mentioned claims will remain pending.

Conclusion

In view of the above amendments and comments, applicant believes the pending application is in condition for allowance, and certainly in better condition for appeal since this amendment, in part, cancels two finally rejected claims with a concomitant addition of only one claim.

Applicant believes no fee is due with this response in addition to the two-month extension of time fee and the fee for filing a notice of appeal. However, if an additional fee is due, please charge our Deposit Account No. 18-1945, under Order No. JJJ-P01-520 from which the undersigned is authorized to draw.

Dated: November 1, 2004

Respectfully submitted,

By _____

Ignacio Perez de la Cruz
Registration No.: 55,535
ROPES & GRAY LLP
45 Rockefeller Plaza
New York, New York 10111-0087
(212) 497-3613
(212) 497-3650 (Fax)
Attorneys/Agents For Applicant

Am J Physiol Lung Cell Mol Physiol 286: L81–L86, 2004.
First published September 5, 2003; 10.1152/ajplung.00160.2003.

BMP4 signaling induces senescence and modulates the oncogenic phenotype of A549 lung adenocarcinoma cells

S. Buckley,[1] W. Shi,[1] B. Driscoll,[1] A. Ferrario,[2] K. Anderson,[3] and D. Warburton[1]
[1]*Developmental Biology,* [2]*Hematology/Oncology, and* [3]*Pediatric Surgery Programs, Children's Hospital of Los Angeles Research Institute, Los Angeles, California 90027*

Submitted 21 May 2003; accepted in final form 28 August 2003

Buckley, S., W. Shi, B. Driscoll, A. Ferrario, K. Anderson, and D. Warburton. BMP4 signaling induces senescence and modulates the oncogenic phenotype of A549 lung adenocarcinoma cells. *Am J Physiol Lung Cell Mol Physiol* 286: L81–L86, 2004. First published September 5, 2003; 10.1152/ajplung.00160.2003.—Lung cancer is the most common visceral malignancy in males, with rapidly increasing incidence in females, and a devastatingly poor prognosis. Transforming growth factor (TGF)-β has been shown to induce senescence in A549 lung cancer cells, and both TGF-β and bone morphogenetic protein (BMP) 2 can suppress the transformed phenotype of A549 cells in vitro. We examined the effects of BMP4, another member of the TGF-β superfamily, on specific oncogenic properties of A549 cancer cells. When A549 cancer cells were treated continuously with 100 ng/ml of BMP4, a senescent phenotype was observed after 2 wk of treatment. The BMP-treated cells appeared larger than untreated cells, grew more slowly, had more senescence-associated β-galactosidase activity, and had less telomerase activity, as measured by the telomeric repeat amplification protocol assay. Invasion through Engelbreth Holm-Swarm matrix was inhibited in the senescent cell population. Senescent BMP4-treated cells had lower ERK activation, VEGF expression, and Bcl2 expression than wild-type cells, consistent with a less proliferative, less angiogenic phenotype with increased susceptibility to death by apoptosis. BMP4 treatment also resulted in sustained elevation of Smad1. In vivo xenograft studies in the flanks of nude mice confirmed that the BMP-treated cells were significantly less tumorigenic than untreated cells. Direct overexpression of Smad1 using adenoviral constructs resulted in cell death within 5 days. These studies suggest that BMP4 pathway signaling can induce senescence and thus negatively regulate the growth of A549 lung cancer cells.

bone morphogenetic protein 4; senescence-associated β-galactosidase activity; telomerase; Engelbreth Holm-Swarm matrix invasion; xenograft tumor

LUNG CANCER is the primary cause of cancer deaths in the United States, with a devastatingly poor prognosis (22). There has been little improvement in 5-year survival rates over the last 20 years, and, for the most common treatments, toxicity exceeds efficacy.

Bone morphogenetic proteins (BMPs) are one of the subgroups of the transforming growth factor-β (TGF-β) superfamily. TGF-β and BMP transduce signals through downstream proteins, Smads, controlling cell proliferation, differentiation, migration, and apoptosis (1, 14). Frequent activating mutations of Smad4 (10) or less common somatic mutations of Smad2 (19) are seen in solid tumors and suggest that these genes may have a suppressor function. A ubiquitously expressed truncated Smad5, Smad5-β, has been implicated in stem cell homeostasis as a mechanism to protect pluripotent stem cells and malignant cells from the growth inhibitory and differentiation signals of BMPs (9). Functionally impaired Smad mutations may also play a role in lung tumorigenesis (24).

The concept of lung cancer growth suppression through TGF-β signaling is supported by several studies. TGF-β has been shown to drive A549 cancer cells into replicative senescence in vitro (11) by mechanisms unknown, and TGF-β or BMP2 treatment can suppress the growth of A549 cells in vitro (17, 18). However, the effects of BMP4 signaling on nonsmall cell lung cancers have not been explored. Herein, we investigate the effects of BMP4 on cell senescence and tumorigenicity in A549 lung cancer cells. We present data demonstrating that BMP4 at a dose of 100 ng/ml is effective in inducing senescence in A549 lung cancer cells in vitro. More importantly, we show that BMP4 pretreatment can significantly reduce tumorigenicity of A549 xenograft tumors generated by these cells in nude mice. We demonstrate that BMP4-mediated overexpression of Smad1 in A549 cells correlates with senescence, whereas direct overexpression of Smad1 using adenoviral vectors results in cell death. These data suggest that BMP4 or downstream targets may be effective in the control of certain lung cancers.

METHODS

Parental cell line. A549 lung carcinoma cells (13) were obtained from ATCC (CCL-185), and parental cultures were maintained in HEPES-buffered RPMI with 10% FCS and antibiotics. The medium was replaced every other day, and the cells were passaged before confluence. As the A549 cell line consists of four distinct clones (2), each BMP4 treatment was done on cells fresh from the ATCC to ensure a reproducible response.

BMP4 treatment. A549 cells were grown in RPMI with 1% FCS ± 100 ng/ml of human recombinant BMP4 (R & D Systems) continuously present. Control cells were grown in parallel in 1% FCS. The medium ± BMP4 was replaced every other day, and the cells were passaged before confluence. At various times during the BMP4 treatment, flasks of A549 cells ± BMP4 were grown to near confluence, trypsinized, and counted by hemocytometer to compare growth rates.

Senescence-associated β-galactosidase assay. Cells were lysed in reporter lysis buffer (Promega, Madison, WI) and centrifuged at 20,800 *g* at 4°C for 1 min, and the supernatants were removed. Proteins were measured with Bio-Rad protein dye (Bio-Rad, Hercules, CA). Cell lysates containing equal amounts of protein were diluted in equal volumes of 2× assay buffer containing 1.33 mg/ml o-nitrophenyl-β-D-galactopyranoside, 2 mM $MgCl_2$, and 100 μl 2-mercaptoethanol in 200 mM phosphate buffer, pH 6.0, and incu-

Address for reprint requests and other correspondence: D. Warburton, MS 35, Children's Hospital Los Angeles, 4650 Sunset Blvd., Los Angeles, CA 90027 (E-mail: dwarburton@chla.usc.edu).

The costs of publication of this article were defrayed in part by the payment of page charges. The article must therefore be hereby marked "*advertisement*" in accordance with 18 U.S.C. Section 1734 solely to indicate this fact.

bated at 37°C for 4 h. The absorbance at 420 nm was measured after the addition of an equal volume of 1 M Na_2CO_3.

Telomeric repeat amplification protocol assay. Sample preparation and telomeric repeat amplification protocol (TRAP) assays were performed according to the TRAP-EZE protocol provided by Serologicals (Norcross, GA) (3). Briefly, at least 10^6 cells for each sample were lysed in 1× 3-([3-cholamidopropyl]dimethylammonio)-1-propanesulfonate lysis buffer. The lysate was clarified by centrifugation, and protein content was measured with Bio-Rad dye. To assay telomerase activity, we incubated samples with a [γ-^{33}P]dATP end-labeled telomerase specific primer at 30°C for 30 min for telomere primer extension. The telomerase products were then amplified by 30 rounds of two-step PCR (94°C/30 s, 60°C/30 s). The samples were subjected to 12.5% nondenaturing polyacrylamide gel electrophoresis in 0.5× TBE buffer (45 mM Tris-borate, 1 mM EDTA) for 1 h at 500 V. Gels were dried and exposed to X-ray film to visualize the telomerase products. Each assay included telomerase-positive A549 cells that had not been treated with BMP4, as a cellular control, as well as a PCR internal amplification control, provided by Intergen, and a PCR contamination control lane consisting of all sample elements with the exception of cell lysate.

Western blotting of proteins. Cells were washed in PBS, lysed in iced radioimmunoprecipitation assay buffer (1% Nonidet P-40, 0.5% sodium deoxycholate, 0.1% SDS in PBS, with 10 mg/ml PMSF, 30 U/ml aprotinin, and 100 mM sodium orthovanadate), and centrifuged at 14,000 *g* for 10 min at 4°C. Protein (20 μg) was electrophoresed through commercially prepared polyacrylamide gels (Novex, San Diego, CA) and transferred to Immobilon membrane (Millipore, Bedford, MA). Proteins of interest were detected with horseradish peroxidase-linked secondary antibodies (Sigma, St. Louis, MO) followed by ECL detection (Amersham, Little Chalfont, UK). We confirmed equal loading by blotting the lower half of the blots with an antibody to actin. Antibodies to VEGF, phosphorylated ERK (p-ERK), Bcl2, interleukin-1β-converting enzyme (ICE), and p-Smad1 were from Santa Cruz Biotechnology (Santa Cruz, CA). Antibody to actin was from ICN (Irvine, CA). Antibody to FLAG, a tagging epitope, was from Sigma.

Cell invasion assay. A commercial cell invasion assay kit (Chemicon, Temecula, CA) was used according to the manufacturer's instructions. The inserts, which contain 8-μm pores, are coated with a thin layer of biological matrix derived from the Engelbreth Holm-Swarm (EHS) mouse tumor. Cells (3.5×10^5) in 300 μl of serum-free RPMI + 0.1% BSA were added to triplicate upper wells, and migration through the matrix to the lower wells, containing 500 μl of RPMI + 10% FCS, was measured after 24-h culture at 37°C. The noninvading cells and matrix were removed with a cotton-tipped swab, and the cells were stained. Cell-free filters were processed as blanks. The stain was eluted with 10% acetic acid, and the absorbance at 560 nm was measured.

Adenoviral transduction of Smad1. FLAG-tagged Smad1 recombinant adenovirus (5) was a kind gift from Dr. M. Fujii (Japan Society for the Promotion of Science, Tokyo). High titer stocks of recombinant virus were grown in 293 cells and purified with a Viraprep kit (Virapur, Carlsbad, CA) according to the manufacturer's instructions. Purified adenovirus containing green fluorescence protein (GFP) or Smad1 was added to nonconfluent cultures of A549 cells at a concentration of 20 live particles/cell in RPMI with 5% FCS. The virus-conditioned medium was removed after overnight incubation, and the cells were further incubated in RPMI and 5% FCS. The GFP-transduced cells were observed daily under fluorescent microscopy for GFP expression, which was seen maximally after 48 h (estimated to be 80–90% of the culture), and persisted until the death of the Smad1-transduced cells around *day 5*. We confirmed overexpression of Smad1 by lysing the Smad1 and control GFP-transduced cells and then Western blotting for FLAG expression.

Tumorigenicity in nude mice. Viable single cell suspensions (4×10^6) from BMP4-treated and untreated A549 cells were injected subcutaneously into the flanks of nude mice obtained from Harlan Sprague-Dawley. Tumor size was measured in three dimensions weekly, and the tumor volume was calculated by the formula (length × width × height × π/6). The animals were killed when necrosis occurred in the larger tumors arising from untreated cells (45 days postinjection). Animal experiments were approved by the Institutional Animal Care and Use Committee and conducted in accordance with Institutional guidelines.

RESULTS

BMP4 treatment induces a senescent morphology in A549 lung cancer cells. Cultures of A549 cells treated continuously with BMP4 showed reduced growth compared with untreated cells (Fig. 1*A*). A change in morphology was apparent after 2 wk of treatment. The slower-growing cells were larger, flattened, and more granular than untreated cells (Fig. 1*B*).

BMP4 treatment induces senescence-activated β-galactosidase activity in A549 cancer cells. A549 cells were treated with BMP4 until the growth rate slowed and the cells assumed an enlarged, flattened appearance compared with untreated cells grown under parallel low-serum conditions. BMP4-treated and untreated cultures were lysed and assayed for senescence-activated β-galactosidase (SA-β-gal; pH 6.0) activity, a biomarker associated with senescence in human cells (23). A fourfold increase in SA-β-gal activity was seen after 17 days of BMP4 treatment (Fig. 2). Increased SA-β-gal activity was sustained through prolonged culture in the presence of BMP4

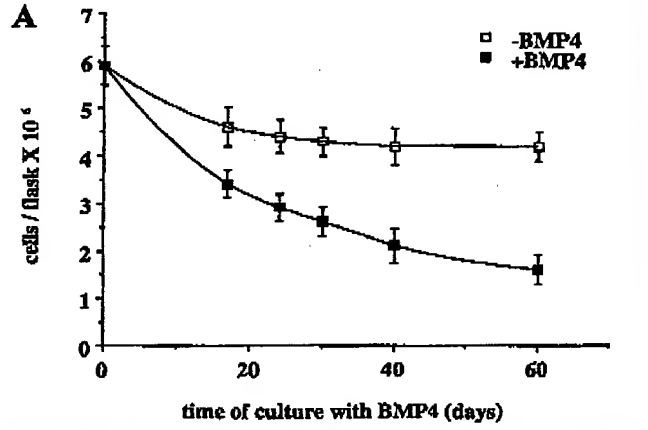

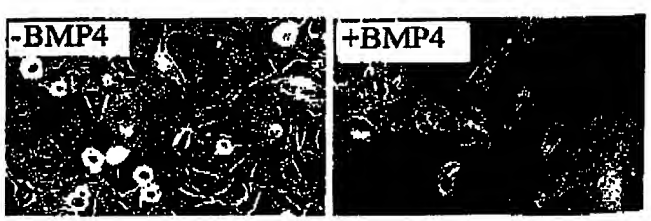

Fig. 1. *A*: bone morphogenetic protein (BMP) 4-treated cells grow more slowly than untreated cells cultured under identical low-serum conditions. At various times during the BMP4 treatment, flasks of A549 cells ± BMP4 were grown to near confluence, trypsinized, and counted by hemocytometer to compare growth rates. *B*: BMP4-treated senescent A549 cells have a larger, more flattened phenotype than quiescent, untreated cells grown in parallel in low serum. *Left*: untreated cells after 21 days (d) of culture. *Right*: BMP4-treated, senescent cells after 21-d culture.

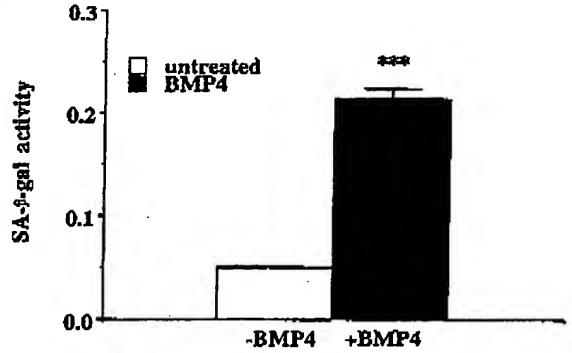

Fig. 2. A549 cells treated with BMP4 for 17 d have significantly higher senescence-activated β-galactosidase (SA-β-gal) activity than untreated cells cultured under identical low-serum conditions. Data are presented ± SD, $n = 4$. ***$P < 0.05$. A549 cells cultured ± 100 ng/ml BMP4 for 17 d were lysed, and the lysates tested for SA-β-gal activity, using o-nitrophenyl-β-D-galactopyranoside as substrate at pH 6.0.

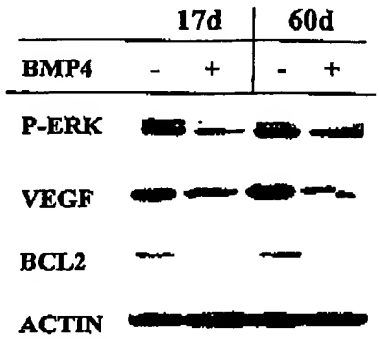

Fig. 4. BMP4 treatment of A549 cells results in a sustained less proliferative, less angiogenic phenotype, as reflected by decreased expression of phosphorylated ERK (p-ERK) and VEGF, as seen in this representative Western blot. The expression of Bcl2 is also decreased in BMP4-treated cells, suggesting that the senescent cells may be more prone to death by apoptosis. Actin was used as loading control.

(60 days) and for at least 1 wk after BMP4 was withdrawn (data not shown).

BMP4 treatment downregulates telomerase activity in A549 cells. A549 cells, in common with many cancer cells, have abundant telomerase activity that correlates with a highly proliferative phenotype (3). A549 cells treated with TGF-β have reduced telomerase activity that is associated with senescence (11). We analyzed lysates of senescent BMP4-treated and quiescent untreated A549 cells for telomerase activity, using the PCR-based TRAP. Autoradiography showed characteristic laddering, representing radiolabeled telomere primer extension, in the wild-type A549 cells (Fig. 3, *lane 5*). Laddering was reduced in untreated A549 cells grown for 17 days in low-serum conditions making them essentially quiescent (*lane 3*) and dramatically reduced in cells treated with BMP4 for 17 days and expressing the senescence biomarker SA-β-gal (*lane 4*).

Fig. 3. BMP4-induced senescence in A549 cells is associated with decreased telomerase activity. The representative autoradiograph shows that A549 cells treated with BMP4 for 17 d (*lane 4*) have greatly decreased telomerase activity compared with untreated cells (*lane 3*), as measured by the laddering, which represents radioactive telomere extension products. Each assay included telomerase-positive parental A549 cells grown in 10% serum as a cellular control (*lane 5*), as well as a PCR internal amplification control (*lane 1*), and a PCR contamination control lane, consisting of all sample elements with the exception of cell lysate (*lane 2*). TRAP, telomeric repeat amplification protocol; WT, wild type.

BMP4-induced senescence in A549 cells is associated with downregulation of p-ERK, VEGF, and Bcl2. Western analysis of lysates of BMP4-treated A549 cells (Fig. 4) suggests a decrease in proliferative and angiogenic phenotypic markers compared with untreated cells cultured under parallel low-serum conditions, as shown by decreased p-ERK and VEGF expression, respectively. The expression of survival factor Bcl2 is lower in BMP4-treated cells, suggesting an increased potential for apoptosis in the senescent population. Despite the decreased Bcl2 levels, a population of cells can survive culture in the presence of BMP4 for 8 wk or more. This survival may reflect the polyclonal nature of the A549 cell line (2), with diverse effects elicited from different subclones.

BMP4-treated A549 cells are less invasive through EHS matrix. We compared the invasive properties of senescent BMP4-treated cells with untreated cells by measuring invasion through EHS matrix (Fig. 5). Migration through EHS matrix was significantly retarded by ~50% in the BMP4-treated cells compared with untreated cells ($P < 0.05$). The nonmigrating population was viable and attached readily to the matrix. The decreased invasion of BMP4-treated A549 cells through a basement membrane model suggests that BMP4 treatment may result in a less metastatic phenotype by downregulating the proteolytic enzymes required for matrix penetration. Wild-type A549 cells are highly metastatic and secrete high levels of matrix metalloproteinase-2 (25).

BMP4-treated A549 cells generate slower-growing xenograft tumors in nude mice. Xenograft tumors were established by subcutaneous injection of 4×10^6 viable untreated or BMP4-treated A549 cells into the flanks of nude mice. The tumor size was recorded weekly, and the tumors were excised when necrosis was observed in the larger tumors generated from untreated cells (45 days postinjection). The tumors from

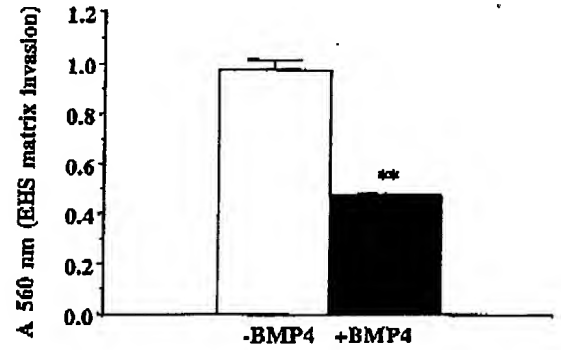

Fig. 5. Cells treated with BMP4 for 17 d are significantly less invasive through Engelbreth Holm-Swarm (EHS) matrix-coated porous inserts than untreated cells grown in identical low-serum conditions. $^{**}P < 0.01$. Data are presented ± SD, $n = 4$. BMP4-treated and untreated A549 cells, cultured under identical low-serum conditions, were plated in serum-free medium on a layer of EHS matrix over a porous filter, atop serum-containing medium. Invasion through matrix was measured after 24 h.

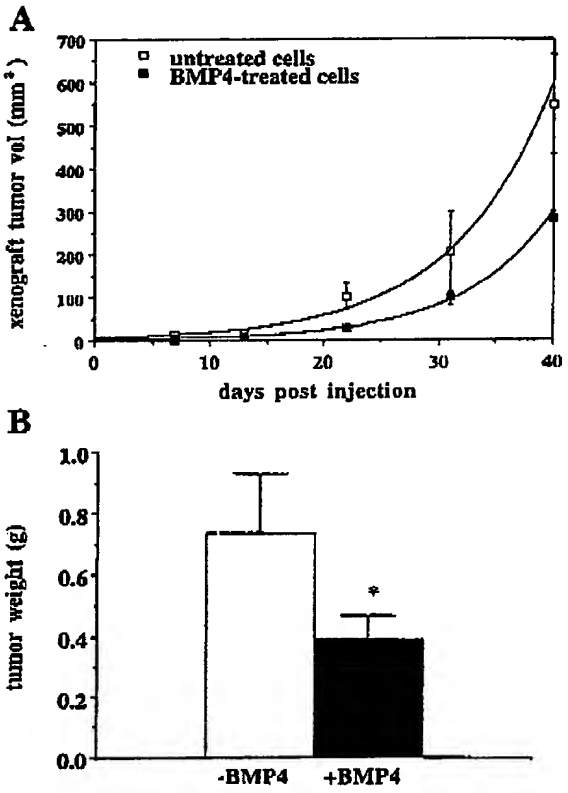

Fig. 6. *A*: BMP4-treated cells resulted in insignificantly smaller xenograft tumors in nude mice compared with untreated cells grown under identical low-serum conditions. Viable BMP4-treated and untreated cells (4×10^6) cultured under identical low-serum conditions were injected into the flanks of nude mice, and the tumors were measured weekly in 3 dimensions. Tumor volume was calculated assuming spheroid shape, using the formula length × width × height × $\pi/6$. The experiment was stopped when necrosis was observed in the larger tumors. Data are expressed as means ± SD (untreated, $n = 6$; BMP4-treated, $n = 8$). *B*: weights of tumors resulting from BMP4-treated A549 cells were significantly less at excision (45 days postinjection) than tumors arising from untreated cells, $^{*}P < 0.05$. Data are presented as means ± SD.

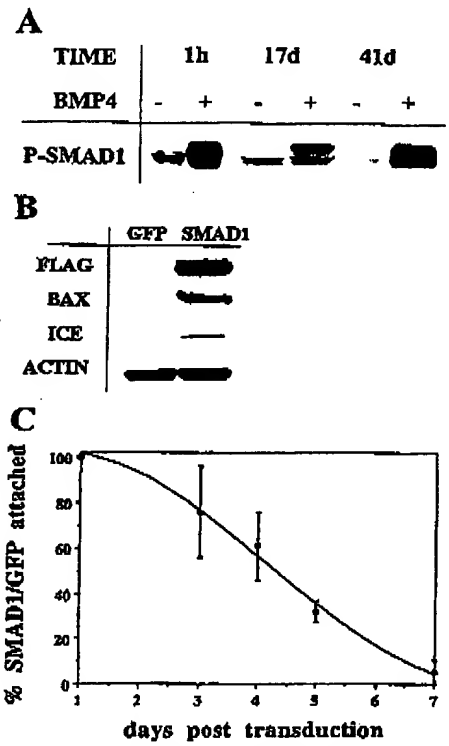

Fig. 7. *A*: representative Western analysis of lysates of A549 cells treated continuously with 100 ng/ml of BMP4 for various periods of time shows sustained activation of Smad1 in the BMP4-treated group compared with cells cultured under identical low-serum conditions. *B*: A549 cells were transduced with adenovirus bearing FLAG-tagged Smad1 or green fluorescence protein (GFP) at the same multiplicity of infection (MOI). Western analysis of FLAG expression in lysates of A549 cells at 48 h posttransduction confirms successful overexpression of Smad1 and shows increased bax and interleukin-1β-converting enzyme (ICE) expression in the cells overexpressing SMAD1. These cells would subsequently die. *C*: flasks of A549 cells were transduced with either adenovirus bearing FLAG-tagged Smad1 or GFP at the same MOI and harvested at various times after GFP expression was detected. Cell counts show that overexpression of Smad1 in A549 cells results in cell death within 5 days.

BMP4-treated A549 cells grew more slowly than tumors from untreated cells (Fig. 6*A*). The weights at excision of tumors arising from BMP4-treated cells were significantly (50%) less than tumors generated by untreated cells (Fig. 6*B*). These data support the in vitro findings, which suggest that the BMP4-treated cells are less proliferative and angiogenic than the quiescent untreated cells.

Smad1 phosphorylation is induced by BMP4 treatment of A549 cells. Western analysis shows that Smad1 is phosphorylated in A549 cells within 1 h after BMP4 treatment (Fig. 7*A*). Interestingly, p-Smad1 is not downregulated with time and remains elevated during culture with BMP4 (up to 40 days), suggesting that Smad1 activation correlates with slowed growth rate and senescence in A549 cells. To determine whether BMP4-induced senescence in A549 cells is receptor mediated, we bypassed the receptors by overexpressing Smad1. Purified recombinant adenoviral vectors bearing FLAG-tagged Smad1 or GFP were transduced into A549 cells. Maximal expression was achieved at 48 h posttransduction, as

detected by fluorescent GFP expression in the control group. The cells were then lysed and analyzed to confirm Smad1 overexpression by Western blotting for FLAG (Fig. 7*B*). Interestingly, overexpression of Smad1 resulted in cell death, rather than senescence. Smad1-transduced cells began lifting off the plate soon after Smad1 overexpression was established, whereas GFP-transduced controls remained viable. Elevated levels of bax and ICE observed in the BMP4-treated cells before lifting from the plate, compared with the GFP-transduced controls, suggested that cell death may be due to apoptosis. Death of the total cell population occurred over several days (Fig. 7*C*).

DISCUSSION

Novel therapeutic approaches to lung cancer are crucial because of the disease's dismal prognosis, which has persisted for more than 20 years (22). Although a cure is the primary goal of such therapies, control of tumor growth may be more achievable and would still afford significant benefits to the patient, such as longer survival and improved quality of life. Several reports demonstrate that members of the BMP family (or downstream targets) can inhibit growth of various cancers in vitro, including breast, skin, thyroid, and multiple myeloma (4, 6, 7, 16, 21). We examined the effects of in vitro BMP4 treatment on human lung cancer cells using the A549 lung cancer cell line derived from type II alveolar epithelial cells (13). These cells are highly proliferative, tumorigenic, and invasive (25) and have abundant telomerase activity (3). We show that BMP4 induces senescence in A549 lung cancer cells in vitro, as characterized by slowed growth rate, increased β-galactosidase expression, and reduced telomerase activity compared with quiescent cells grown in parallel in low serum. Although the BMP4-treated cells express decreased levels of Bcl2, the reduced cell numbers in the treated cultures probably reflect slowed growth rather than apoptosis, since there was no observable cell detachment from the plates and we could detect neither bax nor ICE in these cells (data not shown). In addition, the cultures survived in the presence of BMP4 for up to 8 wk.

The inhibitory action of BMP4 on certain cancer cell lines in vitro has been shown to be related to upregulation of the cyclin-dependent kinase (cdk) inhibitors p21 and p27, with subsequent decreased activities of cdk2 and cdk6 and hypophosphorylation of the retinoblastoma protein pRb (6). In BMP2-mediated cell cycle arrest of breast cancer cells, p21 promoter activity required both Smad1 and -4 and was induced by either BMP2 or constitutively active type 1 BMP receptors (BMPR) (16). The response of A549 lung cancer cells to BMP4 may not be simple cell cycle arrest, as seen with BMP2-treated breast cancer cells, since we found that BMP4-induced senescence was associated with only a modest increase in p21 compared with the untreated cells and no significant changes in the phosphorylation status of Rb (data not shown).

It has been reported that A5DC7 cells, a subline of A549 cells, senesce with long-term culture in low serum but can be restored to normal phenotype within days by their return to 10% serum culture conditions (12). In our experiments, A549 cells grown in low serum for several weeks in parallel with the BMP4-treated group did not show the hallmarks of senescence seen in the BMP4-treated group, i.e., increased SA-β-gal activity and reduced telomerase activity. In addition, we found that the senescence induced by BMP4 in A549 cells was not immediately reversible, since increased levels of p-Smad1, decreased growth rate, and increased SA-β-gal activity persisted for several weeks after the removal of BMP4 and restoration of 10% serum culture conditions (data not shown).

The persistence of the senescent phenotype after removal of the ligand may explain why BMP4-treated A549 cells generate significantly smaller xenograft tumors in nude mice than untreated cells. This is the first report to document the antitumorigenic potential of a BMP family member using A549 cancer cells in an in vivo model. Although in vivo metastasis was not examined in this project, in vitro matrix invasion assays suggest that the BMP4-treated cells are less invasive. Tada et al. (18) have reported that BMP2 at a dose of 100 ng/ml suppresses anchorage-dependent growth in cultured A549 cells.

Sustained overexpression of Smad1 was associated with a senescent, less invasive, and less tumorigenic phenotype in BMP4-treated A549 cells. In contrast, sustained expression of Smad5, which also transduces the BMP4 signal, was not detected (data not shown). Smads are pivotal intracellular nuclear effectors of TGF family members (8). BMP-mediated activation of downstream Smads involves ligand binding to the high-affinity receptor BMPR-1 and subsequent recruitment of BMPR-2 into the complex. This is followed by phosphorylation of Smads 1, 5, and 8, association with Smad4, and translocation to the nucleus. However, before ligand binding, low but measurable preformed receptor complexes have been detected. Receptor mutant studies show that signals induced by binding of BMP2 to preformed receptor complexes activates the Smad pathway, whereas BMP2-induced recruitment of receptors activates a different, Smad-independent pathway via p38 MAPK (15). Additionally, members of the BMP-Smad pathway can also physically interact with components of other signaling pathways to establish cross talk (20). Thus BMP4 ligand may trigger multiple downstream pathways. To determine whether sustained Smad1 activation itself is sufficient to result in senescence, we overexpressed Smad1 in A549 cells. Adenovirus-mediated Smad1 overexpression resulted in the death of A549 cells, rather than senescence, as seen with BMP4 treatment. The Smad1-overexpressing cells started to lift after 48–72 h posttreatment, and all were dead within 1 wk. Whether this response is unique to A549 cells or can be induced in other cancer cell lines remains to be determined. In the other lung cancer cell lines we tested, overexpression of Smad1 in CALU1 (squamous cell carcinoma) cells resulted in senescence yet had no deleterious effects on SW900 (epidermoid carcinoma) cells, indicating cell-specific responses (data not shown).

In A549 cells, activation of BMP4 downstream Smad1 signaling causes cell death, whereas the ligand itself induces a senescent phenotype. Although the specific downstream targets of BMP4 and/or Smad1 that mediate the phenotypic changes described herein remain to be determined, our data suggest that BMP4 and downstream mediators may have potential to control or retard the growth of certain lung cancers.

GRANTS

This work was funded by National Heart, Lung, and Blood Institute Grants HL-44060, HL-44977, HL-61286, HL-60231 and HL-68597.

REFERENCES

1. **Chen W, Fu X, and Sheng Z.** Review of current progress in the structure and function of Smad proteins. *Chin Med J (Engl)* 115: 446–450, 2002.
2. **Croce MV, Colussi AG, Price MR, and Segal-Eiras A.** Identification and characterization of different subpopulations in human lung adenocarcinoma cell line (A549). *Pathol Oncol Res* 5: 197–204, 1999.
3. **Driscoll B, Buckley S, Bui KC, Anderson K, and Warburton D.** Telomerase in alveolar epithelial development and repair. *Am J Physiol Lung Cell Mol Physiol* 279: L1191–L1198, 2000.
4. **Franzen A and Heldin NE.** BMP-7-induced cell cycle arrest of anaplastic thyroid carcinoma cells via p21 (CIP1) and p27 (KIP1). *Biochem Biophys Res Commun* 285: 773–781, 2001.
5. **Fujii M, Takeda K, Imamura T, Aoki H, Sampath TK, Enomoto S, Kawahata M, Kato M, Ichijo H, and Miyazono K.** Roles of bone morphogenetic protein type I receptors and SMAD proteins in osteoblast and chondroblast differentiation. *Mol Biol Cell* 10: 3801–3813, 1999.
6. **Ghosh-Choudbury N, Woodruff K, Qi W, Celeste A, Abboud SL, and Ghosh-Choudbury G.** Bone morphogenetic protein-2 blocks MDA MB231 human breast cancer cell proliferation by inhibiting cyclin-dependent kinase-mediated retinoblastome protein phosphorylation. *Biochem Biophys Res Commun* 272: 705–711, 2000.
7. **Hjertner O, Hjorth-Hansen H, Borset M, Seidel C, Waage A, and Sundan A.** Bone morphogenetic protein-4 inhibits proliferation and induces apoptosis of multiple myeloma cells. *Blood* 97: 516–522, 2001.
8. **Itoh S, Itoh F, Goumans MG, and Ten Dijke P.** Signaling of transforming growth factor-beta family members through Smad proteins. *Eur J Biochem* 267: 6954–6967, 2000.
9. **Jiang Y, Liang H, Guo W, Kottickal LV, and Nagarajan L.** Differential expression of a novel C-terminally truncated splice form of SMAD5 in hematopoietic stem cells and leukemia. *Blood* 95: 3945–3950, 2000.
10. **Jonson T, Albrechtsson E, Axelson J, Heidenblad M, Gorunova L, Johansson B, and Hoglund M.** Altered expression of TGF-β receptors and mitogenic effects of TGF-β in pancreatic carcinomas. *Int J Oncol* 19: 71–81, 2001.
11. **Katakura Y, Nakata E, Miura T, and Shirahata S.** Transforming growth factor β triggers two independent-senescent programs in cancer cells. *Biochem Biophys Res Commun* 255: 110–115, 1999.
12. **Katakura Y, Yamamoto K, Miyake O, Yasuda T, Uehara N, Nakata E, Kawamoto S, and Shirahata S.** Bidirectional regulation of telomerase activity in a subline derived from human lung adenocarcinoma. *Biochem Biophys Res Commun* 237: 313–317, 1997.
13. **Lieber A, Smith B, Szakal A, Nelson-Rees W, and Todaro G.** A continuous tumor cell line from a human lung carcinoma with properties of type II alveolar epithelial cells. *Int J Cancer* 17: 62–70, 1976.
14. **Massague J, Blain SW, and Lo RS.** TGF beta signaling in growth control, cancer, and heritable disorders. *Cell* 103: 295–309, 2000.
15. **Nohe A, Hassel S, Ehrich M, Neubauer F, Sebald W, Henis YI, and Knaus P.** The role of bone morphogenic protein (BMP) receptor oligomerization determines different BMP-2 signaling pathways. *J Biol Chem* 277: 5330–5338, 2002.
16. **Poulint F and Labrie C.** Role of SMAD1 and SMAD4 proteins in the induction of p21WAF1, Cip1 during bone morphogenic protein-induced growth arrest in human breast cancer cells. *J Endocrinol* 172: 187–198, 2002.
17. **Tada A, Kato H, Takennga K, and Hagesawa S.** Transforming growth factor beta 1 increases the expressions of high molecular weight tropomyosin isoforms and vinculin and suppresses the transformed phenotype in lung carcinoma cells. *Cancer Lett* 121: 31–37, 1997.
18. **Tada A, Nishihara T, and Kato H.** Bone morphogenetic protein 2 suppresses the transformed phenotype and restores actin microfilaments of human lung cancer A549 cells. *Oncol Rep* 5: 1137–1140, 1998.
19. **Takagi Y, Koumura H, Futamura M, Aoki S, Yamaguchi K, Kida H, Tanemura H, Shimokara K, and Saji S.** Somatic alterations of the SMAD-2 gene in human colorectal cancers. *Br J Cancer* 78: 1152–1155, 1998.
20. **Von Bubnoff A and Cho KW.** Intracellular BMP signaling in vertebrates: pathway or network? *Dev Biol* 239: 1–14, 2001.
21. **Wach S, Schirmacher P, Protschka M, and Blessing M.** Overexpression of bone morphogenetic protein-6 (BMP-6) in murine epidermis suppresses tumor formation by induction of apoptosis and down-regulation of fos/jun family members. *Oncogene* 20: 7761–7769, 2001.
22. **Wingo PA, Ries LA, Parker SL, and Heath CW Jr.** Long term cancer patient survival in the United States. *Cancer Epidemiol Biomarkers Prev* 7: 271–282, 1998.
23. **Xu HJ, Zhou Y, Wan J, Perng GS, Kruzelock R, Kong CT, Bast RC, Mills GB, Li J, and Hu SX.** Reexpression of the retinoblastoma protein in tumor cells induces senescence and telomerase inhibition. *Oncogene* 13: 2589–2596, 1997.
24. **Yanagisawa K, Uchida K, Nagatake M, Masuda A, Sugiyama M, Saito T, Yamaki K, Takahashi T, and Osada H.** Heterogeneities in the biological and biochemical functions of Smad2 and Smad4 mutants naturally occurring in human lung cancers. *Oncogene* 19: 2305–2311, 2000.
25. **Zucker S, Lysik RM, Malik M, Bauer BA, Caamano J, and Klein-Szanto AJ.** Secretion of gelatinases and tissue inhibitors of metalloproteinases by human lung cancer cell lines and revertant cell lines: not an invariant correlation with metastasis. *Int J Cancer* 52: 366–371, 1992.

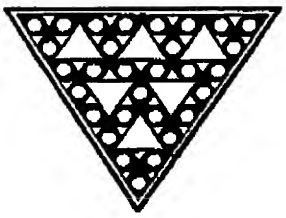

THE JOURNAL OF BIOLOGICAL CHEMISTRY
Vol. 276, No. 33, Issue of August 17, pp. 31133–31141, 2001
Printed in U.S.A.

Bone Morphogenetic Protein-2 Inhibits Serum Deprivation-induced Apoptosis of Neonatal Cardiac Myocytes through Activation of the Smad1 Pathway*

Received for publication, February 15, 2001, and in revised form, May 31, 2001
Published, JBC Papers in Press, June 14, 2001, DOI 10.1074/jbc.M101463200

Masahiro Izumi‡, Yasushi Fujio‡, Keita Kunisada‡, Shinji Negoro‡, Eiro Tone‡, Masanobu Funamoto‡, Tomoaki Osugi‡, Yuichi Oshima‡, Yoshikazu Nakaoka‡, Tadamitsu Kishimoto§, Keiko Yamauchi-Takihara‡, and Hisao Hirota‡¶

From the ‡Department of Molecular Medicine, Osaka University Graduate School of Medicine, and §Osaka University, 2-2 Yamadaoka, Suita City, Osaka 565-0871, Japan

Bone morphogenetic protein (BMP)-2 has been shown to induce ectopic expression of cardiac transcription factors and beating cardiomyocytes in non-precardiac mesodermal cells, suggesting that BMP-2 is an inductive signaling molecule that participates in cardiac development. However, direct evidence of the effects of BMP-2 on cardiac myocytes has not been reported. To examine the role of BMP-2 and its receptors, we studied the ability of BMP-2 to promote survival of isolated neonatal rat cardiac myocytes. BMP receptors IA, IB, and II and activin receptor I were found to be expressed in myocytes, and BMP-2 phosphorylated Smad1 and p38 MAPK. Interestingly, BMP-2 promoted survival and inhibited apoptosis of serum-deprived myocytes, although it did not strongly induce hypertrophic growth. To explore the mechanisms for this protective effect, an adenovirus-based vector system was used. Similar to BMP-2, Smad1 promoted survival that was repressed by Smad6. Moreover, BMP-2 and Smad1 enhanced the expression of the anti-apoptotic molecule Bcl-x_L. Antisense oligonucleotides to *bcl-*x_L attenuated the survival effected by BMP-2. Overall, our findings suggest that BMP-2 prevents apoptosis of myocytes by induction of Bcl-x_L via a Smad1 pathway and might be a novel survival factor without any hypertrophic effect on myocytes.

Bone morphogenetic protein (BMP)[1]-2, a member of the transforming growth factor-β superfamily, signals through the heterotetrameric complex of type I and II serine/threonine kinase receptors (1, 2). Downstream of this receptor complex, at least two distinct intracellular pathways have been suggested to mediate inductive signals from the cell membrane to the nucleus.

One pathway involves a family of transcription factors collectively known as Smad proteins. Thus far, eight mammalian Smad proteins, specified as Smad1–8, have been isolated. They can be classified into three subgroups by their structures and functions: pathway-restricted, common mediator, and inhibitory Smad proteins. Smad1, Smad5, and probably Smad8/MADH6 are pathway-restricted Smad proteins, which are activated by BMP receptors. Smad4 is a common mediator Smad, whereas Smad6 and Smad7 are classified in the inhibitory Smad subgroup. Following binding of BMPs to their receptors, Smad1 and Smad5 are phosphorylated by BMP receptors, form hetero-oligomeric complexes with Smad4, translocate into the nucleus, and modulate transcription of a variety of target genes (3–5). Another pathway is the MAPK cascade initiated by TAK-1 (6). TAK-1 was originally identified as a member of the MAPK kinase kinase family activated in response to transforming growth factor-β and BMP-4 (6). More recently, it has been reported that TAK-1 functions as a mediator of the MKK6/p38 MAPK and MKK7/JNK pathways (7–9).

After initial activation of receptors, BMP-2 elicits multiple effects ranging from cell differentiation to regulation of early embryogenesis. BMP-2 was originally identified as a molecule that induces bone and cartilage formation and is now considered a multifunctional cytokine (10, 11). Interestingly, BMP-2 induces ectopic expression of cardiac transcription factors and beating cardiomyocytes in non-precardiac mesodermal chick cells, and BMP-2-deficient mouse embryos exhibit a defect in cardiac development manifested by abnormal development of the heart (12, 13). These data suggest that BMPs are inductive signaling molecules that participate in development of the heart. In addition to cardiac development, BMP-2 has been reported to exert both pro-apoptotic and anti-apoptotic effects, depending on cell types and circumstances (14–16). Therefore, it is of interest to examine whether BMP-2 might also regulate survival of cardiac myocytes.

Recent evidence that apoptosis of cardiac myocytes is a feature in several myocardial disease states, including ischemic heart disease and congestive heart failure, has raised hopes that inhibition of myocyte apoptosis can prevent the loss of contractile cells and thus provide a new target in a multimodal therapeutic approach to cardiac disease (17). Several groups have reported that insulin-like growth factor-1, cardiotrophin-1, leukemia inhibitory factor (LIF), and neuregulin reduce myocyte apoptosis after ischemia, serum withdrawal, myocyte

* This work was supported by research grants from the Ministry of Education, Science, Sports, and Culture of Japan, the Japan Heart Foundation, the Senri Life Science Foundation, the Japan Cardiovascular Research Foundation, the Mochida Memorial Foundation for Medical and Pharmaceutical Research, and the Natio Foundation. The costs of publication of this article were defrayed in part by the payment of page charges. This article must therefore be hereby marked "*advertisement*" in accordance with 18 U.S.C. Section 1734 solely to indicate this fact.

¶ To whom correspondence should be addressed. Tel.: 81-6-6879-3835; Fax: 81-6-6879-3839; E-mail: hirota@imed3.med.osaka-u.ac.jp.

[1] The abbreviations used are: BMP, bone morphogenetic protein; BMPR, BMP receptor; MAPK, mitogen-activated protein kinase; TAK-1, transforming growth factor-β-activated kinase-1; MKK, MAP kinase kinase; JNK, c-Jun N-terminal kinase; LIF, leukemia inhibitory factor; ERK, extracellular signal-regulated kinase; PCR, polymerase chain reaction; FCS, fetal calf serum; BNP, brain natriuretic peptide; PBS, phosphate-buffered saline; MTS, 3-(4,5-dimethylthiazol-2-yl)-5-(3-carboxymethoxyphenyl)-2-(4-sulfophenyl)-2*H*-tetrazolium; TUNEL, terminal deoxynucleotidyltransferase-mediated dUTP nick end labeling; ELISA, enzyme-linked immunosorbent assay; ActR-I, activin receptor I; Stat, signal transducer and activator of transcription.

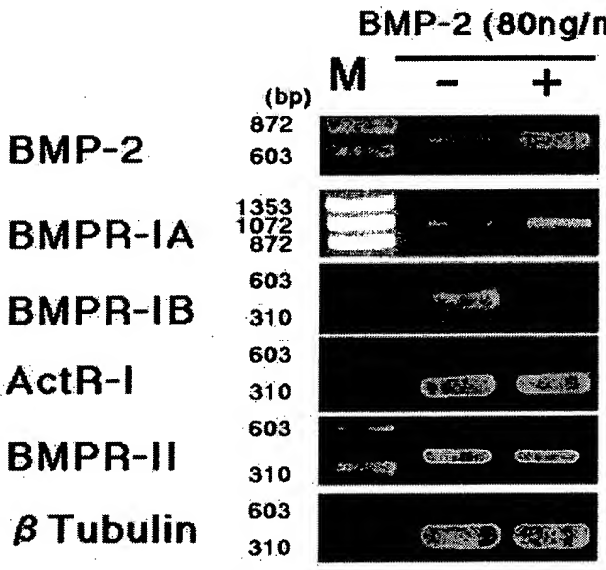

FIG. 1. **Expression of BMP-2 and its receptors in cardiac myocytes.** Total RNA from freshly cultured neonatal rat cardiac myocytes treated with BMP-2 (80 ng/ml) or untreated was reverse-transcribed into cDNA and amplified with BMP-2 or BMP receptor isoform-specific primers as described under "Experimental Procedures." β-Tubulin expression was also assayed as a control. *Lane M* contains molecular size markers (in base pairs (*bp*)).

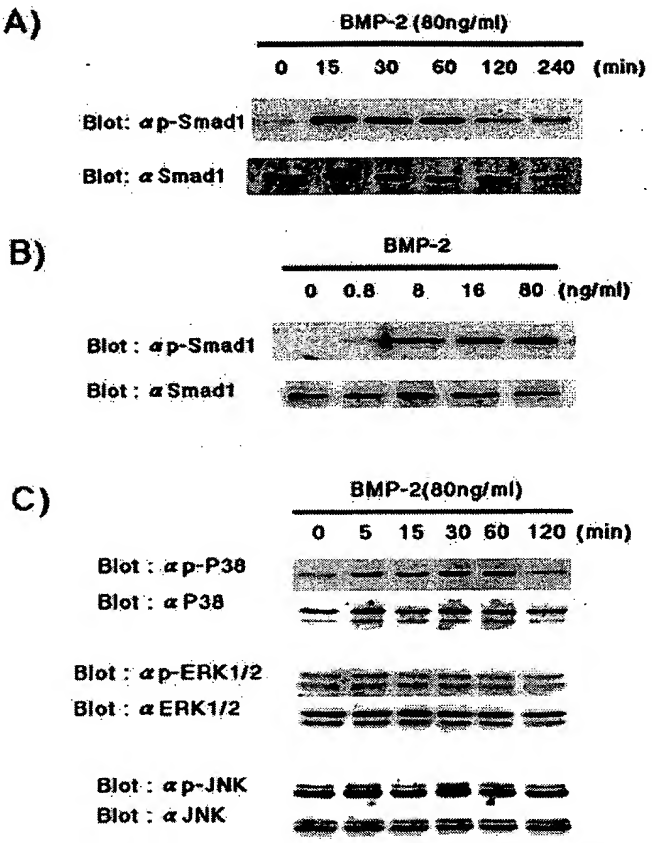

FIG. 2. **BMP-2 activates Smad1 and p38 MAPK.** *A*, neonatal rat cardiac myocytes were treated with BMP-2 (80 ng/ml) for the indicated periods of time. Cell lysates (20 μg of proteins) were subjected to immunoblotting with anti-phospho-Smad1 antibody (*αp-Smad1*; *upper panel*) and subsequently with anti-Smad1 antibody (*αSmad1*; *lower panel*). Experiments were performed three times with similar results. Representative data are shown. *B*, cardiac myocytes were treated with various concentrations of BMP-2 for 30 min. Cell lysates were subjected to immunoblotting with anti-phospho-Smad1 antibody (*upper panel*) and subsequently with anti-Smad1 antibody (*lower panel*). *C*, cell lysates (20 μg of proteins) were subjected to immunoblotting with anti-phospho-p38 MAPK (*αp-P38*), anti-phospho-ERK1/2 (*α pERK1/2*), and anti-phospho-JNK (*αp-JNK*) antibodies (*upper panels*) and subsequently with anti-p38 MAPK (*αP38*), anti-ERK1/2 (*αERK1/2*), and anti-JNK (*αJNK*) antibodies (*lower panels*).

stretch, and treatment with the cardiotoxic hemotherapeutic drug doxorubicin (18–22). However, these factors simultaneously induce cardiac hypertrophy. Although cardioprotective factors can thus be considered clinically suitable for treating heart failure, the hypertrophic effect accompanying their cardioprotective function may promote structural and geometric changes in the left ventricle that are commonly referred to as remodeling. Progressive, adverse remodeling of the myocardium may lead to ventricular dilatation and congestive heart failure (23).

Our study demonstrates that human BMP-2 promotes survival of neonatal rat cardiac myocytes *in vitro* without any significant change in cell size. This survival effect is accompanied by a marked reduction in the proportion of apoptotic cells in BMP-2-treated cultures. We also describe the survival effect of BMP-2 involving an increase in Bcl-x_L via a Smad1 signaling pathway. These data support the concept that the BMP-2/Smad1 signaling system plays an important role in regulation of the myocardium and suggest that BMP-2 as an attenuator of apoptosis in cardiac myocytes has therapeutic and prognostic potential.

EXPERIMENTAL PROCEDURES

Reagents—Recombinant human BMP-2 (80 mg/ml; Yamanouchi Co., Ltd., Tokyo), recombinant human LIF (106 units/ml; PeproTech EC, Ltd., London), and norepinephrine (1 mg/ml; Sankyo Co., Ltd., Tokyo) were used this study. Anti-Smad1, anti-Smad6, anti-p38 MAPK, anti-ERK1/2, anti-JNK, anti-Bcl-x_L, and anti-Bcl-2 antibodies were purchased from Santa Cruz Biotechnology (Santa Cruz, CA). Anti-α-tubulin monoclonal antibody was from Calbiochem, and phospho-Smad1, p38 MAPK, and ERK1/2 were from New England Biolabs Inc. (Beverly, MA). All other chemicals were reagents of molecular biology grade obtained from standard commercial sources.

Cell Culture—Primary cultures of neonatal cardiac myocytes were prepared from the ventricles of 1–2-day-old Wistar rats obtained from Kiwa Dobutsu (Wakayama, Japan) as described previously (24).

Reverse Transcription-PCR Assay—10 μg of total RNA was prepared by the acid guanidinium thiocyanate/phenol/chloroform method (25). Total RNA (0.1 μg) was subjected to first-strand synthesis using oligo(dT) (Amersham Pharmacia Biotech, Uppsala) and Moloney murine leukemia virus reverse transcriptase (Life Technologies, Inc.) at 37 °C for 2 h, and the reaction was stopped by incubation at 70 °C for 10 min. The primers used for gene amplification of BMP-2, BMP receptors (BMPRs), and β-tubulin by PCR were synthesized according to the sequence previously reported (26–28).

Western Blot Analysis—Neonatal rat cardiac myocytes were cultured at a cell density of 3×10^5/ml in six-well dishes in duplicate. After being cultured with Medium 199 with 10% fetal calf serum (FCS) for 24 h, the medium was changed to Medium 199 with 1% FCS and incubated for 24 h. Thereafter, cardiac myocytes were cultured without serum for another 12 h. The cells were then stimulated with BMP-2. Western blotting was performed as previously described (24).

Northern Blot Analysis—Northern blotting was performed as previously described (29). RNAs from cardiac myocytes were prepared as described above. Mouse *bcl-x* cDNA, kindly donated by Dr. Y. Tsujimoto (Osaka University Medical School), was used as a probe. Mouse brain natriuretic peptide (BNP) cDNA, kindly donated by Dr. K. R. Chien (University of California, San Diego, CA), was used as a probe. Mouse *junB* cDNA was purchased from American Type Culture Collection.

Immunohistochemistry—For examination of changes in myocyte phenotypes produced by BMP-2, LIF, and norepinephrine, cardiac myocytes were grown on slides and fixed in 2% (w/v) formaldehyde for 15 min at room temperature and permeabilized with 0.1% Triton X-100/

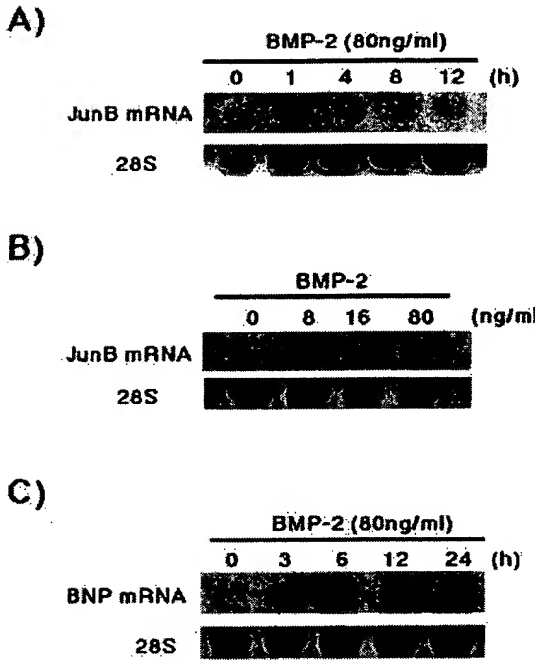

FIG. 3. **BMP-2 induces *junB* and BNP mRNAs.** *A*, neonatal rat cardiac myocytes were treated with BMP-2 (80 ng/ml) for the indicated periods of time. *junB* mRNA expression was examined by Northern blot analysis. Experiments were performed three times with similar results. Representative data are shown. *B*, cardiac myocytes were treated with various concentrations of BMP-2 for 1 h. *C*, cardiac myocytes were treated with 80 ng/ml BMP-2 for the indicated periods of time. BNP mRNA expression was examined by Northern blot analysis.

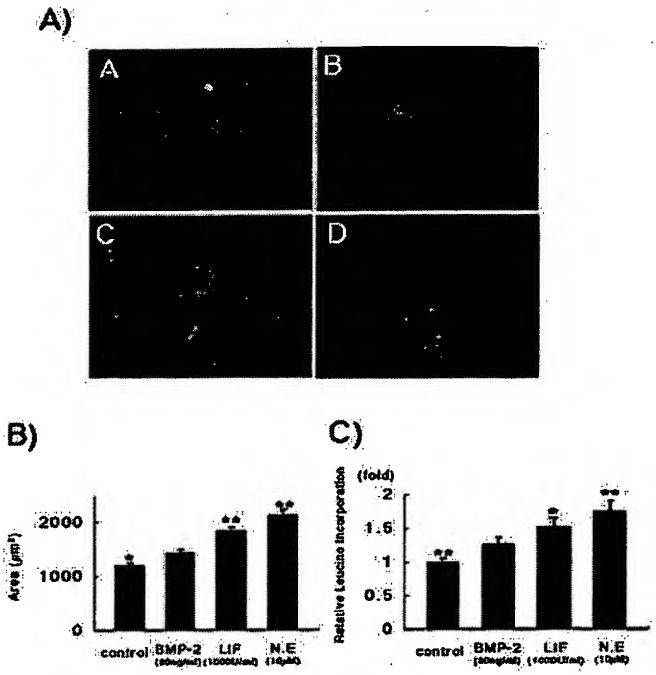

FIG. 4. **BMP-2 does not induce hypertrophic growth of neonatal myocytes.** *A*, neonatal rat cardiac myocytes were plated onto chamber slides and incubated for 48 h with no addition (*panel A*) or with the addition of 80 ng/ml BMP-2 (*panel B*), 1×10^3 units/ml LIF (*panel C*), or 2 μg/ml norepinephrine (*panel D*). Cells were labeled with anti-α-actinin antibody and viewed with a confocal microscope (magnification × 40). *B*, cardiac myocytes were treated with 80 ng/ml BMP-2, 1×10^3 units/ml LIF, or 2 μg/ml norepinephrine (*N.E*) for 48 h. Cardiac myocytes (100 cells for each treatment) were traced, and cell-surface areas were measured with the aid of the Macscope program. Each *bar* represents the mean ± S.D. *, $p < 0.01$ *versus* BMP-2; **, $p < 0.0001$ *versus* BMP-2. *C*, cardiac myocytes were treated with 80 ng/ml BMP-2, 1×10^3 units/ml LIF, or 2 μg/ml norepinephrine and co-incubated with [^{3}H]leucine for 24 h. Aliquots were counted with a scintillation counter. The data are expressed as relative absorbance normalized to the mean absorbance of untreated control cells. Each *bar* represents the mean ± S.D. (n = three experiments). *, $p < 0.05$ *versus* BMP-2; **, $p < 0.01$ *versus* BMP-2.

phosphate-buffered saline (PBS). Following three PBS washes, the chamber slides were incubated in 1% bovine serum albumin/PBS for 1 h to block nonspecific sites. Subsequently, the cells were stained for 1 h in 0.05% Tween 20 and 1% bovine serum albumin/PBS with a mouse anti-rabbit α-actinin monoclonal antibody. Following another three PBS washes, the slides were incubated for 30 min in 0.05% Tween 20 and 1% bovine serum albumin/PBS with rhodamine B isothiocyanate-conjugated anti-mouse IgG as a secondary antibody and finally mounted on glass coverslips.

Cardiac Myocyte Surface—To measure the cell-surface areas, light photomicrographs of beating cells (100 cells from six visual fields) were obtained with an Olympus IMT-2 microscope, and cell surfaces were traced with the Macscope program (Mitani Co., Tokyo).

Leucine Incorporation—To examine the effect of BMP-2 on protein synthesis, the incorporation of [^{3}H]leucine was measured. Cultured myocytes were treated with BMP-2 (80 ng/ml), LIF (1×10^3 units/ml), or norepinephrine (2 μg/ml) and co-incubated with [^{3}H]leucine (1 μCi/ml) for 24 h. The cells were washed three times with PBS and then treated with 5% trichloroacetic at 4 °C for 10 min to precipitate the protein. The precipitates were dissolved in 0.1 N NaOH, and aliquots were counted with a scintillation counter.

Cell Viability Assay—Cell viability was quantitated with the MTS (inner salt) cell respiratory assay (Promega, Madison, WI) (30, 31). Neonatal rat cardiac myocytes were cultured at a density of 2×10^4/100 μl in 96-well dishes. After culturing in Medium 199 with 10% FCS for 24 h, the medium was changed to Medium 199 with 1% FCS, and the cells were incubated for 24 h. Next, the cardiac myocytes were cultured without serum for another 12 h and stimulated with BMP-2 or LIF. 48 h later, MTS was incubated with the cells for 1 h at 37 °C in a humidified 5% CO_2 atmosphere. The absorbance was then recorded at 490 nm with a 96-well plate reader. Each experiment was carried out in triplicate and repeated in three independent experiments.

Apoptosis Assays—Apoptosis was evaluated with the terminal deoxynucleotidyltransferase-mediated dUTP nick end labeling (TUNEL) assay and cell death detection ELISA. The TUNEL assay was performed as previously described (32), and the cells were analyzed by fluorescence microscopy. For quantitative analysis, 600 α-actinin-positive cardiac myocytes were counted, and the number of TUNEL-positive cells among them was expressed as a percentage. The cell death detection assay (Roche Molecular Biochemicals) measures the presence of the soluble histone-DNA complex as a result of DNA fragmentation (33). For this assay, neonatal rat cardiac myocytes were cultured at a density of 5×10^5/1 ml in 6-cm dishes. After culturing in Medium 199 with 10% FCS for 24 h, the medium was changed to Medium 199 with 1% FCS, and the cells were incubated for 24 h. Next, the cardiac myocytes were cultured without serum for another 12 h and stimulated with BMP-2. 48 h later, all cells were collected in lysis buffer and subjected to capture ELISA according to the manufacturer's protocol. Each experiment was carried out in triplicate and repeated in three independent experiments.

Antisense Assay—The antisense and sense phosphorothioate oligonucleotides were designed as described by Wang *et al.* (34): antisense, CTGAGACATTTTTAT and sense, ATAAAAATGTCTCAG. This region of murine *bcl-x_L* is completely identical to that of rat *bcl-x_L* (35). Antisense oligonucleotide assays were performed according to previously described methods (36).

Generation of Recombinant Adenovirus and Protocol for Adenoviral Infection—The recombinant adenoviruses expressing Smad proteins were kindly donated by Dr. K. Miyazono (Tokyo University Medical School) (37). The recombinant viruses were purified and concentrated as described previously (38). They were prepared for experiments at high multiplicity of infections. 36 h after plating, cardiac myocytes were transfected with adenoviral vectors in Medium 199 with 10% FCS at a multiplicity of infection of 20 and incubated for 12 h. After removal of the viral suspension, cardiac myocytes were serum-starved for 6 h and

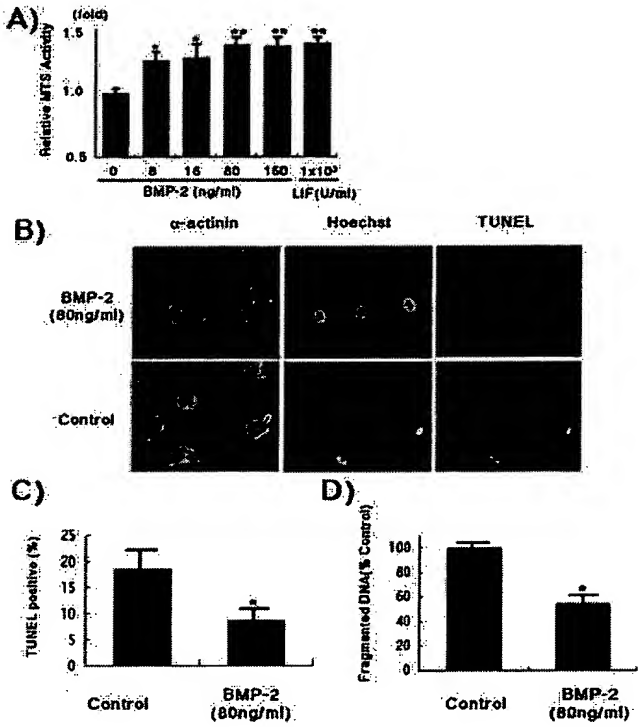

FIG. 5. **BMP-2 promotes survival and diminishes apoptotic cell death in neonatal rat cardiac myocyte primary cultures.** *A*, neonatal rat cardiac myocytes were treated with various concentrations of BMP-2 or 1 × 10^3 units/ml LIF for 48 h. The viability of cardiac myocytes was determined by the MTS cell respiration assay, and the data are expressed as relative absorbance normalized to the mean absorbance of untreated control cells. Each *bar* represents the mean ± S.D. (n = three experiments). *, $p < 0.05$ *versus* control; **, $p < 0.01$ *versus* control. *B*, shown is a representative image of TUNEL-positive cardiac myocytes in culture (magnification × 100). Cardiac myocytes were plated onto chamber slides and incubated for 48 h with or without (*Control*) the addition of BMP-2 (80 ng/ml). Cells were subjected to Hoechst dye, TUNEL, and anti-α-actinin antibody staining. *C*, shown are the results from the quantitative analysis of the percentage of cells undergoing apoptosis as measured by the TUNEL technique. Each *bar* represents the mean ± S.D. (n = six experiments). *, $p < 0.01$ *versus* control. *D*, neonatal rat cardiac myocytes were treated with BMP-2 (80 ng/ml) for 48 h. To quantify apoptosis, commercially available ELISA was used to detect histone-associated DNA fragments. The data are expressed as percentages of the values obtained with untreated control cells. Each *bar* represents the mean ± S.D. (n = three experiments). *, $p < 0.01$ *versus* control.

stimulated with reagents. The adenoviral vector expressing β-galactosidase (referred to as Ad-β-gal) was used as a control.

Statistical Analysis—Data are presented as means ± S.E. Statistical analysis was carried out using unpaired Student's t tests. A p value of <0.05 was considered significant.

RESULTS

Reverse Transcription-PCR Analysis of RNAs for BMP-2 and BMP Receptors—mRNA expression of BMP receptors was analyzed in cardiac myocytes grown in the absence or presence of BMP-2 (80 ng/ml). Cultures were assayed for the expression of BMP-2, BMPR-IA, BMPR-IB, BMPR-II, and activin receptor I (ActR-I) mRNAs by reverse transcription-PCR after 3 h in culture. As shown in Fig. 1, mRNAs for BMPR-IB, ActR-I, and BMPR-II were readily apparent in control cultures, whereas mRNAs for BMP-2 and BMPR-IA were less abundant. Cultures grown in the presence of BMP-2 expressed BMP-2, BMPR-IA, BMPR-II, and ActR-I mRNAs. Although this PCR method is not quantitative, the induction of BMP-2 and BMPR-IA mRNAs following exposure to BMP-2 was striking. These observations indicate that treatment with BMP-2 can activate heart cells through its receptors.

BMP-2 Induces the Activation of Smad1 and p38 MAPK in Neonatal Rat Cardiac Myocytes—To determine whether BMP-2 transduces signals in neonatal cardiac myocytes, we examined the phosphorylation of Smad1, p38 MAPK, ERK1/2, and JNK after BMP-2 stimulation by Western blot analysis. After 8 h of culture in serum-deprived medium, cardiac myocytes were stimulated with BMP-2 (80 ng/ml) for the times indicated (Fig. 2*A*). Smad1 was rapidly phosphorylated within 15 min in cardiac myocytes, followed by a decrease within 2 h. As shown in Fig. 2*B*, BMP-2 also activated Smad1 in a dose-dependent manner. The amounts of Smad1 protein were the same for each period (Fig. 2, *A* and *B*, *lower panels*). In the MAPK family, p38 MAPK was rapidly phosphorylated within 5 min, whereas ERK1/2 and JNK were not activated (Fig. 2*C*).

BMP-2 Induces the Expression of junB and BNP mRNAs—The induction of immediate-early genes precedes the late phenotypic changes in cardiomyocytes following stimulation of G-protein-coupled receptors *in vitro* (39–41) and cardiac hypertrophy *in vivo* (42). We therefore determined whether stimulation of cardiomyocytes with BMP-2 would induce *junB* gene expression. Stimulation with BMP-2 resulted in the rapid and transient induction of *junB* mRNA (Fig. 3*A*). BMP-2 also induced *junB* mRNA expression in a dose-dependent manner (Fig. 3*B*). Since the reactivation of an embryonic pattern of gene expression is a hallmark of cardiomyocyte hypertrophy, we therefore determined whether stimulation of cardiomyocytes with BMP-2 would induce BNP gene expression. As shown in Fig. 3*C*, enhancement of BNP mRNA expression was detected within 6 h, with a maximum level at 12 h, followed by a decrease within 24 h.

BMP-2 Does Not Induce Hypertrophic Growth of Cardiac Myocytes—Neonatal rat ventricular cardiomyocytes respond to various hypertrophic stimuli by an increase in individual cell size, assembly of myofibrils, and induction of the BNP gene. To assess the effects of BMP-2 on these morphological features of a hypertrophic response, cardiomyocytes were treated with BMP-2 (80 ng/ml) and stained with an anti-α-actinin antibody. Unstimulated cells and LIF/norepinephrine-treated cells served as negative and positive controls, respectively. Interestingly, BMP-2 did not induce a strong hypertrophic response in cardiac myocytes in comparison with LIF and norepinephrine, but did induce BNP gene expression (Fig. 4*A*). To quantify hypertrophic effects, we measured the cell-surface area and the incorporation of [^{3}H]leucine as described under "Experimental Procedures." As shown in Fig. 4 (*B* and *C*), the increase in cell size and [^{3}H]leucine incorporation induced by BMP-2 was significantly less than those induced by LIF or norepinephrine. These findings suggest that the hypertrophic effects of BMP-2 are significantly less than those of LIF and norepinephrine.

BMP-2 Promotes Survival and Diminishes Apoptotic Cell Death through the Induction of Bcl-x_L—Primary cultures of neonatal rat ventricular myocytes maintained in serum-free medium exhibited a gradual reduction in cell numbers. We performed an MTS cell respiration assay to measure cell viability in primary cultures of neonatal rat cardiac myocytes. The myocytes were cultured in the presence or absence of BMP-2 for 48 h. As shown in Fig. 5*A*, BMP-2 promoted myocardial cell survival in a dose-dependent manner. LIF-treated cells served as positive controls. On the other hand, BMP-2 could not promote survival of cardiac non-myocytes (data not shown). We examined next whether the survival effect of BMP-2 was mediated by inhibition of programmed cell death (apoptosis). We performed the TUNEL assay and cell death detection ELISA on primary cultures of neonatal rat cardiac myocytes. About 18%

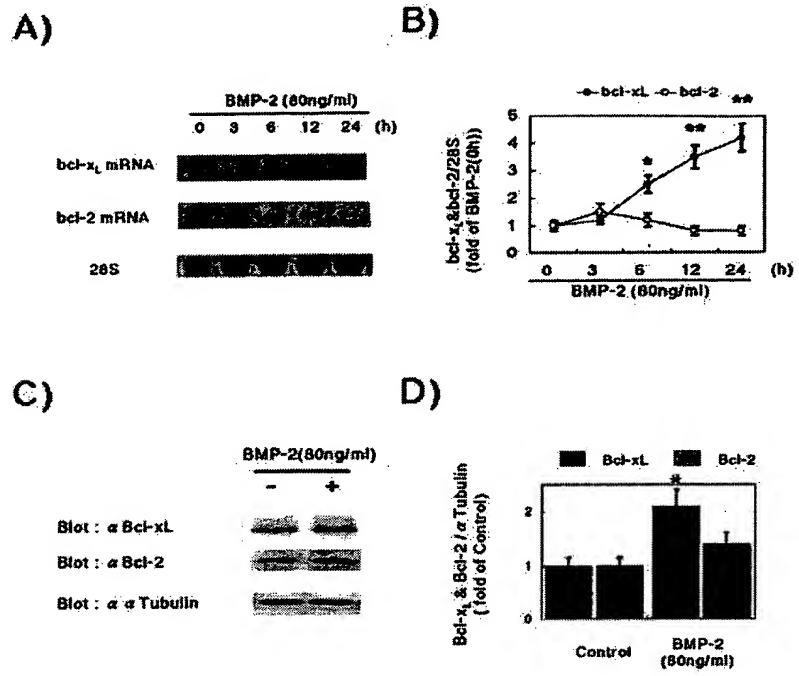

FIG. 6. **BMP-2 induces *bcl-x_L* in neonatal rat cardiac myocyte primary cultures.** *A*, neonatal rat cardiac myocytes were treated with BMP-2 (80 ng/ml) for the indicated periods of time. *bcl-x_L* and *bcl-2* mRNA expression was examined by Northern blot analysis. *B*, densitometry was used to assess the relative intensity of the band for *bcl-x_L* and *bcl-2* as a ratio in comparison with the intensity of the band for 28 S rRNA. The data are expressed as relative absorbance normalized to the mean absorbance of untreated control cells. Values represent the means ± S.D. (n = three experiments.) *, $p < 0.05$ *versus* control; **, $p < 0.01$ *versus* control. *C*, cardiac myocytes were treated with BMP-2 (80 ng/ml) for 24 h. Cells were directly lysed with SDS-polyacrylamide gel electrophoresis solution, and the cell lysates were Western-blotted with anti-Bcl-x_L (*αBcl-xL*), anti-Bcl-2 (*αBcl-2*), and anti-α-tubulin (*α αTubulin*) antibodies. *D*, densitometry was used to assess the relative intensity of the band for Bcl-x_L and Bcl-2 as a ratio in comparison with the intensity of the band for α-tubulin. The data are expressed as relative absorbance normalized to the mean absorbance of untreated control cells. Values represent the means ± S.D. (n = three experiments). *, $p < 0.05$ *versus* control.

of the cardiac myocytes maintained in serum-deprived medium for 48 h showed positive TUNEL staining (Fig. 5*B*). As shown in Fig. 5*C*, BMP-2 (80 ng/ml) significantly reduced TUNEL-positive cells. Cell death detection ELISA also demonstrated that BMP-2 significantly suppressed serum deprivation-induced nuclear fragmentation (Fig. 5*D*). These results indicate that BMP-2 acts as a survival factor at least in part by preventing programmed cell death in neonatal rat cardiac myocytes.

To investigate the molecular mechanism that relates to the anti-apoptotic effect of BMP-2, we examined the expression of *bcl-x_L* and *bcl-2*, which are anti-apoptotic members of *bcl-2* families. Neonatal rat cardiac myocytes were treated with BMP-2 (80 ng/ml) for the indicated periods of time. Upon examination by Northern blot analysis, expression of *bcl-x_L* and *bcl-2* mRNAs showed enhancement of *bcl-x_L* gene expression in cardiac myocytes, with the maximum level attained at 24 h, whereas no enhancement of *bcl-2* gene expression was detected (Fig. 6, *A* and *B*). We also examined the expression of Bcl-x_L and Bcl-2 proteins by Western blot analysis in cardiac myocytes treated with BMP-2 (80 ng/ml) for 24 h. A high level of Bcl-x_L was also detected in BMP-2-treated cells, but no up-regulation of Bcl-2 (Fig. 6, *C* and *D*). These results indicate that BMP-2 may promote cardiac myocyte survival through the induction of Bcl-x_L.

Antisense Oligonucleotides to bcl-x_L Attenuate the Anti-apoptotic Effect of BMP-2—To demonstrate the specificity of *bcl-x_L* antisense oligonucleotides, cardiac myocytes were treated with *bcl-x_L* antisense or sense oligonucleotides in the presence or absence of BMP-2 for 48 h. The myocytes were subsequently examined with the MTS cell respiratory assay. In the presence of antisense oligonucleotides, the increase in Bcl-x_L induced by BMP-2 was inhibited, but not in the presence of sense oligonucleotides (Fig. 7*A*). Antisense oligonucleotides against *bcl-x_L* mRNA canceled the BMP-2-mediated protective effect on cell survival (Fig. 7*B*). Although the sense nucleotides also inhibited BMP-2-mediated cell protection, their inhibitory effect was significantly less than that of antisense oligonucleotides (Fig. 7*B*).

Smad1 in the Adenoviral Vector Promotes Survival in Neonatal Rat Cardiac Myocytes—We investigated the molecular mechanisms that regulate *bcl-x_L* gene expression upon BMP-2 stimulation in cardiac myocytes using an adenovirus-based vector system that allows for highly efficient transfection of DNAs into many cell types. In our study, we demonstrated that activation of BMP receptors resulted in the activation of downstream signaling pathways, including Smad1 and p38 MAPK. To identify the downstream effector for BMP-2-mediated protection of cell survival through the induction of *bcl-x_L*, the effects of Smad1 on cell survival and *bcl-x_L* induction were examined. We performed an MTS respiratory cell assay, a TUNEL assay, and cell death detection ELISA in cultured cardiac myocytes transfected with adenoviral vectors expressing Smad1 (referred to as Ad-Smad1) in the presence or absence of BMP-2 for 48 h. Interestingly, the phosphorylation of Smad1 was detected in cultured cardiac myocytes transfected with Ad-Smad1 (Fig. 8*A*). As shown in Fig. 8*B*, Smad1 promoted cell survival, which was enhanced by the presence of BMP-2. TUNEL-positive cells were significantly reduced in cardiac myocytes transfected with Ad-Smad1 compared with those in untransfected cardiac myocytes (Fig. 8*C*). Cell death detection ELISA also showed that fragmented DNA was significantly reduced in cardiac myocytes transfected with Ad-Smad1 (Fig. 8*D*). Altogether, these results indicate that the survival effect of Smad1 is mediated by inhibition of apoptosis. Moreover, the expression of the *bcl-x_L* gene and protein was increased in cultured cardiac myocytes transfected with Ad-Smad1 (Fig. 9, *A–D*). These findings suggest that BMP-2 promotes cardiac muscle survival through the induction of *bcl-x_L* via the Smad signaling pathway.

Smad6 in the Adenoviral Vector Inhibits the Anti-apoptotic Effect—To examine whether Smad6 inhibits the Smad1-mediated protective effect on cell survival by inhibition of apoptosis, we performed an MTS respiratory cell assay and TUNEL assay of cultured cardiac myocytes transfected with adenoviral vectors expressing Smad6 (referred to as Ad-Smad6) or Ad-β-gal in the presence or absence of BMP-2 for 48 h. As shown in Fig. 10*A*, Smad6 inhibited BMP-2-mediated phosphorylation of

Smad1 as determined by Western blot analysis and also inhibited BMP-2-mediated protection of cell survival by prevention of apoptosis (Fig. 10, *B* and *C*). These findings again indicate that the Smad pathway is essential for the induction of cardiac protection.

DISCUSSION

The importance of BMP-2 in development of the heart is highlighted by the characterization of mice with targeted disruption of BMP-2 and the findings of BMP-2-induced beating cardiomyocytes in non-precardiac mesodermal chick cells (12, 13). In the study reported here, we have documented the expression of BMP-2 receptors and signaling pathways in the postnatal myocardium. Furthermore, we demonstrated the occurrence of BMP-2-induced novel phenotypic changes in neonatal cardiac myocytes.

BMP signaling at the plasma membrane is mediated by a subset of transmembrane serine/threonine kinase receptors (1, 2). However, a certain redundancy in the ligand binding of type I receptors has been reported (7, 43). Three structurally related type I receptors, BMPR-IA and BMPR-IB (7) and ActR-IA, and one type II receptor, BMPR-II (44), have been identified as the specific receptors for BMPs. We observed all these receptors to be expressed in cardiomyocytes. Presumably, BMP-2 binds to BMPR-II in cardiac myocytes, after which BMPR-IA, BMPR-IB, or ActR-I is recruited to the BMP-2·BMPR-II complex. We demonstrated, in terms of intracellular signaling pathways, the activation of Smad1 and p38 MAPK, but not of ERK1/2 or JNK, by stimulation with BMP-2. In support of our data, Zhang *et al.* (45) reported the selective activation of p38 MAPK (but not JNK and ERK1/2) in myocardia from cardiac-specific activated TAK-1 transgenic mice, whereas treatment with BMP-2 was shown to activate TAK-1 in other cell systems, accompanied by both p38 MAPK and JNK (6–9).

BMP-2, a pleiotropic cytokine involved in regulating growth and differentiation, can exert both pro-apoptotic and anti-apoptotic effects (11–13). BMP-induced apoptosis has been reported *in vivo*, *e.g.* in rhombomeres 3 and 5 (46) and in the interdigit field of the limb (11, 47) in the developing chick. On the other hand, BMPs have been found to be involved in a sequence of interactions that influence neuronal survival (48, 49). The regulation of apoptosis by BMPs is complex, being influenced by the degree of differentiation and intrinsic susceptibility of target cells as well as by localized cellular interactions.

In this report, we provide the first evidence that BMP-2 can promote survival without hypertrophy of cardiac myocytes. There is a growing list of stimuli that induce hypertrophic growth of cardiac myocytes, including α_1-adrenergic agents, mechanical stretch, thyroid hormone, fibroblast growth factors, heparin-binding epidermal growth factor-like growth factor, endothelin, insulin-like growth factor-1, neuregulin, LIF, cardiotrophin-1, angiotensin II, and interleukin-1β (18–22, 50–54). Among these, angiotensin II (55) and interleukin-1β (56) have been reported to be hypertrophic and pro-apoptotic stimuli, whereas insulin-like growth factor-1, neuregulin, LIF, and cardiotrophin-1 are hypertrophic and anti-apoptotic factors. Although cardioprotective factors can be considered clinically suitable for treating subjects with heart failure (57), the hypertrophic effect accompanying the cardioprotective function of these factors may promote structural and geometric changes in the left ventricle that are commonly referred to as remodeling. Progressive, adverse remodeling of the myocardium may lead to ventricular dilatation and congestive heart failure. Compared with other survival factors, BMP-2 did not strongly promote hypertrophic growth of neonatal cardiac myocytes, suggesting that BMP-2 may be a good candidate for clinical application.

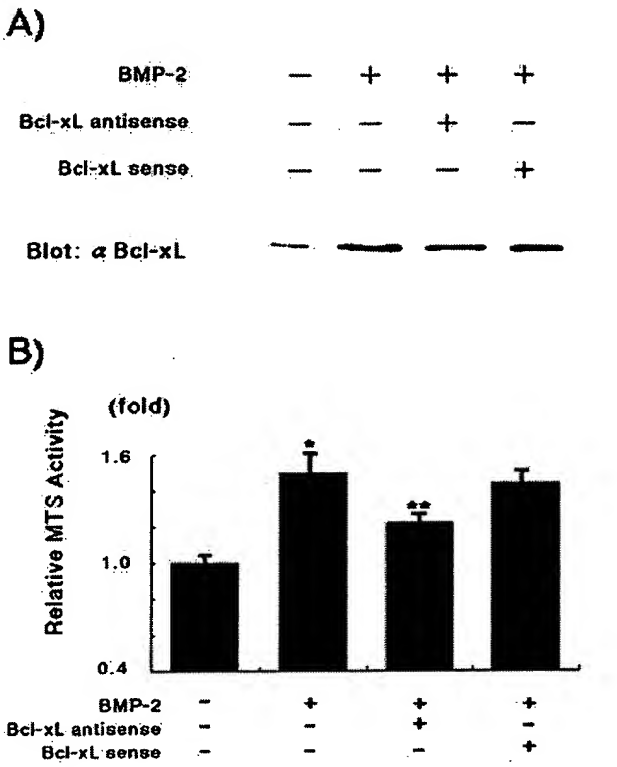

FIG. 7. **Antisense oligonucleotides to *bcl-x_L* attenuate the anti-apoptotic effect of BMP-2.** *A*, neonatal rat cardiac myocytes were treated with BMP-2 (80 ng/ml) in the presence of antisense or sense oligonucleotides (5 μM) for 24 h. Cells were directly lysed with SDS-polyacrylamide gel electrophoresis solution. The cell lysates were Western-blotted with anti-Bcl-x_L antibody (*αBcl-xL*). Experiments were performed three times with similar results. Representative data are shown. *B*, cardiac myocytes were treated with BMP-2 (80 ng/ml) in the presence of antisense or sense oligonucleotides (5 μM) for 48 h. The viability of cardiac myocytes was determined by an MTS cell respiration assay, and the data are expressed as relative absorbance normalized to the mean absorbance of untreated control cells. Each *bar* represents the mean ± S.D. (n = three experiments). *, $p < 0.01$ *versus* control; **, $p < 0.01$ *versus* BMP-2 with sense *bcl-x_L*.

With respect to the mechanisms that relate to the anti-apoptotic effect of BMP-2, we focused on Bcl-x_L expression in cardiomyocytes since Bcl-x_L has a critical role in anti-apoptosis, counteracting apoptotic signals in a variety of cells, including cardiomyocytes (58). We have provided direct evidence of BMP-2-promoted cardiac muscle survival through the induction of Bcl-x_L. Antisense oligonucleotides against *bcl-x_L* mRNA reduced the BMP-2-mediated cytoprotection with a corresponding reduction in the Bcl-x_L protein levels. These observations indicate that the induction of the *bcl-x_L* gene in cardiac myocytes might be a key molecular event for BMP-2-induced myocardial protection.

We next used an adenovirus-based vector system that allows for highly efficient DNA transfection in many cell types to investigate the molecular mechanisms by which *bcl-x_L* gene expression is regulated following BMP-2 stimulation in cardiac myocytes. The efficiency of expression examined with the *lacZ* gene in cardiac myocytes infected by adenovirus was found to exceed 90% (data not shown). To assess whether Smad1 alone is sufficient to induce cardiac myocyte protection, the Smad1-expressing adenovirus was used. Smad1 was found to promote

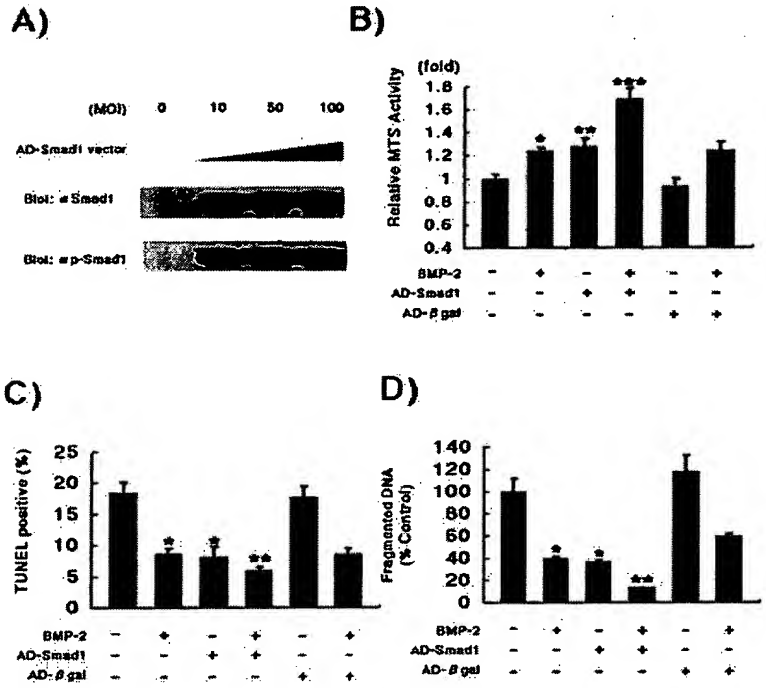

FIG. 8. **Smad1 in an adenoviral vector promotes survival and diminishes apoptotic cell death in neonatal rat cardiac myocyte primary cultures.** *A*, neonatal rat cardiac myocytes were transfected with Ad-Smad1 at the indicated multiplicity of infection (*MOI*) and incubated for 12 h. Cell lysates (20 μg of proteins) were subjected to immunoblotting with anti-Smad1 (*αSmad1*) and anti-phospho-Smad1 (*αp-Smad1*) antibodies. *B*, cardiac myocytes were transfected with Ad-Smad1. Next, the myocytes were incubated with or without BMP-2 (80 ng/ml) for 48 h. Ad-β-gal was used as a negative control. The viability of cardiac myocytes was determined with the MTS cell respiration assay, and the data are expressed as relative absorbance normalized to the mean absorbance of untreated control cells. Each *bar* represents the mean ± S.D. (n = three experiments). *, $p < 0.01$ *versus* control; **, $p < 0.05$ *versus* control; ***, $p < 0.05$ *versus* Ad-Smad1 or BMP-2. *C*, cardiac myocytes were transfected with Ad-Smad1 with or without BMP-2 (80 ng/ml) for 48 h. Shown are the results from the quantitative analysis of the percentage of cells undergoing apoptosis as measured by the TUNEL technique. Each *bar* represents the mean ± S.D. (n = six experiments). *, $p < 0.001$ *versus* control; **, $p < 0.01$ *versus* BMP-2. *D*, to quantify apoptosis, commercially available ELISA was used to detect histone-associated DNA fragments. The data are expressed as a percentage of the fragments seen in untreated control cells. Each *bar* represents the mean ± S.D. (n = three experiments). *, $p < 0.05$ *versus* control, **, $p < 0.01$ *versus* BMP-2.

FIG. 9. **Smad1 induces *bcl-x_L* in neonatal rat cardiac myocyte primary cultures.** *A*, neonatal rat cardiac myocytes were transfected with Ad-Smad1 (*Smad1 (adeno)*) or Ad-β-gal (*β-gal (adeno)*). Next, the myocytes were cultured without serum for another 24 h. *bcl-x_L* mRNA expression was examined by Northern blot analysis. *B*, densitometry was used to assess the relative intensity of the band for *bcl-x_L* mRNA as a ratio in comparison with the intensity of the band for 28 S rRNA. The data are expressed as relative intensity. Values represent the means ± S.D. (n = three experiments). *, $p < 0.01$ *versus* control. *C*, cardiac myocytes were transfected with Ad-Smad1 or Ad-β-gal with BMP-2 (80 ng/ml). Next, the myocytes were cultured without serum for another 24 h. The cell lysates were Western-blotted with anti-Bcl-x_L antibody. *D*, densitometry was used to assess the relative intensity of the band for Bcl-x_L as a ratio in comparison with the intensity of the band for α-tubulin. The data are expressed as relative intensity. Values are the means ± S.D. (n = three experiments). *, $p < 0.01$ *versus* control.

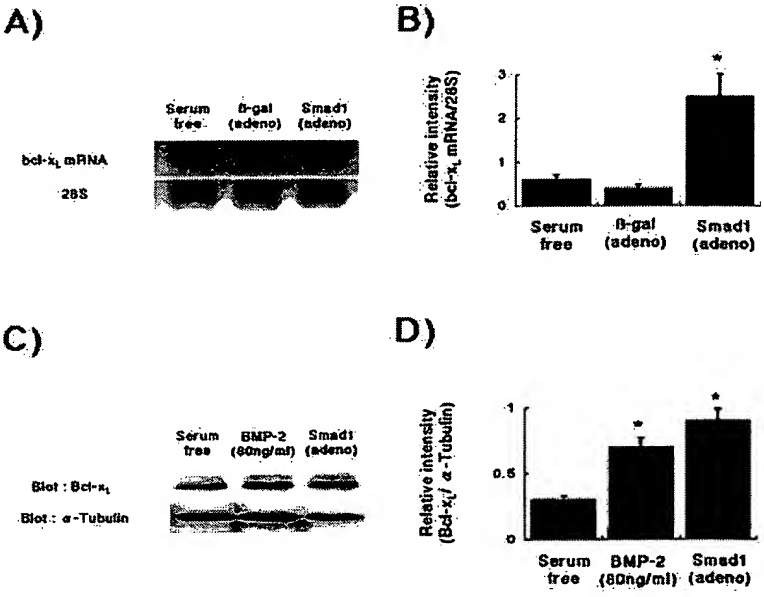

survival, which was enhanced by the presence of BMP-2. This may have been because Smad1 efficiently translocated into the nucleus upon ligand stimulation. Our findings thus suggest that Smad1 is a major signaling molecule for cardiac survival via BMP pathways.

Smad6 has been shown to inhibit the effects of pathway-

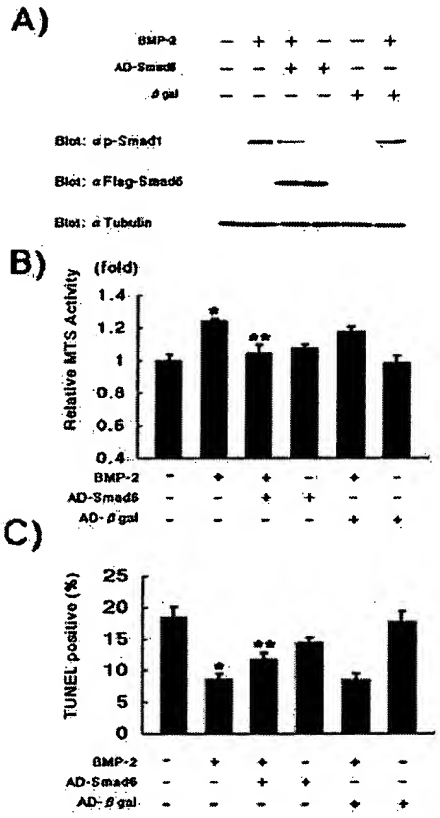

FIG. 10. **Smad6 in the adenoviral vector inhibits the anti-apoptotic effect and induction of *bcl-x_L* by BMP-2 and Smad1.** *A*, cardiac myocytes were transfected with adenoviral vectors expressing FLAG-tagged Smad6 or β-galactosidase (*β-gal*). Next, the myocytes were stimulated with BMP-2 (80 ng/ml) for 30 min. Cell lysates (20 μg of proteins) were subjected to immunoblotting with anti-phospho-Smad1 (*αp-Smad1*), anti-FLAG-tagged Smad6 (*αFlag-Smad6*), and anti-α-tubulin (*αTubulin*) antibodies. Experiments were performed three times with similar results. *B*, the viability of cardiac myocytes was determined by the MTS cell respiration assay, and the data are expressed as relative absorbance normalized to the mean absorbance of untreated control cells. Each *bar* represents the mean ± S.D. (n = three experiments). *, $p < 0.01$ *versus* control; **, $p < 0.05$ *versus* BMP-2. *C*, cardiac myocytes were transfected with Ad-Smad6 or Ad-β-gal. Next, the myocytes were incubated with or without BMP-2 (80 ng/ml) for 48 h. Shown are the results from the quantitative analysis of the percentage of cells undergoing apoptosis as measured by the TUNEL technique. Each *bar* represents the mean ± S.D. (n = six experiments). *, $p < 0.01$ *versus* control; **, $p < 0.01$ *versus* BMP-2.

restricted Smad proteins by competing for binding to activated type I receptors. It was also shown that Smad6 inhibits the activity of Smad1 by competing for complex formation with Smad4 (37). In the present report, we showed that the BMP-2-promoted survival effect was completely blocked in myocytes expressing Smad6. These findings again indicate that the Smad pathway is essential for the induction of cardiac protection.

However, it is still possible that the MAPK pathway may be related to BMP-2-induced anti-apoptosis because we have not examined whether the activation of p38 MAPK by BMP-2 can activate anti-apoptotic mechanisms in cardiac myocyte cells. Although Smad6 was recently reported to function as a negative regulator of the TAK-1 pathway in BMP-2 signaling, in addition to the previously reported Smad pathways (59), we found that Smad6 did not reduce BMP-2-induced p38 MAPK activation in cardiac myocytes (data not shown). Moriguchi *et al.* (7) have shown the existence of a kinase cascade consisting of TAK-1/MKK6/p38 MAPK downstream of BMP. Other reports have shown that treatment of cells with ceramide (8), interleukin-1β (60), and transforming growth factor-β (6) results in activation of the TAK-1/JNK cascade. JNK and p38 MAPK, collectively known as stress-activated protein kinases, are involved in pro-apoptosis, probably by inducing expression of a Fas ligand (61). On the basis of these findings, we conclude that BMP-2-induced anti-apoptosis is most likely mediated by the Smad signaling cascade. So far, intracellular signaling pathways leading to anti-apoptotic effects of cardiotrophic factors such as insulin-like growth factor-1, cardiotrophin-1, LIF, and neuregulin have been reported to involve ERK, phosphatidylinositol 3-kinase/Akt, and Stat activation (20, 22, 62). In this study, we have demonstrated Smad1/Bcl-x_L as a novel pathway for survival of cardiac myocytes. Whether the BMP-2/Smad1 pathway is essential for cardiac protection under stress conditions *in vivo* cannot be answered on the basis of our data alone. Cardiac-specific gene overexpression and deletion may be more informative.

In conclusion, we have provided the first evidence that BMP-2 can attenuate serum withdrawal-induced apoptosis in cardiac myocytes. The up-regulation of Bcl-x_L via the Smad1 pathway might be responsible for this protective effect. Our findings support the concept that the BMP-2/Smad1 signaling system plays an important role in regulation of the myocardium and suggest that BMP-2 could be a new therapeutic agent for cardiac heart failure.

Acknowledgment—We are grateful to J. Hironaka for technical support.

REFERENCES

1. Massague, J., and Weis-Garcia, F. (1996) *Cancer Surv.* **27**, 41–64
2. ten Dijke, P., Miyazono, K., and Heldin, C. H. (1996) *Curr. Opin. Cell Biol.* **8**, 139–145
3. Heldin, C. H., Miyazono, K., and ten Dijke, P. (1997) *Nature* **390**, 465–471
4. Derynck, R., Zhang, Y., and Feng, X. H. (1998) *Cell* **95**, 737–740
5. Massague, J. (1998) *Annu. Rev. Biochem.* **67**, 753–791
6. Yamaguchi, K., Shirakabe, K., Shibuya, H., Irie, K., Oishi, I., Ueno, N., Taniguchi, T., Nishida, E., and Matsumoto, K. (1995) *Science* **270**, 2008–2011
7. Moriguchi, T., Kuroyanagi, N., Yamaguchi, K., Gotoh, Y., Irie, K., Kano, T., Shirakabe, K., Muro, Y., Shibuya, H., Matsumoto, K., Nishida, E., and Hagiwara, M. (1996) *J. Biol. Chem.* **271**, 13675–13679
8. Shirakabe, K., Yamaguchi, K., Shibuya, H., Irie, K., Matsuda, S., Moriguchi, T., Gotoh, Y., Matsumoto, K., and Nishida, E. (1997) *J. Biol. Chem.* **272**, 8141–8144
9. Yao, Z., Zhou, G., Wang, X. S., Brown, A., Diener, K., Gan, H., and Tan, T. H. (1999) *J. Biol. Chem.* **274**, 2118–2125
10. Wozney, J. M., Rosen, V., Celeste, A. J., Mitsock, L. M., Whitters, M. J., Kriz, R. W., Hewick, R. M., and Wang, E. A. (1988) *Science* **242**, 1528–1534
11. Hogan, B. L. (1996) *Genes Dev.* **10**, 1580–1594
12. Rosen, V., and Thies, R. S. (1992) *Trends Genet.* **8**, 97–102
13. Reddi, A. H. (1994) *Curr. Opin. Genet. Dev.* **4**, 737–744
14. Yokouchi, Y., Sakiyama, J., Kameda, T., Iba, H., Suzuki, A., Ueno, N., and Kuroiwa, A. (1996) *Development* **122**, 3725–3734
15. Iwasaki, S., Iguchi, M., Watanabe, K., Hoshino, R., Tsujimoto, M., and Kohno, M. (1999) *J. Biol. Chem.* **274**, 26503–26510
16. Bhatia, M., Bonnet, D., Wu, D., Murdoch, B., Wrana, J., Gallacher, L., and Dick, J. E. (1999) *J. Exp. Med.* **189**, 1139–1148
17. Haunstetter, A., and Izumo, S. (1998) *Circ. Res.* **82**, 1111–1129
18. Buerke, M., Murohara, T., Skurk, C., Nuss, C., Tomaselli, K., and Lefer, A. M. (1995) *Proc. Natl. Acad. Sci. U. S. A.* **92**, 8031–8035
19. Li, Q., Li, B., Wang, X., Leri, A., Jana, K. P., Liu, Y., Kajstura, J., Baserga, R., and Anversa, P. (1997) *J. Clin. Invest.* **100**, 1991–1999
20. Fujio, Y., Kunisada, K., Hirota, H., Yamauchi-Takihara, K., and Kishimoto, T. (1997) *J. Clin. Invest.* **99**, 2898–2905
21. Zhao, Y. Y., Sawyer, D. R., Ragavendra, R., Baliga, R., Opel, D. J., Han, X., Marchionni, M. A., and Kelly, R. A. (1998) *J. Biol. Chem.* **273**, 10261–10269
22. Sheng, Z., Knowlton, K., Chen, J., Hoshijima, M., Brown, J. H., and Chien, K. R. (1997) *J. Biol. Chem.* **272**, 5783–5791
23. Zannad, F., Alla, F., Dousset B., Peres A., and Pitt B. (2000) *Circulation* **102**, 2700–2706
24. Kunisada, K., Hirota, H., Fujio, Y., Matsui, H., Tani, Y., Yamauchi-Takihara, K., and Kishimoto, T. (1996) *Circulation* **94**, 2626–2632
25. Chomczynski, P., and Sacchi, N. (1987) *Anal. Biochem.* **162**, 156–159
26. Roelen, B. A., Goumans, M. J., van Rooijen, M. A., and Mummery, C. L. (1997) *Int. J. Dev. Biol.* **41**, 541–549
27. Iantosca, M. R., McPherson, C. E., Ho, S. Y., and Maxwell, G. D. (1999) *J. Neurosci. Res.* **56**, 248–258

28. Kunisada, K., Negoro, S., Tone, E., Funamoto, M., Osugi, T., Yamada, S., Okabe, M., Kishimoto, T., and Yamauchi-Takihara, K. (2000) *Proc. Natl. Acad. Sci. U. S. A.* **97,** 315–319
29. Boise, L. H., Gonzalez-Garcia, M., Postema, C. E., Ding, L., Lindsten, T., Turka, L. A., Mao, X., Nunez, G., and Thompson, C. B. (1993) *Cell* **74,** 597–608
30. Berridge, M. V., and Tan, A. S. (1993) *Arch. Biochem. Biophys.* **303,** 474–482
31. Cory, A. H., Owen, T. C., Barltrop, J. A., and Cory, J. G. (1991) *Cancer Commun.* **3,** 207–212
32. Negoro, S., Oh, H., Tone, E., Kunisada, K., Fujio, Y., Kenneth, W., Kishimoto, T., and Yamauchi-Takihara, K. (2001) *Circulation* **103,** 555–561
33. Thome, M., Schneider, P., Hofmann, K., Fickenscher, H., Meinl, E., Neipel, F., Mattmann, C., Burns, K., Bodmer, J. L., Schroter, M., Scaffidi, C., Krammer, P. H., Peter, M. E., and Tschopp, J. (1997) *Nature* **386,** 517–521
34. Wang, Z., Karras, J. G., Howard, R. G., and Rothstein, T. L. (1995) *J. Immunol.* **155,** 3722–3725
35. Shiraiwa, N., Inohara, N., Okada, S., Yuzaki, M., Shoji, S., and Ohta, S. (1996) *J. Biol. Chem.* **271,** 13258–13265
36. Ackermann, E. J., Taylor, J. K., Narayana, R., and Bennett, C. F. (1999) *J. Biol. Chem.* **274,** 11245–11252
37. Fujii, M., Takeda, K., Imamura, T., Aoki, H., Sampath, T. K., Enomoto, S., Kawabata, M., Kato, M., Ichijo, H., and Miyazono, K. (1999) *Mol. Biol. Cell* **10,** 3801–3813
38. Becker, T. C., Noel, R. J., Coats, W. S., Gomez-Foix, A. M., Alam, T., Gerard, R. D., and Newgard, C. B. (1994) *Methods Cell Biol.* **43,** 161–189
39. Shubeita, H. E., McDonough, P. M., Harris, A. N., Knowlton, K. U., Glembotski, C. C., Brown, J. H., and Chien, K. R. (1990) *J. Biol. Chem.* **265,** 20555–20562
40. Ito, H., Hirata, Y., Hiroe, M., Tsujino, M., Adachi, S., Takamoto, T., Nitta, M., Taniguchi, K., and Marumo, F. (1991) *Circ. Res.* **69,** 209–215
41. Iwaki, K., Sukhatme, V. P., Shubeita, H. E., and Chien, K. R. (1990) *J. Biol. Chem.* **265,** 13809–13817
42. Izumo, S., Nadal-Ginard, B., and Mahdavi, V. (1988) *Proc. Natl. Acad. Sci. U. S. A.* **85,** 339–343
43. Rosenzweig, B. L., Imamura, T., Okadome, T., Cox, G. N., Yamashita, H., ten Dijke, P., Heldin, C. H., and Miyazono, K. (1995) *Proc. Natl. Acad. Sci. U. S. A.* **92,** 7632–7636
44. Nohno, T., Ishikawa, T., Saito, T., Hosokawa, K., Noji, S., Wolsing, D. H., and Rosenbaum, J. S. (1995) *J. Biol. Chem.* **270,** 22522–22526
45. Zhang, D., Gaussin, V., Taffet, G. E., Belaguli, N. S., Yamada, M., Schwartz, R. J., Michael, L. H., Overbeek, P. A., and Schneider, M. D. (2000) *Nat. Med.* **6,** 556–563
46. Graham, A., Francis-West, P., Brickell, P., and Lumsden, A. (1994) *Nature* **372,** 684–686
47. Zou, H., and Niswander, L. (1996) *Science* **272,** 738–741
48. Mehler, M. F., Mabie, P. C., Zhang, D., and Kessler, J. A. (1997) *Trends Neurosci.* **20,** 309–317
49. Varley, J. E., and Maxwell, G. D. (1996) *Exp. Neurol.* **140,** 84–94
50. Rokosh, D. G., Stewart, A. F., Chang, K. C., Bailey, B. A., Karliner, J. S., Camacho, S. A., Long, C. S., and Simpson, P. C. (1996) *J. Biol. Chem.* **271,** 5839–5843
51. Ramirez, M. T., Sah, V. P., Zhao, X. L., Hunter, J. J., Chien, K. R., and Brown, J. H. (1997) *J. Biol. Chem.* **272,** 14057–14061
52. Kaye, D., Pimental, D., Prasad, S., Maki, T., Berger, H. J., McNeil, P. L., Smith, T. W., and Kelly, R. A. (1996) *J. Clin. Invest.* **97,** 281–291
53. Bogoyevitch, M. A., Glennon, P. E., Andersson, M. B., Clerk, A., Lazou, A., Marshall, C. J., Parker, P. J., and Sugden, P. H. (1994) *J. Biol. Chem.* **269,** 1110–1119
54. Sadoshima, J., and Izumo, S. (1993) *EMBO J.* **12,** 1681–1689
55. Kajstura, J., Cigola, E., Malhotra, A., Li, P., Cheng, W., Meggs, L. G., and Anversa, P. (1997) *J. Mol. Cell. Cardiol.* **29,** 859–870
56. Singh, K., Balligand, J. L., Fischer, T. A., Smith, T. W., and Kelly, R. A. (1996) *J. Biol. Chem.* **271,** 1111–1117
57. Hirota, H., Chen, J., Betz, U. A. K., Rajewsky, K., Gu, Y., Ross, J. J., Muller, W., and Chien, K. R. (1999) *Cell* **97,** 189–198
58. Imamura, T., Takase, M., Nishihara, A., Oeda, E., Hanai, J., Kawabata, M., and Miyazono, K. (1997) *Nature* **389,** 622–626
59. Kimura, N., Matsuo, R., Shibuya, H., Nakashima, K., and Taga, T. (2000) *J. Biol. Chem.* **275,** 17647–17652
60. Ninomiya-Tsuji, J., Kishimoto, K., Hiyama, A., Inoue, J., Cao, Z., and Matsumoto, K. (1999) *Nature* **398,** 252–256
61. Le-Niculescu, H., Bonfoco, E., Kasuya, Y., Claret, F. X., Green, D. R., and Karin, M. (1999) *Mol. Cell. Biol.* **19,** 751–763
62. Oh, H., Fujio, Y., Kunisada, K., Hirota, H., Matui, H., Kishimoto, T., and Yamauchi-Takihara, K. (1998) *J. Biol. Chem.* **273,** 9703–9710

THE JOURNAL OF BONE & JOINT SURGERY · JBJS.ORG | VOLUME 83-A · SUPPLEMENT 1, PART 1 · 2001

BONE MORPHOGENETIC PROTEIN-7 MODULATES GENES THAT MAINTAIN THE VASCULAR SMOOTH MUSCLE CELL PHENOTYPE IN CULTURE

BY HAIMANTI DORAI, PHD, AND T. KUBER SAMPATH, PHD

Investigation performed at Creative BioMolecules Inc., Hopkinton, Massachusetts

Background: The vasculature is an important component in the musculoskeletal system, and vascularization is a key event in the development of normal cartilage and bone formation. Blood vessels deliver nutrients, oxygen, and precursor cells to maintain the structural and functional integrity of joints and soft and hard tissues. Therefore, agents that help to inhibit proliferation and retain the phenotype of vascular smooth muscle cells (SMCs) are of critical importance. In this study, we examined the capacity of bone morphogenetic protein-7 (BMP-7) to inhibit the proliferation of SMCs and maintain their phenotype.

Methods: A thymidine-incorporation assay was used to monitor the proliferative activity of SMCs on stimulation with platelet-derived growth factor (PDGF) and transforming growth factor-beta (TGF-β), agents known to be stimulatory for these cells. Reverse transcriptase-polymerase chain reaction (RT-PCR), Northern blot analysis, and enzyme-linked immunosorbent assay (ELISA) were used to monitor the modulation of various genes and gene products. Immunolocalization of SMC specific markers was also performed.

Results: BMP-7 inhibited both serum-stimulated and growth factor-induced (PDGF-BB and TGF-β1) SMC growth, as measured by ^{3}H-thymidine uptake and cell number, in primary human aortic smooth muscle (HASM) cell cultures. The addition of BMP-7 stimulated the expression of developmentally regulated as well as SMC-specific markers, namely, Id-1 and Id-2, α-actin, and SMC-specific heavy-chain myosin, as examined by semiquantitative and quantitative RT-PCR and by Northern blot analysis. Additionally, BMP-7 exhibited anti-inflammatory activity by downregulating intercellular adhesion molecule-1 (ICAM-1) expression. The collagen type III/I ratio that becomes lower with the transdifferentiation of SMCs into myofibroblasts is maintained in BMP-7-treated cultures compared with untreated controls. Studies on the mechanism of action indicate that BMP-7 treatment induces cyclin-dependent kinase-2 inhibitor, p21, which was inhibited during PDGF-BB-induced proliferation of SMCs. Finally, BMP-7 upregulates the expression of the inhibitory Smads, Smad6 and Smad7, which are known to inhibit TGF-β superfamily signaling.

Conclusions: These results suggest that BMP-7 maintains the expression of the vascular SMC phenotype. Thus, BMP-7 may prevent vascular proliferative disorders and potentially could act as a palliative agent following damage to the vasculature.

Clinical Relevance: In musculoskeletal disorders in which the vasculature plays an important role, BMP-7 may be of benefit as an anti-inflammatory and anti-proliferative agent for vascular endothelium and help maintain vascular integrity.

Vascular trauma due to metabolic, mechanical, or immunological insult is characterized by changes in the vascular endothelium, including migration and proliferation of smooth muscle cells (SMCs), loss of expression of SMC phenotype, enhanced extracellular-matrix synthesis, and cell death due to apoptosis and necrosis. These cellular changes gradually result in intimal thickening of the blood vessel and loss of elasticity in the vasculature[1]. Vasculature also plays an important role in endochondral ossification[2], and vascularization is a key event in the development of normal cartilage and bone.

A number of local and systemic factors participate in the maintenance of vascular integrity[3,4]. Platelet-derived growth factor (PDGF), basic fibroblast growth factor (bFGF), and insulin-like growth factor-1 (IGF-1) are known to exert strong growth-promoting activity on SMCs *in vitro*[5] and play critical roles in the migration and proliferation of SMCs *in vivo*[6,7]. Notably, these growth factors are detected at high concentrations within vascular proliferative lesions[8]. Conversely, systemic factors such as gamma-interferon and progesterone have been shown to exhibit growth-inhibitory activity on SMCs[9,10]. TGF-β, a bifunctional growth-regulatory molecule

for vascular SMCs, stimulates or inhibits cell growth, depending on the cell culture conditions, the presence of other growth-regulatory molecules, and the dose and frequency with which they are employed[11]. It has been shown that the injury site has high concentrations of TGF-β, which subsequently cause an enhanced extracellular-matrix production leading to intimal thickening in blood vessels. Thus, the regulation of SMC proliferation and expression of SMC phenotype is a dynamic process, tightly governed by local and systemic factors to maintain the vascular integrity and continuous blood flow *in vivo*.

Bone morphogenetic proteins (BMPs), also called osteogenic proteins (OPs), are members of the TGF-β superfamily, originally identified by their ability to induce endochondral bone formation at an extraskeletal site[12,13]. They have been shown to regulate the migration, proliferation, and differentiation of pluripotent progenitor cells involved in the development of organ systems during embryogenesis and in adult tissue repair[14]. We have shown that systemic administration of recombinant human BMP-7 is capable of protecting heart[15], brain[16,17], and in particular kidney function following ischemia-reperfusion injury in rat models[18]. The tissue protective function of BMP-7 may be complex; however, we demonstrated that BMP-7 maintains the expression of vascular smooth muscle phenotype in peritubular capillaries after ischemic acute renal failure (ARF) in the rat[18]. In addition, administration of BMP-7 in norepinephrine-induced ARF in rats has been shown to improve renal function by increasing the glomeruli filtration rate, renal blood flow, and urine flow rate[19].

In this study, we show that BMP-7 inhibits proliferation and stimulates the expression of the SMC phenotype when it is added to human aorta-derived SMCs in culture. This BMP-7-induced growth-inhibitory effect was also observed when the SMC proliferation was stimulated by PDGF-BB and TGF-β, suggesting that in addition to its role in the prevention of ischemic injury, BMP-7 may be a cytoprotective agent for vascular proliferative disorders.

Materials and Methods

Cell Culture

Human primary aortic smooth muscle cells (HASM) were purchased from Clonetics (San Diego, California). They were grown in growth medium provided by the same company. Cells from passages 4-9 were used for all experiments.

^{3}H-Thymidine Incorporation

HASM cells were plated into 24-well plates at a concentration of 4×10^4 cells/well such that they were 60-70% confluent the next day. At this time, they were rendered quiescent by changing the medium to Dulbecco's modified Eagle medium (DMEM) (Gibco BRL, Gaithersburg, Maryland) containing 0.1% serum for 60-72 hours. The medium was then replaced with DMEM containing 1% serum with or without various concentrations of a homogenous preparation of recombinant human mature BMP-7[20], PDGF-BB, or TGF-β (Upstate Biologicals, Syracuse, New York) for 24 hours. During the last 3 hours of culture, cells were labeled with [methyl-^{3}H]-thymidine (Dupont/NEN, Boston, Massachusetts) at 1 μCi/ml/well in thymidine-free medium. At the end of the incubation period, the cells were fixed in 75% methanol/25% acetic acid (v/v) for at least 2 hours, followed by several washes with 80% methanol. Incorporated ^{3}H-thymidine was measured in a liquid scintillation counter. All experiments were performed multiple times employing cells from different passages (passages 4-9). The data presented are representative of one such experiment.

Cell Counting

HASM cells were plated into a 24-well plate at a concentration of 8×10^3 cells/well. After 24 hours, various concentrations of BMP-7, PDGF-BB, or TGF-β1 were added and the cells were incubated for a total of 72 hours. The total cell number was determined at 0, 24, 48, and 72 hours with use of a hemocytometer and trypan blue staining for viable cells. Cells from four wells were combined for an average reading.

Long-Term Cultures of HASM Cells

Eight 100-mm dishes were plated with HASM cells at a concentration of 1.2×10^6 cells/dish. After 24 hours, 100 ng/ml BMP-7 was added to four plates and an equal amount of vehicle was added to the other four. The day that the cultures reached confluence was noted and marked as day 0. The medium was changed that day and every other day thereafter, and fresh BMP-7 was added. Beginning day 3 and every other day thereafter, one plate from each group was harvested and total RNA was isolated. Thus, total RNA was made from BMP-7-treated and untreated cultures on day 3, 5, 7, and 9, respectively.

Total RNA Preparation and Semiquantitative Reverse Transcriptase-Polymerase Chain Reaction (RT-PCR) Analysis

Total RNA from HASM cells was isolated with TRIzol as indicated (Gibco BRL). Contaminating genomic DNA was removed with RNAase-free DNAase following the manufacturer's protocol. Complementary DNA was synthesized with Superscript reverse transcriptase (Gibco BRL) as described in the same protocol. Four micrograms of DNAase-treated RNA was incubated with 2 μl oligo dT at 70°C for 10 minutes. Next, 14 μl of 5× buffer, 7 μl DTT (0.1 *M*), 3.5 μl of each nucleotide (10 m*M*), 1.5 μl RNAase inhibitor, and 2 μl Superscript reverse transcriptase (Gibco BRL) were added to each reaction. The samples were incubated for 10 minutes at room temperature, 50 minutes at 42°C, 10 minutes at 50°C, and 5 minutes at 90°C. RNAase-H (1 μl) (Gibco BRL) was added to the reactions, and samples were incubated for 20 minutes at 37°C. PCR was performed as indicated by the manufacturer (Perkin-Elmer, Norwalk, Connecticut) with the following primers: α-actin sense 5'GCT CAC GGA GGC ACC CCT GAA, antisense 5'CTG ATA GGA CAT TGT TAG CAT; glyceraldehyde-3-phosphate (GAPDH) sense 5'ACC ACA GTC CAT GCC ATC AC, antisense 5'TCC ACC ACC CTG TTG CTG TA; collagen III sense 5'GGT GTG GAC GTT GGC CCT GTT TGC, antisense 5'CTA AGT AAC CGT ACG GTG TCC C; collagen I

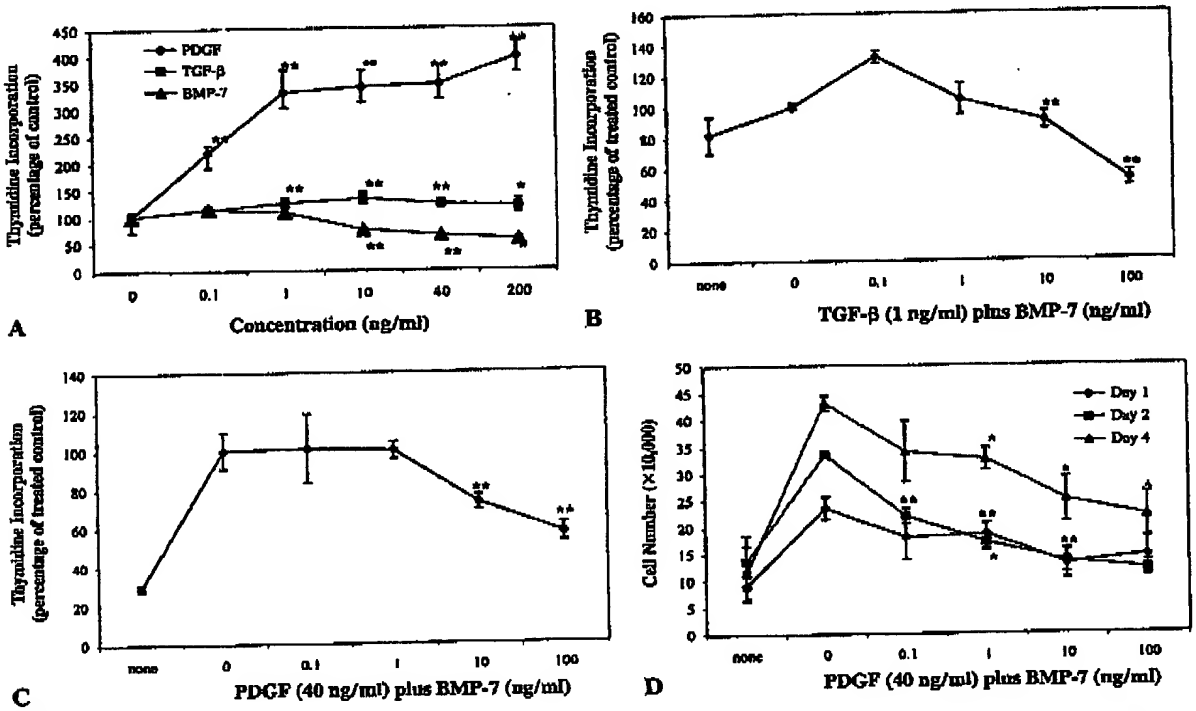

Fig. 1

Effect of bone morphogenetic protein-7 (BMP-7), transforming growth factor-beta (TGF-β), and platelet-derived growth factor-BB (PDGF-BB) on human aortic smooth muscle cell proliferation. First, 4 x 10^4 cells were serum-starved for 48 hours. They were then induced to proliferate in medium containing 1% serum. At this time, various concentrations of BMP-7, TGF-β, or PDGF-BB (A) or various concentrations of BMP-7 plus 1 ng/ml TGF-β (B) or various concentrations of BMP-7 plus 40 ng/ml PDGF (C) were added. The cells were further incubated for 24 hours. They were pulsed during the last 4 hours with ^{3}H-thymidine at 1 μCi/ml. For cell-number studies, the PDGF-BB (40 ng/ml) and BMP-7 (100 ng/ml)-treated cultures were harvested at days 2, 3, and 4 and counted (D). The data are given as the mean and the standard deviation (in quadruplicates); values were normalized to counts per minute (cpm) incorporated by control cultures. *$p < 0.05$ and **$p < 0.01$ compared with 0 ng/ml growth factor. (Adapted, with permission of Wiley-Liss, a subsidiary of John Wiley and Sons, Inc., from Doral H, Vukicevic S, Sampath TK. Bone morphogenetic protein-7 [osteogenic protein-1] inhibits smooth muscle cell proliferation and stimulates the expression of markers that are characteristic of SMC phenotype in vitro. J Cell Physiol. 2000;184:37-45.)

sense 5′TGA CTT GAG ACT CAG CCA CCC A, antisense 5′AGG TTG CCA GTC TCC TCA TCC A; and intercellular adhesion molecule-1 (ICAM-1) sense 5′GGG AAT CCA GCC CCT AAT CTG A, ICAM-1 antisense 5′GAC TGT CCC AGC TTT CCC ATG T.

Reactions included 5 μl of 10× buffer, 3 μl of 25 m*M* $MgCl_2$, 1 μl of 10 m*M* dNTP, 1 μl of 20 μ*M* 3′ primer, 1 μl of 20 μ*M* 5′ primer, 0.5 μl Taq polymerase (Perkin-Elmer, Foster City, California), and 1 μl cDNA. Samples were incubated for 5 minutes at 94°C followed by 25–40 cycles of 45 seconds at 94°C, 45 seconds at 59°C, 1 minute at 72°C, and final extension at 72°C for 10 minutes in a Perkin-Elmer DNA Thermal Cycler. To compare the relative quantity of the RT-PCR reactions, the transcription level of GAPDH was used as a control. GAPDH gene expression was found to be similar at all time points examined, enabling analysis of the relative levels of gene expression for the desired genes. PCR primer sets were optimized with use of human placental and embryonic cDNA libraries purchased from Clonetech (Palo Alto, California). The PCR product was verified at least twice.

Quantitative RT-PCR Analysis

cDNA was generated by reverse-transcribing 1 μg of total RNA in a volume of 100 μl with use of a kit provided by Promega (Madison, Wisconsin). This cDNA (2 μl) was then used as a template for PCR reactions. Quantitative PCR was performed with use of a PE Biosystems 5700 SDS with SYBR Green core reagents (PE Biosytems, Foster City, California). Reactions were performed in triplicate and quantitated to that of β-actin, which remained unchanged by the addition of BMP-7. The primers used were β-actin sense 5′CTG GAA CGG TGA AGG TGA CA, antisense 5′CGG CCA CAT TGT GAA CTT TG; p21 sense 5′CCC GTT TCT CCA CCT AGA CTG T, antisense 5′TCA GCA TTG TGC GAG GAG CT; Smad6 sense 5′GCC ACT GGA TCT GTC CGA TT, antisense 5′CAC CCG GAG CAG TGA TGA G; Smad7 sense 5′CTG GGA GGG ACA TGC TTA GC, antisense 5′TCA GCC TAG GAT GGT ACC TTG G; α-actin sense 5′CCA GCA GAT GTG GAT CAG CA,

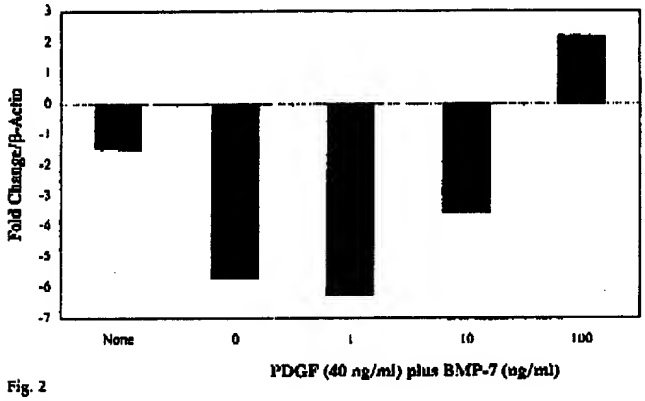

Fig. 2

Effect of bone morphogenetic protein-7 (BMP-7) on p21 expression in platelet-derived growth factor (PDGF)-treated human aortic smooth muscle cultures. First, 1 x 10^6 cells were serum-starved for 48 hours before the addition of various concentrations of BMP-7 and PDGF (40 ng/ml) in medium containing 1% serum. They were further incubated for 24 hours. Subsequently, the cDNA was isolated and subjected to quantitative reverse transcriptase-polymerase chain reaction with use of the human β-actin and p21 primers.

antisense 5′AAG CAT TTG CGG TGG ACA AT; Id-1 sense 5′AGA ACC GCA AGG TGA GCA A, antisense 5′TCC ACC TGA AGG TCC CTG ATG; Id-2 sense 5′CCA CCC TCA ACA CGG ATA TCA, antisense 5′ACA CAG TGC TTT GCT GTC ATT TG; Id-3 sense 5′GCG GCA GAG CTG GTC TTC, antisense 5′TCA GGG CAA CAG AAC CTT TCT C; basic calponin sense 5′AGG AGC TGA GAG AGT GGA TCG A, antisense 5′TCG CAA AGA ATG ATG CCA TCT; and H-chain myosin sense 5′TCA ACA TGC AGG CGC TCA, antisense 5′ CGT CTC ATA CTC GTG AAG CTG TCT.

Northern Blot Analysis

Five micrograms of total RNA was electrophoresed in a 1.2% formaldehyde-agarose gel and blotted onto nitrocellulose filters that were hybridized with randomly primed ^{32}P-labeled Smad6 cDNA probe as described[21]. The hybridized filters were washed in 30 m*M* NaCl, 3 m*M* sodium citrate, and 0.1% sodium dodecyl sulfate at 55°C and autoradiographed on Kodak XAR film at –80°C on phosphor screen. To correct for differences in RNA loading, the filters were washed at 80°C in 50% formamide solution and rehybridized with a radiolabeled GAPDH probe. The GAPDH probe was generated from RT-PCR product.

ICAM-1 Estimation by ELISA

HASM cells were plated at 5 × 10^4 cells/well in a 24-well plate, in growth medium containing 5% fetal bovine serum (FBS). The next day, the medium was replaced with medium containing 0.1% FBS. Then, 1 ng/ml of IL-1β (R&D Systems, Minneapolis, Minnesota) and various concentrations of BMP-7 were added as indicated. Three or five days later, the medium was removed and the cell layer was washed twice with phosphate buffered saline (PBS) and lysed in 0.5 ml PBS by three freeze-thaw cycles. Finally, 20-100 μl of cell lysates was analyzed for soluble human ICAM-1 with use of ELISA kits (R&D Systems). Recombinant human ICAM-1 and IL-6 were provided by the manufacturer and used as standards.

The results are indicated as units/mg of protein in cell lysates.

Results

SMCs Express BMP-7 Receptors

Prior to evaluating the direct effect of BMP-7 on vascular SMCs, we examined cultures of HASM cells for the presence of BMP-7 and its type-I and II receptors by RT-PCR. Although there was no detectable BMP-7, BMP type-I receptors ALK-3 (ActR-IA) and ALK-6 (BMPR-IB) were abundant. The presence of several type-I receptors for BMPs [ALK-2 (ActR-I), ALK-3 (BMPR-IA), and ALK-6 (BMPR-IB)] in vascular SMC also has been reported previously[22-24]. Although we were unable to detect BMP type-II receptors (BMPR-II), we found abundant activin type-IIB receptor (ActR-IIB), which has been shown to function as a type-II receptor for BMP-7[25]. Similarly, BMP-2 has been shown to bind to ActR-II and ActR-IIB in the presence of the appropriate type-I receptors[26].

BMP-7 Inhibits Serum and Growth Factor-Induced Proliferation of SMCs

We examined the effect of exogenously added BMP-7 on cell growth in HASM cell cultures by ^{3}H-thymidine incorporation into DNA. Prior to the addition of BMP-7, cells were synchronized by serum starvation for 60-72 hours and then induced to proliferate by providing the medium with 1% serum. Various concentrations of BMP-7 with or without PDGF-BB or TGF-β1 were added. BMP-7 exhibits a biphasic effect on the serum-induced proliferation of HASM cells in culture (Fig. 1-A). At very low concentrations (0.1-1.0 ng/ml), BMP-7 had a small but reproducible stimulatory effect (about 10%) on these cells, whereas at higher concentrations (10-200 ng/ml) it inhibited the serum-induced HASM cell proliferation in a dose-dependent manner. About 60% inhibition of proliferation was obtained within 24 hours by the addition of BMP-7 (200 ng/ml). Under identical experimental conditions, TGF-β1 (1 ng/ml) and PDGF-BB (40 ng/ml) stimulated the proliferation of HASM cells by 30% and 300%, respectively (Fig. 1-A). Interestingly, when BMP-7 was added in conjunction with these growth factors, the same biphasic pattern was observed as seen with BMP-7 alone (Figs. 1-B and 1-C). At very low concentrations (0.1-1 ng/ml), BMP-7 had either no effect or a small but reproducible stimulatory effect, whereas at higher concentrations (10-200 ng/ml), BMP-7 was able to inhibit the stimulatory activity of TGF-β1 and PDGF-BB in a dose-dependent manner. In accordance with reduced ^{3}H-thymidine incorporation into DNA, the cell number was also decreased when cells were treated with BMP-7 and PDGF as compared with PDGF alone (Fig. 1-D).

Several cell-cycle proteins, including cyclin-dependent kinase-2 (cdk-2) and cdk-2 kinase inhibitor, p21 (cip), mediate SMC proliferation[27-29], and BMP-7 inhibits the proliferative activity of PDGF in HASM cells. Therefore, we examined the

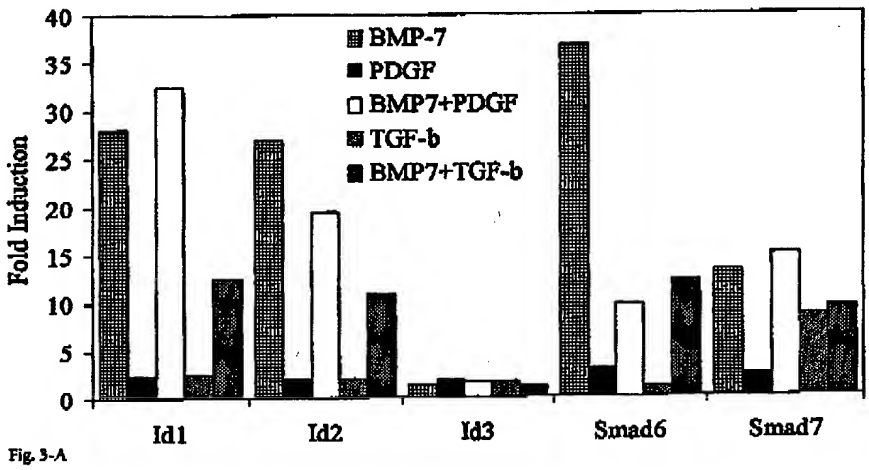

Fig. 3-A

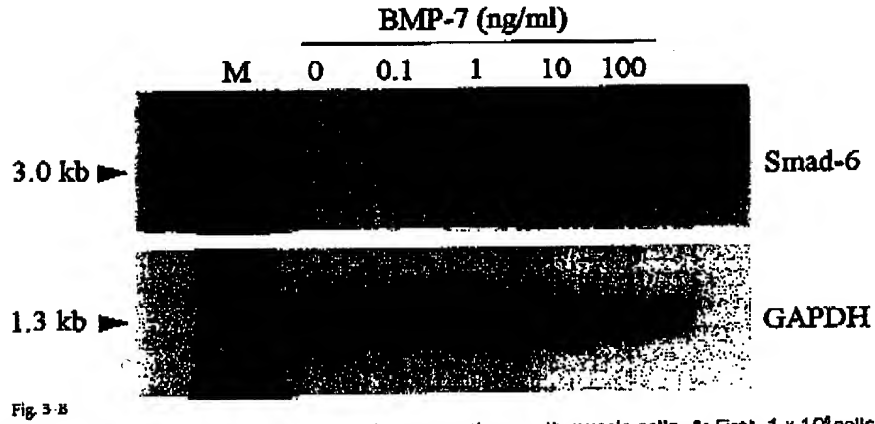

Fig. 3-B

Fig. 3 Genes induced by bone morphogenetic protein-7 (BMP-7) in human aortic smooth muscle cells. **A:** First, 1 x 10^6 cells were treated with BMP-7 (100 ng/ml) and/or transforming growth factor-beta (TGF-β) (1 ng/ml) and/or platelet-derived growth factor (PDGF) (40 ng/ml) for 24 hours. Subsequently, total RNA was made. Next, 1 µg of total RNA was used to prepare cDNA, which was then subjected to quantitative reverse transcriptase-polymerase chain reaction. **B:** First, 1 x 10^6 cells were treated with various concentrations of BMP-7 for 48 hours. Total RNA was then extracted, and 5 µg of each sample was subjected to a Northern blot analysis. The probe used was a HindIII-RI fragment of Smad6 cDNA[23].

effect of BMP-7 on these cell-cycle-modulated genes by quantitative RT-PCR. As shown in Figure 2, 40 ng PDGF-BB per ml dramatically downregulated the expression of cdk-2 kinase inhibitor, p21, which was completely neutralized by BMP-7 in a dose-dependent manner. Correspondingly, the cdk-2 kinase gene expression was upregulated by PDGF and this effect was inhibited by BMP-7.

BMP-7 Induces the Expression of Inhibitors of Helix-Loop-Helix Transcription Factors and Inhibitory Smads

Id proteins control cell differentiation by interfering with DNA binding of transcription factors. Previously, it was shown that BMP-2 upregulated Id-1 in the process of osteoblast differentiation of myoblast cell line C2C12[29]. Investigating the mechanism of BMP-7 action, we found that the expression of inhibitors of helix-loop-helix transcription factors Id-1 and Id-2 was dramatically upregulated by BMP-7 (Fig. 3-A). Greater than 25-fold induction of both Id-1 and Id-2 was obtained by 100 ng/ml BMP-7. In contrast, TGF-β and PDGF had little or no effect on the expression of Ids. This induction was rapid and was detected at the earliest time point we have examined: 15 minutes after the addition of BMP-7. When BMP-7 was added in conjunction with TGF-β or PDGF, Id-1 and Id-2 were induced to a lesser extent.

The inhibitory Smads, Smad6 and Smad7, have been shown to act as an inhibitor of Smad phosphorylation in the BMP and TGF-β signaling pathway and have been implicated in the control of these pathways[21,30,32]. Both Smad6 (35-fold) and Smad7 (15-fold) were induced by 100 ng/ml BMP-7 (Fig. 3-A). Under identical culture conditions, PDGF had no effect on the expression of these two genes and TGF-β induced only Smad7. A dose-dependent induction of Smad6 could be detected by Northern blot analysis of the same RNA (Fig. 3-B).

BMP-7 Downregulates Endogenous and Induced ICAM-1

One key feature of vascular proliferative disorders is inflam-

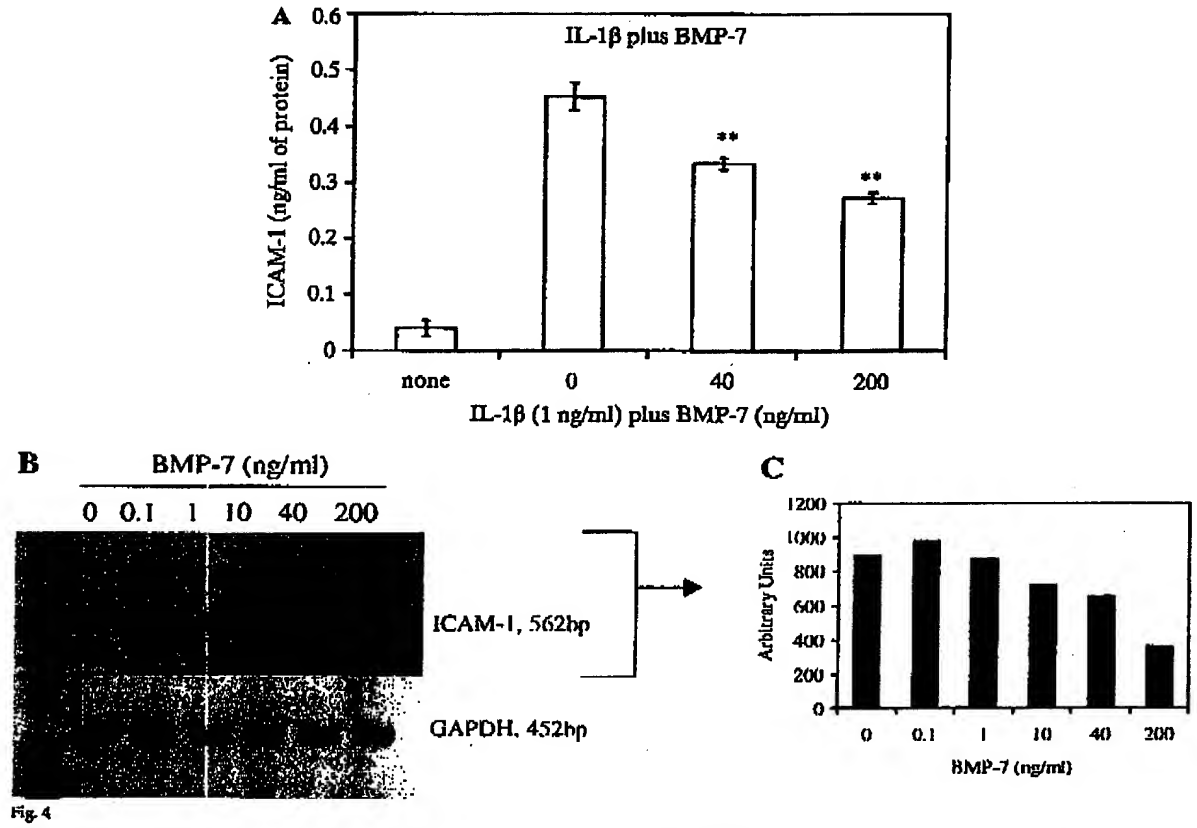

Fig. 4

Fig. 4 Effect of bone morphogenetic protein-7 (BMP-7) on the endogenous and interleukin-1β (IL-1β)-induced intercellular adhesion molecule-1 (ICAM-1). **A:** Cells were plated in a 24-well plate (4 x 10^5 cells/well). The next day, growth medium was replaced with medium containing 0.1% serum. IL-1β (1 ng/ml) and various concentrations of BMP-7 were added. After 5 days of incubation, soluble ICAM-1 in lysed cells was measured by enzyme-linked immunosorbent assay. **B:** First, 1 x 10^6 cells were treated with various concentrations of BMP-7 for 24 hours. The cells were harvested, and total RNA was made. Next, 1 μg of total RNA was used to prepare cDNA, which was then subjected to semiquantitative reverse transcriptase-polymerase chain reaction with use of human glyceraldehyde-3-phosphate (GAPDH) and ICAM-1 primers. One-fifth of the reaction was subjected to agarose gel electrophoresis and photographed. M = DNA marker. **C:** Densitometer scan of the ICAM-1 gel photograph.

mation. IL-1β and other pro-inflammatory cytokines from aggregating macrophages and monocytes induce in turn the expression of ICAM-1, MCP-1, and other pro-inflammatory cytokines in SMC cells. IL-1β (1 ng/ml) dramatically induced the expression of ICAM-1, which can be inhibited to as much as 40% by 200 ng/ml BMP-7 (Fig. 4-A). Additionally, BMP-7 can dose-dependently downregulate the expression of endogenous ICAM-1 (Figs. 4-B and 4-C) and IL-6 (data not shown) as examined by semiquantitative RT-PCR.

BMP-7 Maintains the Expression of Markers Characteristic of SMC Phenotype

When primary HASM cells are maintained in culture for long periods, they tend to adopt a more fibroblast-like morphology with a concomitant loss of SMC markers such as α-actin and SMC-specific H-chain myosin. We found that HASM cultures containing BMP-7 (100 ng/ml) maintained the expression of α-actin beyond day 6 in confluent cultures, whereas untreated cultures started to loose α-actin expression as early as day 3 (Fig. 5-A). As it has been shown that in atherosclerotic lesions type-I collagen synthesis is enhanced compared with that of type-III collagen, we examined the ability of BMP-7 to maintain type-III collagen synthesis in long-term cultures by semiquantitative RT-PCR. Although the expression of collagen type I remained unaltered beyond day 3 following confluence in treated and untreated cultures (Fig. 5-A), the expression of collagen type III was significantly decreased over the same time period in untreated cultures (Fig. 5-A). However, its expression remained unaltered or even enhanced in BMP-7-treated cultures. This is confirmed by densitometer scanning of the gel followed by calculations of ratios (collagen III/GAPDH). Furthermore, BMP-7 induced a dose-dependent increase in the expression of α-actin, basic calponin, and H-chain myosin as examined by quantitative and semiquantitative RT-PCR (Figs. 5-B and 5-C). Additionally, there was a discernable change in morphology (Fig. 5-D) from needle-

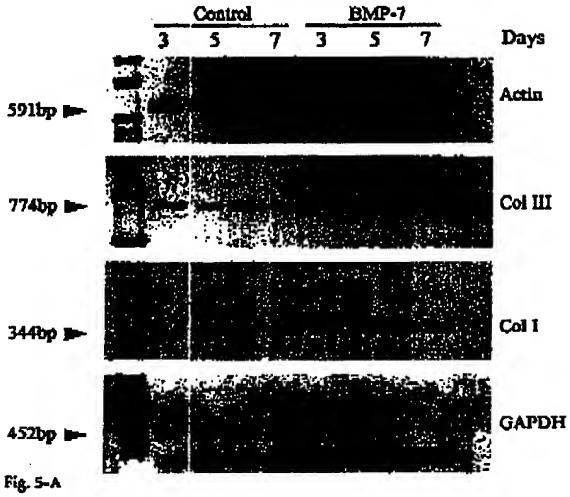

Fig. 5-A

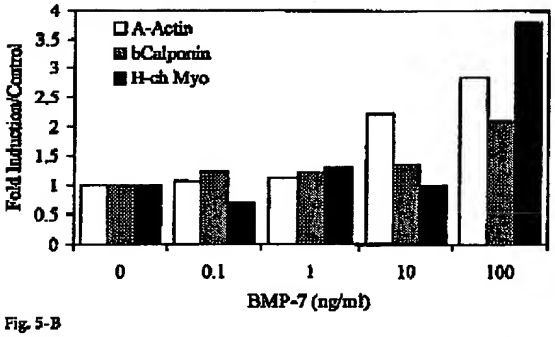

Fig. 5-B

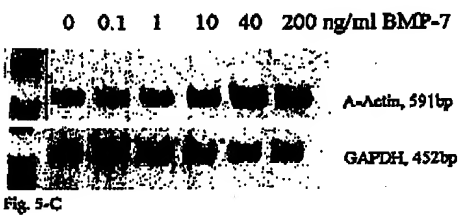

Fig. 5-C

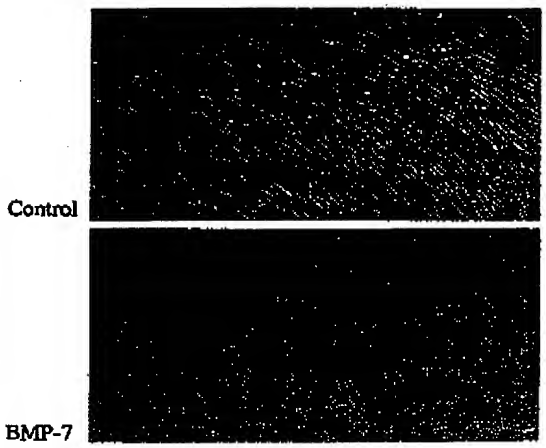

Fig. 5-D

Fig. 5 Effect of bone morphogenetic protein-7 (BMP-7) on the expression of smooth muscle cell markers. **A:** First, 2 x 10^6 cells were treated with 100 ng/ml BMP-7 for various times in long-term cultures; then, they were harvested and cDNA was synthesized. Semiquantitative reverse transcriptase-polymerase chain reaction (RT-PCR) was carried out with use of the primers shown. Lanes 1-4, control, day 3, 5, 7, and 9, respectively; lanes 5-8, 100 ng/ml BMP-7, day 3, 5, 7, and 9, respectively. **B:** First, 1 x 10^6 cells were treated with various concentrations of BMP-7 for 24 hours. Cells were harvested, and total RNA was made. Then, 1 µg of total RNA was used to prepare cDNA, which was then subjected to quantitative RT-PCR. **C:** First, 1 x 10^6 cells were treated with various concentrations of BMP-7 for 24 hours. The cells were harvested, and total RNA was made. Next, 1 µg of total RNA was used to prepare cDNA, which was then subjected to semiquantitative RT-PCR with use of human glyceraldehyde-3-phosphate (GAPDH) and α-actin primers. One-fifth of the reaction was subjected to agarose gel electrophoresis and photographed. **D:** First, 5 x 10^5 cells were plated in growth medium and treated with 100 ng/ml BMP-7 or vehicle for 9 days. They were then photographed. Magnification is 20x.

shaped fibroblast-like cells that are stacked on top of each other to more randomly organized smaller cells at the addition of BMP-7 to these cultures. The true appearance of SMCs in culture is unclear.

Discussion

We show here that HASM cells when treated with recombinant human BMP-7 (also called osteogenic protein-1 [OP-1]) inhibit serum-stimulated cell proliferation in culture over a wide range of physiologic concentrations (10-200 ng/ml). Notably, this BMP-7-mediated inhibition of SMC proliferation was more pronounced when cell growth had been stimulated with PDGF-BB or TGF-β, suggesting for the first time a potential role for BMPs in the prevention of SMC proliferation following vascular injury. The inhibitory effect of BMP-7 was due in part to an increased expression of the inhibitor of cyclin-dependent kinase-2, p21, which was inhibited during PDGF-BB-mediated cell proliferation. BMP-7 also induced the expression of developmentally regulated genes such as Id-1 and Id-2, which are required for several key cellular differentiation pathways and inhibitory Smads. Smad6 and Smad7, which negate both the TGF-β and TGF-β superfamily of proteins, mediated downstream signaling. Concurrently, BMP-7-mediated inhibition of cell growth is accompanied by enhanced expression of markers that are characteristic of the SMC phenotype, α-actin, SMC-specific heavy-chain myosin, and maintenance of the type III/I collagen ratio. Finally, BMP-7 downregulated endogenous and IL-1β induced ICAM-1, a cell-surface molecule known to play a role in neutrophil adhesion and activation during inflammation. Our findings suggest that BMP-7 may provide a basis for developing therapeutic strategies to effectively suppress SMC prolifera-

tion, delay the onset of inflammation, and diminish the formation of connective tissue in and around the vascular endothelium associated with vascular proliferative disorders[1].

Several peptide growth factors (PDGF, FGF, IGF-1, and TGF-β), pro-inflammatory cytokines (interleukin-1 [IL-1] and tumor necrosis factor-alpha [TNF-α]), and agents such as nitric oxide and lipids are known to regulate migration, proliferation, and differentiation of vascular SMCs[4,7,32-34]. Specifically, following injury, the migration and proliferation of SMCs are stimulated by (1) the paracrine action of PDGF-BB, released by platelets at their activation[4], (2) the autocrine action of PDGF-AA induced by the pro-inflammatory cytokines (IL-1 and TNF-α), and (3) TGF-β[33,34]. In addition, FGF and IGF-1 are released locally by activated SMCs[4] that act on SMC growth. Studies attempting to antagonize the activities of growth factors PDGF, FGF, and TGF-β and their receptors using specific antibodies and antisense oligonucleotides[35,36] have provided protection against SMC proliferation following balloon angioplasty and thus help to reduce myo-intimal thickening. In addition, therapeutic modalities such as the infusion of IFN-gamma[37] and anti-ICAM[38] antibodies have been reported to diminish intimal thickening in various animal models. Since an ideal artery contains SMCs that are both contractile and quiescent with respect to proliferation, therapies that would decrease the likelihood of SMC hyperplasia and consequent luminal occlusion may provide cytoprotection against the vascular proliferative disorders and delayed dysfunction that occur after organ transplantation.

Although BMPs were originally identified in bone, their morphogenic roles have been widely documented in a wide variety of other nonskeletal tissues[14]. BMPs are novel growth and differentiation factors constituting a large subfamily in the TGF-β superfamily of proteins. BMPs have been shown to play inductive roles in migration and proliferation of pluripotent stem cells[39] and have a subsequent differentiation into lineage-specific cell types during morphogenesis. Furthermore, BMPs are capable of stimulating the expression of phenotypes characteristic to a specific cell type[40] and serve as maintenance factors during the repair and regeneration of adult tissue[18,41]. Therefore, when BMPs are made available in and around the vascular endothelium, they may assist in maintaining SMCs in a contractile and quiescent state rather than aid in the proliferation and loss of phenotype at vascular injury and as observed in various proliferative disorders. To support this notion, BMP-2, a related member of BMP-7, has been shown to inhibit rat vascular smooth muscle proliferation *in vitro* and to inhibit injury-induced intimal hyperplasia when administered locally by adenovirus-mediated gene transfer following balloon angioplasty in rats[42]. Our present study supports and extends these observations. Potentially, BMPs can be used to maintain the expression of SMC phenotype in cultures during cell expansion in order to engineer functional vascular grafts for clinical need. Since the effect of BMPs on cell growth and differentiation is dependent on the developmental stage of the responding cells, it is likely that the presence of the BMPs in the culture medium will help to differentiate the expanded cells into the more "mature" contractile quiescent SMCs.

Among TGF-β superfamily proteins, TGF-β has been studied in the context of vascular integrity *in vitro* and *in vivo*[43]. This morphogen is a bifunctional growth regulator of SMCs that was shown to stimulate or inhibit the growth of SMCs depending on the conditions of cell culture, the presence of other regulatory molecules, the sequence of their addition, and the concentration of TGF-β[44]. Moreover, several studies have shown that TGF-β is potent in stimulating the deposition of connective tissues by SMCs[45]. Under our culture conditions, TGF-β had a proliferative effect on serum-stimulated DNA synthesis of SMCs. Thus, the beneficial effect of BMP-7 on SMCs does not appear comparable with that of TGF-β. Although the mode of action of the BMP-7 activity is currently unknown, the results suggest that BMP-7 upregulates both Smad6 and Smad7, the two inhibitory Smads in the TGF-β superfamily. Under these conditions, Smad7 but not Smad6 was upregulated by TGF-β, whereas neither was induced by PDGF. Additionally, it has been shown that BMP-7 upregulates Smad7 expression in lung cancer cell lines[45] and in myoblast cell line C2C12 (unpublished observation). *In vivo* studies have shown that both Smad6 and Smad7 were induced in vascular endothelium at mechanical stimulus[46], suggesting potential protection against vascular injury. The fact that Smad6 is important for the inhibition of BMP signaling[39] suggests that this molecule may in part be involved in the regulation of the effects of BMP on SMCs.

The observed cytoprotective effect of BMPs on vascular SMC may provide a basis for developing therapeutic agents for intervention against vascular proliferative disorders. ■

Haimanti Dorai, PhD
T. Kuber Sampath, PhD
Curis Inc, 21 Erie Street, Cambridge, MA 02139. E-mail adddress for H. Dorai: hdorai@curis.com

The authors did not receive grants or outside funding in support of their research or preparation of this manuscript. One or more of the authors received payments or other benefits or a commitment or agreement to provide such benefits from a commercial entity (Creative Biomolecule) No commercial entity paid or directed, or agreed to pay or direct, any benefits to any research fund, foundation, educational institution, or other charitable or nonprofit organization with which the authors are affiliated or associated.

References

1. **Ross R, Glomset JA.** Atherosclerosis and the arterial smooth muscle cell: proliferation of smooth muscle is a key event in the genesis of the lesions of atherosclerosis. *Science.* 1973;180:1332-9.

2. **Bittner K, Vischer P, Bartholmes P, Bruckner P.** Role of subchondral vascular system in endochondral ossification: endothelial cells specifically derepress iste differentiation in resting chondrocytes in vitro. *Exp Cell Res.* 1998;238:491-7.

3. **Ross R.** The pathogenesis of atherosclerosis—an update. *N Engl J Med.* 1986;314:488-500.

4. **Ross R.** The pathogenesis of atherosclerosis: a perspective for the

1990s. *Nature.* 1993;362:801-9.

5. **Baskaya NK, Taub R, Zellner K, King G.** Insulin, insulin-like growth factor I and platelet-derived growth factor interact additively in the induction of the protooncogene c-myc and cellular proliferation in cultured bovine aortic smooth muscle cells. *Mol Endocrinol.* 1989;3:1183-90.
6. **Heldin CH, Westermark B.** Platelet-derived growth factor: mechanism of action and possible in vivo function. *Cell Regul.* 1990;1:555-66.
7. **Burgess WH, Maciag T.** The heparin-binding (fibroblast) growth factor family of proteins. *Annu Rev Biochem.* 1989;58:575-606.
8. **Ross R, Masuda J, Raines EW, Gown AM, Katsuda S, Sasahara M, Malden LT, Masuko H, Sato H.** Localization of PDGF-BB protein in macrophages in all phases of atherogenesis. *Science.* 1990;248:1009-12.
9. **Hansson GK, Hellstrand L, Rymo L, Rubbia L, Gabbiani G.** Interferon gamma inhibits both proliferation and expression of differentiation-specific alpha-smooth muscle actin in arterial smooth muscle cells. *J Exp Med.* 1989;170:1595-1608.
10. **Lee WS, Harder JA, Yoshizumi M, Lee ME, Haber E.** Progesterone inhibits arterial smooth muscle cell proliferation. *Nat Med.* 1997;3:1005-8.
11. **Battegay EJ, Raines EW, Seifert RA, Bowen-Pope DF, Ross R.** TGF-beta induces bimodal proliferation of connective tissue cells via complex control of an autocrine PDGF loop. *Cell.* 1990;63:515-24.
12. **Urist MR.** Bone: formation by autoinduction. *Science.* 1965;150:893-9.
13. **Sampath TK, Reddi AH.** Dissociative extraction and reconstitution of extracellular matrix components involved in local bone differentiation. *Proc Natl Acad Sci U S A.* 1981;78:7599-603.
14. **Hogan BL.** Bone morphogenetic proteins in development. *Curr Opin Genet Dev.* 1996;6:432-8.
15. **Lefer AM, Tsao PS, Ma XL, Sampath TK.** Anti-ischemic and endothelial protective actions of recombinant human osteogenic protein (hOP-1). *J Mol Cell Cardiol.* 1992;24:585-93.
16. **Kawamata T, Ren J, Chen TC, Charette M, Finkelstein SP.** Intracisternal osteogenic protein-1 enhances functional recovery following focal stroke. *Neuroreport.* 1998;9:1441-5.
17. **Ren J, Kaplan PL, Charette MF, Speller H, Finkelstein SP.** Time window of intracisternal osteogenic protein-1 in enhancing functional recovery after stroke. *Neuropharmacology.* 2000;39:860-5.
18. **Vukicevic S, Basic V, Rogic D, Basic N, Shih MS, Shepard A, Jin D, Dattatreyamurty B, Jones W, Doral H, Ryan S, Griffiths D, Mallakal J, Jelic M, Pastorcic M, Stavljenic A, Sampath TK.** Osteogenic protein-1 (bone morphogenetic protein-7) reduces severity of injury after ischemic acute renal failure in rat. *J Clin Invest.* 1998;102:202-14.
19. **Chan T, Falk S, Conger J.** Effect of osteogenic protein-1 on the course of norepinephrine induced acute renal failure. *J Am Soc Nephrol.* 1997;8:272IA.
20. **Sampath TK, Maliakal JC, Hauschka PV, Jones WK, Sasak H, Tucker RF, White KH, Coughlin JE, Tucker MM, Pang RH, et al.** Recombinant human osteogenic protein-1 (hOP-1) induces new bone formation in vivo with a specific activity comparable with natural bovine osteogenic protein and stimulates osteoblast proliferation and differentiation in vitro. *J Biol Chem.* 1992;267:20352-62.
21. **Takase M, Imamura T, Sampath TK, Takeda K, Ichijo H, Miyazono K, Kawabata M.** Induction of Smad6 mRNA by bone morphogenetic protein. *Biochem Biophys Res Commun.* 1998;244:26-9.
22. **Agrotis A, Samuel M, Prapas G, Bobik A.** Vascular smooth muscle cells express multiple type I receptors for TGF-beta, activin, and bone morphogenic proteins. *Biochem Biophys Res Commun.* 1996;219:613-8.
23. **Doral H, Shepard A, Mallakal J, Oppermann H, Vukicevic S, Sampath TK.** Osteogenic protein-1 (OP-1/BMP-7) modulates smooth muscle growth and maintains the expression of cell phenotype and protects against cell injury mediated by nephrotoxic and inflammatory agents in vitro. *J Am Soc Nephrol.* 1997;8:136A.
24. **Doral H, Vukicevic S, Sampath TK.** Bone morphogenetic protein-7 (osteogenic protein-1) inhibits smooth muscle cell proliferation and stimulates the expression of markers that are characteristic of SMC phenotype in vitro. *J Cell Physiol.* 2000;184:37-45.
25. **Macias-Silva M, Hoodless PA, Tang SJ, Buchwald M, Wrana JL.** Specific activation of Smad1 signaling pathways by the BMP7 type I receptor, ALK2. *J Biol Chem.* 1998;273:25628-36.
26. **Letsou A, Arora K, Wrana JL, Simin K, Twombly V, Jamal J, Staehling-Hampton K, Hoffmann FM, Gelbart WM, Massague J, O'Connor MB.** Drosophila Dpp signaling is mediated by the punt gene product: a dual ligand-binding type II receptor of the TGF beta receptor family. *Cell.* 1995;80:899-908.
27. **Suzuki JI, Isobe M, Morishita R, Aoki M, Horie S, Okubo Y, Kaneda Y, Sawa Y, Matsuda H, Ogihara T, Sekiguchi M.** Prevention of graft coronary arteriosclerosis by antidense cdk-2 kinase oligonucleotides. *Nature/Medicine.* 3:900-3.
28. **Fukui R, Shibata N, Kohbayashi E, Amakawa M, Furutama D, Hoshiga M, Negoro N, Nakakouji T, Ii M, Ishihara T, Ohsawa N.** Inhibition of smooth muscle cell migration by p21 cyclin-dependent kinase inhibitor (Cip1). *Atherosclerosis.* 1997;132:53-9.
29. **Katagiri T, Yamaguchi A, Komaki M, Abe E, Takahashi N, Ikeda T, Rosen V, Wozney JM, Fujisawa-Sehara A, Suda T.** Bone morphogenetic protein-2 converts the differentiation pathway of C2C12 myoblasts into the osteoblast lineage. *J Cell Biol.* 1994;127:1755-66.
30. **Imamura T, Takase M, Nishihara A, Oeda E, Hanai J, Kawabata M, Miyazono K.** Smad6 inhibits signalling by the TGF-beta superfamily. *Nature.* 1997;389:622-6.
31. **Nakao A, Afrakhte M, Moren A, Nakayama T, Christian JL, Heuchel R, Itoh S, Kawabata M, Heldin NE, Heldin CH, ten Dijke P.** Identification of Smad7, a TGFbeta-inducible antagonist of TGF-beta signalling. *Nature.* 1997;389:631-5.
32. **Old LJ.** Tissue necrosis factor (TNF). *Science.* 1985;230:630-2.
33. **Libby P, Friedman GB, Salomon RN.** Cytokines as modulators of cell proliferation in fibrotic diseases. *Am Rev Respir Dis.* 1989;140:1114-7.
34. **Raines EW, Dower SK, Ross R.** Interleukin-1 mitogenic activity for fibroblasts and smooth muscle cells is due to PDGF-AA. *Science.* 1989;243:393-6.
35. **Fems GA, Raines EW, Sprugel KH, Motani AS, Reidy MA, Ross R.** Inhibition of neointimal smooth muscle accumulation after angioplasty by an antibody to PDGF. *Science.* 1991;253:1129-32.
36. **Simon M, Edelman ER, Dekeyser JL, Langer R, Rosenberg RD.** Anti-sense c-myb oligonucleotide inhibit intimal arterial smooth muscle accumulation in vivo. *Nature.* 1992;359:67-70.
37. **Stopeck AT, Vahedian M, Williams SK.** Transfer and expression of interferon gamma gene in human endothelial cells inhibits vascular smooth muscle cell growth in vitro. *Cell Transplant.* 1997;6:1-8.
38. **Yasukawa H, Imaizumi T, Matsuoka H, Nakashima A, Morimatsu M.** Inhibition of intimal hyperplasia after balloon injury by antibodies to intercellular adhesion molecule-1 and lymphocyte function-associated antigen-1. *Circulation.* 1997;95:1515-22.
39. **Reddi AH.** Role of morphogenic proteins in skeletal tissue engineering and regeneration. *Nat Biotechnol.* 1998;16:247-52.
40. **Maliakal JC, Ashahina I, Hauschka PV, Sampath TK.** Osteogenic protein-1 (BMP-7) inhibits cell proliferation and stimulates the expression of markers characteristic of osteoblast phenotype in rat osteosarcoma (17/2.8) cells. *Growth Factors.* 1994;11:227-34.
41. **Hruska KA, Guo G, Wozniak M, Martin D, Miller S, Liapis H, Loveday K, Klahr S, Sampath TK, Morrissey J.** Osteogenic protein-1 prevents renal fibrogenesis associated with ureteral obstruction. *Am J Physiol Renal Physiol.* 2000;279:F130-43.
42. **Nakaoka T, Gonda K, Ogita T, Otawara-Hamamoto Y, Okabe F, Kira Y, Hanli K, Miyazono K, Takuwa Y, Fujita T.** Inhibition of rat vascular smooth muscle proliferation in vitro and in vivo by bone morphogenetic protein-2. *J Clin Invest.* 1997;100:2824-32.
43. **Roberts AB, Sporn MB.** The transforming growth factor-βs. *Peptide Growth Factors and Their Receptors.* 1990;1:419-72.
44. **Majack RA.** Beta-type transforming growth factor specifies organizational behavior in vascular smooth muscle cell cultures. *J Cell Biol.* 1987;105:465-71.
45. **Afrakhte M, Moren A, Jossan S, Itoh S, Sampath K, Westermark B, Heldin CH, Heldin NE, ten Dijke P.** Induction of inhibitory Smad6 and Smad7 mRNA by TGF-beta family members. *Biochem Biophys Res Commun.* 1998;249:505-11.
46. **Topper JN, Cai J, Qiu Y, Anderson KR, Xu YY, Deeds JD, Feeley R, Gimeno CJ, Woolf EA, Tayber O, Mays GG, Sampson BA, Schoen FJ, Gimbrone MA Jr, Falb D.** Vascular MADs: two novel MAD-related genes selectively inducible by flow in human vascular endothelium. *Proc Natl Acad Sci U S A.* 1997;94:9314-19.

Available online at www.sciencedirect.com
SCIENCE DIRECT®
ELSEVIER
Biochemical and Biophysical Research Communications 316 (2004) 100–106
BBRC
www.elsevier.com/locate/ybbrc

BMP-2 modulates the proliferation and differentiation of normal and cancerous gastric cells

Xian-Zi Wen, Satoshi Miyake,[1] Yoshimitsu Akiyama, and Yasuhito Yuasa*

Department of Molecular Oncology, Graduate School of Medicine and Dentistry, Tokyo Medical and Dental University, 1-5-45 Yushima, Bunkyo-ku, Tokyo 113-8519, Japan

Received 14 January 2004

Abstract

Bone morphogenetic protein 2 (BMP-2), a member of the transforming growth factor β super-family, has been shown to act as an antiproliferative agent for a variety of cell lines by activating signaling cascades that cause cell cycle arrest. However, the biological effect and mechanism of action of BMP-2 on gastric cells remain unknown. In the present study, we showed that recombinant human BMP-2 dose-dependently inhibited the growth of OUMS37 rat gastric cells and MKN74 human gastric cancer cells. The antiproliferation seems to be due to cell cycle arrest in the G_1-phase, which was revealed by flow cytometric assays. BMP-2 increased the level of p21/WAF1/CIP1, suggesting that BMP-2-mediated inhibition of cell proliferation may be induced through p21/WAF1/CIP1. In addition, BMP-2 increased the expression of pepsinogen II, a differentiation marker of the stomach, in MKN74 cells. These results indicate that BMP-2 plays important roles in modulating the proliferation and differentiation of gastric epithelial cells.

Keywords: BMP-2; Proliferation; p21/WAF1/CIP1; Differentiation; Pepsinogen

Bone morphogenetic proteins (BMPs) were initially identified based on their ability to induce bone and cartilage formation when implanted subcutaneously or intramuscularly into animals [1,2]. BMPs are structurally similar to the transforming growth factor β (TGF-β) super-family [3,4]. BMP-2, a member of this large family of proteins, stimulates the growth and differentiation of osteogenic and chondrogenic cells during bone remodeling and also plays important roles in embryogenesis [2,3,5,6]. Similar to TGF-β, BMPs exert their effect via specific type I and type II serine–threonine kinase receptors (BMPR). Binding of BMP-2 to the type II receptor induces oligomerization of the receptor complex, resulting in phosphorylation of the type I receptor and recruitment of downstream signaling protein, Smad1, Smad5, and Smad8 [7,8]. Among the latter, Smad1 has been extensively studied as the target of BMPR signaling. Type I BMPR-phosphorylated Smad1 heterodimerizes with Smad4, translocates to the nucleus to act as a transcription factor, and then induces genes that mediate the biological activity of BMP-2 [9].

Epithelial–mesenchymal interactions are necessary for the normal development of various digestive organs [10,11]. When the proventricular epithelium begins to form glands, only BMP-2 of the BMP family is expressed in the chicken proventricular mesenchyme at a high level. Virus-mediated BMP-2 overexpression results in an increase in the number of glands formed and expression of embryonic chicken pepsinogen (ECPg), one of the differentiation markers of glandular epithelial cells. On the other hand, the gland formation and expression of ECPg are inhibited by ectopic expression of noggin [12], which can block the action of BMP by binding directly to BMP-2 or BMP-4 with high affinity. Two type I receptors for BMP are expressed in the mouse embryonic stomach [13], and the earliest discernible defect in some Smad5-deficient mouse embryos is a vestigial foregut [14]. Thus, the BMP pathway may be involved in gastric differentiation.

* Corresponding author. Fax: +81-3-5803-0125.
E-mail address: yuasa.monc@tmd.ac.jp (Y. Yuasa).
[1] Present address: Department of Developmental Biology, Graduate School of Medicine, Tohoku University, 2-1, Seiryo-machi, Aoba-ku, Sendai 980-8575, Japan.

0006-291X/$ - see front matter © 2004 Elsevier Inc. All rights reserved.
doi:10.1016/j.bbrc.2004.02.016

Juvenile polyposis (JP) is an autosomal dominant gastrointestinal hamartomatous polyposis syndrome, in which patients are at risk for developing gastrointestinal cancers [15,16]. Thirteen of 54 JP patients had germline *BMPRIA* mutations, and patients with *BMPRIA* mutations had a more prominent JP phenotype than those without [17], suggesting high tumor-suppressive activity of BMPRIA. It has been reported that *BMP-2* and *BMP-4* mRNA expression was found in some human gastric cancer cell lines [18]. This accumulated evidence indicates that the BMP pathway might be involved in gastric cell growth control.

BMP-2 inhibits the proliferation of smooth muscle cells, primary mesangial cells, prostate cancer cells, and breast cancer cells [19–22]. Up to now, there have been a number of studies on TGF-β–Smad signaling molecules in gastric carcinogenesis [23,24]. However, although BMPs and their receptors are closely related to the respective TGF-β ligands and receptors, their potential roles in gastric carcinogenesis are still unknown. Here, we examined the effects of BMP-2 on normal and cancerous gastric cells.

Materials and methods

Cell lines and cell culture. The cell lines used in this study comprised a rat gastric epithelial cell line, OUMS37 [25] (kind gift from Dr. Masayoshi Namba, Okayama University Medical School, Japan), and a human gastric cancer cell line, MKN74 (obtained from Riken Cell Bank, Tsukuba, Japan). For routine culture, OUMS37 cells were grown in Dulbecco's modified Eagle's medium and MKN74 cells in RPMI 1640. Both cell lines were cultured at 37 °C under a 5% CO_2 and 95% air atmosphere in the respective medium supplemented with 10% fetal bovine serum and 50 μg/ml kanamycin.

cDNA synthesis and PCR analysis. Total RNA was isolated from the cell lines using a Quickprep RNA purification kit (Amersham Pharmacia Biotech, Buckinghamshire, England). Isolated RNA (2 μg) was pre-incubated with 0.4 μg of 12–18-mer oligo(dT) at 70 °C for 10 min and then with 10 mM dNTP, 0.1 M dithiothreitol, and 1 μl Superscript II (RNaseH (–) reverse transcriptase; Life Technologies, Gaithersburg, MD) at 42 °C for 1 h, according to the protocols recommended by the manufacturer. The synthesized cDNA was then amplified by the PCR method. Each PCR cycle consisted of 94 °C for 1 min, 55 °C for 2 min, and 72 °C for 1 min, followed by final extension at 72 °C for 10 min. The PCRs for *BMPRIA* and *BMPRII* comprised 24 cycles in a 25 μl mixture containing 1 μl of the synthesized cDNA. The product sizes and primer sequences used were as follows: *hBMPRIA* (GenBank Accession No. NM_004329), 316 bp, 5′-ATCATGG CTGACATCTACAGC-3′ and 5′-ACATCTTGGGATTCAACCAT C-3′; and *hBMPRII* (GenBank Accession No. XM_028038), 587 bp, 5′-AGCAGCAGAACCCTTCCCAAG-3′ and 5′-CCAGAGAATTA GGCCTCTGT-3′. These primers were designed from the sequences with high homology between the human and rat, and the PCR products were confirmed by sequencing. As an internal control for RT-PCR, glyceraldehyde-3-phosphate dehydrogenase (*GAPDH*) transcripts were amplified from the same cDNA samples as described previously [26].

For RT-PCR analysis of *pepsinogen C* (GenBank Accession No. NM_002630), which encodes protein pepsinogen II, total RNA (2 μg) from MKN74 cells treated with 100 ng/ml of recombinant human BMP-2 (rhBMP-2) (obtained from Yamanouchi Pharmaceutical Company, Japan) or the same volume of vehicle (LF6: 5 mM glutamic acid, 5 mM sodium chloride, 2.5% glycine, 0.5% galactose, and 0.01% Tween 80) for 48 h was used for cDNA synthesis. The synthesized cDNA was amplified by the semi-quantitative RT-PCR method, as follows. We used a forward primer (5′-GACACAGGCACCTCTCT GCTC-3′) and a reverse primer (5′-GACCTGAGGAAGACATCCC C-3′). PCR for *pepsinogen C* was performed for 30 cycles and 35 cycles in a 25 μl mixture consisting of 1 μl cDNA, 2.5 μl of 10× buffer, 2 μl of 2.5 mM dNTP, 10 pmol of each primer, and 1 U *Taq* DNA polymerase (Biotech International, Bentley, Australia), and each PCR cycle consisted of 94 °C for 1 min, 56 °C for 2 min, and 72 °C for 1 min, with final extension at 72 °C for 10 min. The PCR products were confirmed by sequencing.

Cell proliferation assays. Cell proliferation assays with rhBMP-2 were conducted as follows. OUMS37 cells and MKN74 cells were plated at 2×10^4 or 5×10^4 cells/well, respectively, in a 24-well plate in the respective medium. After culturing for 4–5 h, rhBMP-2 was added to give different concentrations (10, 50, and 100 ng/ml). Cell proliferation was evaluated on day 3 (OUMS37) or 6 (MKN74) by determining the number of cells with a Cell Counting Kit 8 (Dojindo, Kumamoto, Japan) according to the protocol recommended by the manufacturer. As a control, the same volume of vehicle was added to each well.

Flow cytometric analysis. For cell cycle analysis, near 50% confluent cells were synchronized in the G_0/G_1 phase by overnight incubation in serum-free medium. Cells were then incubated in the complete medium containing 100 ng/ml rhBMP-2. After 48 h (OUMS37) or 72 h (MKN74) incubation, the cells were trypsinized and washed with PBS, and then fixed in 70% ethanol for 30 min at −20 °C. The cells were then centrifuged at 1500*g* for 4 min. For nuclear staining, the cells were treated with 1 ml of 100 ng/ml RNaseA at 37 °C for 20 min, centrifuged and re-suspended in 69 μM propidium iodide, and then incubated at room temperature for 20 min. The cells were then analyzed by flow cytometry on FACStar Plus (Becton–Dickinson Immunocytometry System, San Jose, CA). Data were analyzed for 20,000 viable cells as determined by forward and right angle light scatter, stored as frequency histograms, and subsequently analyzed by MODFIT software (Verity, Topsham, ME).

Luciferase assay. The human *p21/WAF1/CIP1* promoter luciferase reporter (*p21*-Luc) construct was described previously [27]. This reporter construct contains the *p21* promoter from −2699 to +45 bp in the pGL2-basic vector. MKN74 cells were plated at 5×10^4 cells/well (24-well plate) 1 day before transfection. The cells were transfected with 300 ng of *p21*-Luc construct and 10 ng pRL-SV40 vector using Trans IT-LT1 transfection reagent (Mirus, Madison, WI) according to the protocol recommended by the manufacturer. Beginning on the next day, the cells were incubated for another 24 h with or without 100 ng/ml rhBMP-2. The cells were then harvested and a dual luciferase test was performed using a Dual Luciferase Assay Kit (Promega, Madison, WI) as described by the manufacturer with a Lumicounter 700 (Microtech Niti-on, Chiba, Japan). Each assay was performed in duplicate and experiments were repeated three times. The results were expressed as fold activation, that is, the ratio of normalized luciferase activity on treatment with rhBMP-2 to that with the vehicle.

Western blot analysis. Approximately 30–50% confluent cultures of OUMS37 and MKN74 cells were incubated with 100 ng/ml rhBMP-2 for 24 and 48 h, respectively. The cells were lysed with NP-40 lysis buffer (150 mM sodium chloride, 1% NP-40, 50 mM Tris, pH 8.0, 1 μg/ml aprotinin, 1 μg/ml leupeptin, 1 μg/ml pepstatin, and 50 μg/ml PMSF). Protein concentrations were measured with a Bio-Rad DC protein assay kit (Bio-Rad Laboratories, Hercules, CA). The total cell lysates (80 μg per lane) were separated on 12% SDS–polyacrylamide gels and the proteins were electroblotted onto Immobilon-P transfer membranes (Millipore, Bedford, MA). The blots were probed separately with antibodies against p21/WAF1/CIP1 diluted 1:100 (Santa Cruz Biotechnology, Santa Cruz, CA), and α-tubulin diluted 1:2000 (Santa Cruz). Secondary goat anti-rabbit and anti-mouse antibodies were purchased from Santa Cruz Biotechnology.

Determination of the secreted pepsinogen II protein was performed as follows. About 20% confluent culture of MKN74 cells was incubated with 100 ng/ml rhBMP-2 for 4 days. The medium was then changed and rhBMP-2 (100 ng/ml) was added for further 2 days, then 40 μl aliquots of the medium of cultured cells were separated on 10% SDS–polyacrylamide gels and the products were blotted onto Immobilon-P transfer membranes (Millipore, Bedford, MA). The blots were probed with antibodies against pepsinogen II diluted 1:1000 (The Binding Site Limited, Birmingham, UK). Secondary sheep anti-human pepsinogen II (IgG fraction) antibodies were purchased from The Binding Site Limited.

Results

BMP receptors are expressed in OUMS37 and MKN74 cells

To determine if the BMP-2 signaling pathway is intact, we investigated the mRNA expression of *BMPRIA* and *BMPRII* in OUMS37 and MKN74 cells. RT-PCR analysis revealed that *BMPRIA* and *BMPRII* were abundantly expressed in both cell lines (Fig. 1).

BMP-2 inhibits the proliferation of OUMS37 and MKN74 cells

We analyzed the effects of BMP-2 on the proliferation of OUMS37 and MKN74 cells with the Cell Counting kit 8. Growing OUMS37 and MKN74 cells were treated with increasing concentration of rhBMP-2. As shown in Fig. 2, BMP-2 inhibited cell growth in a dose-dependent manner in both cell types. Approximately 60% and 50% growth inhibition of OUMS37 and MKN74 cells was observed with 100 ng/ml BMP-2. We also directly calculated the number of cells with a hemocytometer, and obtained similar results (data not shown).

The responsiveness of OUMS37 and MKN74 cells to rhBMP-2 was also evidenced by alterations in cell shape.

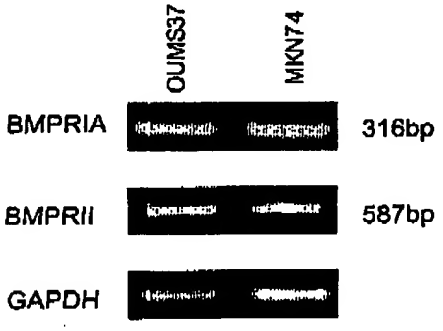

Fig. 1. *BMPRIA* and *BMPRII* are expressed in OUMS37 and MKN74 cell lines. Total RNA (2 μg) isolated from OUMS37 and MKN74 cell lines was used for cDNA synthesis, and then PCRs were performed as described under Materials and methods. The upper panel shows type *IA BMP receptor*, and the middle one shows type *II BMP receptor*. *GAPDH* was used as a control.

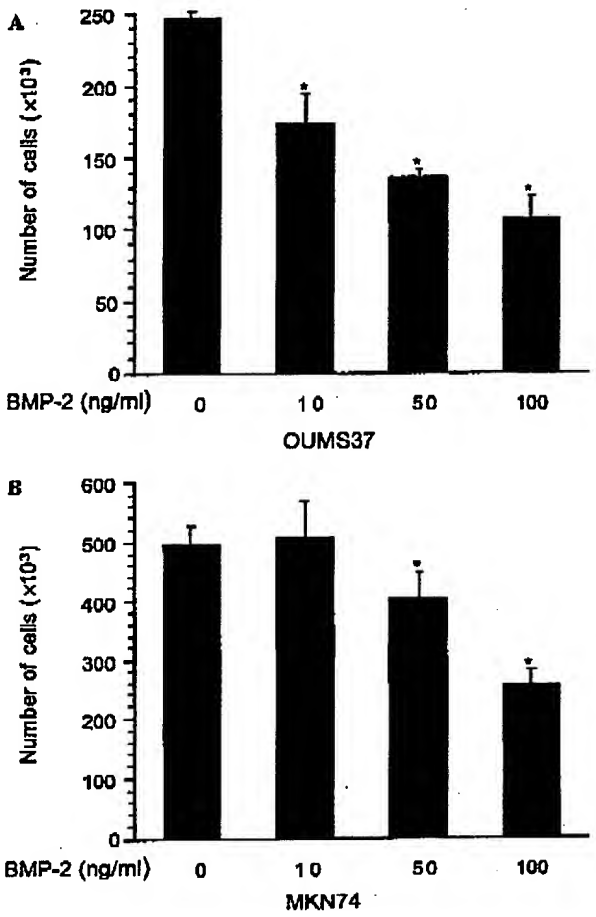

Fig. 2. Effects of BMP-2 on OUMS37 (A) and MKN74 (B) cell proliferation. OUMS37 and MKN74 cells were incubated with different concentrations of rhBMP-2 as described under Materials and methods. The numbers of cells were determined for each treatment. Means ± SD of three independent experiments. $^*P < 0.05$ vs untreated cells.

The majority of OUMS37 and MKN74 cells treated with rhBMP-2 adopted a more enlarged shape with close intercellular contacts and a decreased proportion of nucleus to cytoplasm compared with untreated cells (Fig. 3). These data indicated that BMP-2 dose-dependently inhibited the proliferation of OUMS37 and MKN74 cells, and changed the cell morphology.

BMP-2 causes cell cycle arrest in the G_1-phase in OUMS37 and MKN74 cells

A possible explanation for the observed growth inhibition of OUMS37 and MKN74 cells in response to BMP-2 is either apoptosis or inhibition of new DNA synthesis. We examined the effects of BMP-2 on OUMS37 and MKN74 cell cycle progression by means of FACS analysis. OUMS37 and MKN74 cells

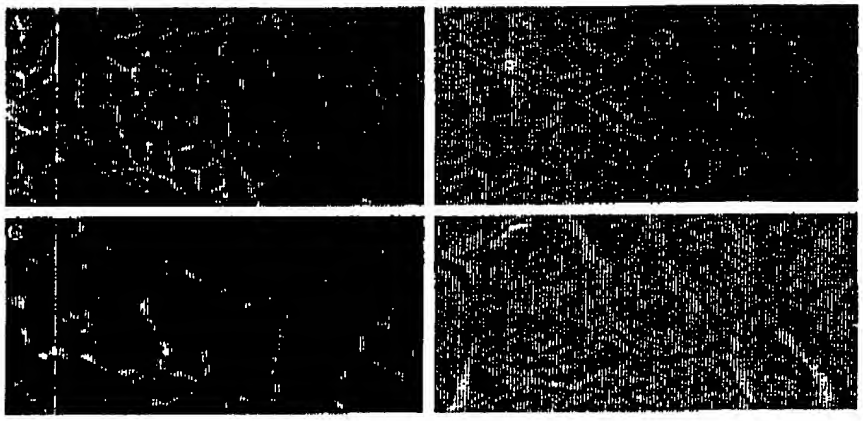

Fig. 3. Morphological changes of OUMS37 and MKN74 cells. The upper panels (A and B) show OUMS37 cells and the lower ones (C and D) MKN74 cells. OUMS37 and MKN74 cells were incubated with 100 ng/ml concentration of rhBMP-2 for 4 or 5 days, respectively. Cells treated with BMP-2 (B and D) adopted a more enlarged shape with close intercellular contacts and a decreased proportion of nucleus as to cytoplasm compared with untreated cells (A and C). Magnification 200×.

Table 1
Flow cytometric analysis of OUMS37 and MKN74 cells for G_1- and S-phase

Name of cell	BMP-2	% of cells in G_1-phase	% of cells in S-phase
OUMS37	–	69.0 ± 1.2	24.1 ± 0.8
	+	78.0 ± 0.4	15.5 ± 0.2
MKN74	–	54.3 ± 2.3	40.3 ± 1.4
	+	65.8 ± 1.8	28.2 ± 0.5

incubated with 100 ng/ml rhBMP-2 showed approximately 36% and 30% decreases in the S-phase, respectively (Table 1). The decrease in the S-phase population was accompanied by an increase in the cell number at the G_1-phase of the cell cycle. These data suggest that rhBMP-2 inhibits OUMS37 and MKN74 cell proliferation by arresting them at the G_1-phase of the cell cycle.

BMP-2 up-regulates the expression of CDK inhibitor p21/WAF1/CIP1 in OUMS37 and MKN74 cells

Cyclin-dependent kinase inhibitors (CDKIs) are involved in the cell cycle arrest induced by many growth inhibitors including TGF-β [28]. p21/WAF1/CIP1, one of the CDKI, was up-regulated by rhBMP-2 in some cell systems [19,22]. We therefore examined whether or not rhBMP-2 activates the *p21/WAF1/CIP1* promoter in MKN74 cells. rhBMP-2 stimulation resulted in about 2-fold transcriptional activation of the *p21/WAF1/CIP1* promoter construct compared with the same volume of vehicle (Fig. 4A).

To confirm the up-regulation of the endogenous p21/WAF1/CIP1 protein by BMP-2 in OUMS37 and

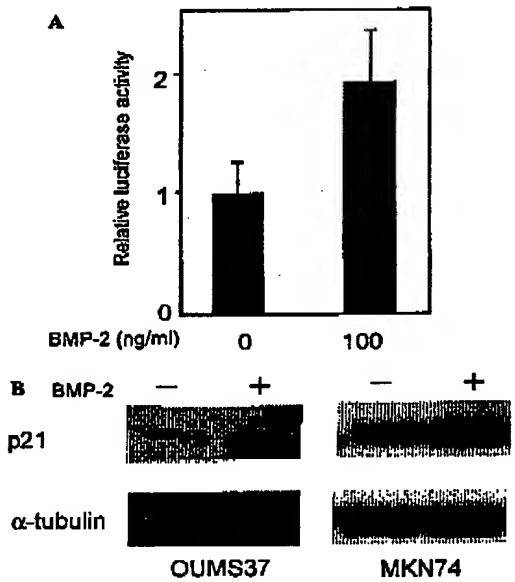

Fig. 4. (A) BMP-2 activates the *p21* promoter in MKN74 human gastric cancer cells. MKN74 cells were transfected with the *p21* promoter luciferase-reporter plasmid. Beginning on the next day, the cells were incubated for 24 h with or without 100 ng/ml rhBMP-2. The results were expressed as fold activation as described under Materials and methods. These results are representative of three independent experiments carried out in duplicate. (B) BMP-2 up-regulated the p21 protein level in OUMS37 and MKN74 cells. OUMS37 and MKN74 cells were incubated with 100 ng/ml BMP-2 for 24 and 48 h, respectively. Equal amounts of cell lysates were analyzed by Western blotting. α-Tubulin was used as a loading control.

MKN74 cells, we analyzed the protein level of p21/WAF1/CIP1 by Western blot assay. As shown in Fig. 4B, rhBMP-2 increased the p21 protein levels in

OUM37 and MKN74 cells. These data constitute evidence that the growth inhibition of OUMS37 and MKN74 cells in response to BMP-2 may be caused by an increased level of p21/WAF1/CIP1.

BMP-2 up-regulates pepsinogen II expression

To determine whether or not BMP-2 up-regulates the transcription of endogenous *pepsinogen C*, a differentiation marker of glandular epithelial cells of the stomach, MKN74 cells treated with rhBMP-2 for 48 h were assayed for the *pepsinogen C* mRNA level by RT-PCR. MKN74 cells treated with the same volume of vehicle were used as a control. As shown in Fig. 5A, the internal standard *GAPDH* mRNA level remained constant in cells treated with rhBMP-2 or the same volume of vehicle (refer to the *GAPDH* panel). MKN74 cells treated with rhBMP-2 expressed the *pepsinogen C* transcript, whereas the control only showed a faint level of expression (refer to the *pepsinogen C* panel, 30 cycles), indicating that rhBMP-2 had up-regulated the transcription of the endogenous *pepsinogen C* gene in MKN74 cells.

To ascertain whether or not BMP-2 up-regulates the pepsinogen II protein, a translation product of *pepsinogen C*, we conducted Western blot analysis to determine the secreted pepsinogen II protein. The medium from MKN74 cells treated with rhBMP-2 contained pepsinogen II (a molecular mass of approximately 40 kDa), but the control exhibited only a very slight level of the protein (Fig. 5B), demonstrating that rhBMP-2 had also up-regulated the protein level of pepsinogen II in MKN74 cells.

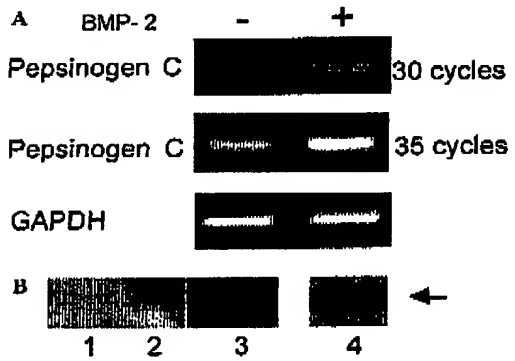

Fig. 5. Up-regulation of the pepsinogen II mRNA and protein in MKN74 cells. MKN74 cells were cultured with rhBMP-2 for 2 days. mRNA and proteins were analyzed as described under Materials and methods. (A) RT-PCR analysis of *pepsinogen C* encoding the pepsinogen II protein. *GAPDH* was used as a control. (B) Western blot analysis of pepsinogen II. Lane 1, fresh medium with 10% FBS; lane 2, medium of untreated MKN74 cells; lane 3, medium of MKN74 cells treated with rhBMP-2; and lane 4, human normal stomach mucosa as a positive control.

Discussion

Our data constituted the first evidence that BMP-2 inhibits the proliferation of OUMS37 rat gastric cells and MKN74 human gastric cancer cells. The inhibition may be due to an increased level of p21/WAF1/CIP1, a cyclin-dependent kinase inhibitor, in response to BMP-2 in both cell types. BMP-2 also up-regulated pepsinogen II, a differentiation marker of glandular epithelial cells of the stomach, in MKN74 cells.

BMPs are members of the TGF-β super-family of cytokines and, like TGF-β, employ similar signal transduction pathways. It has been reported that the TGF-β signal suppresses the growth of gastric epithelial cells [23] and is involved in gastric carcinogenesis [29–32]. Many gastric cancer cells including MKN74 exhibit functional impairment in the TGF-β pathway [33]. Because MKN74 cells express the wild type TGF-βRII and Smad4 proteins [33], the exact mechanism of resistance to TGF-β has not been clarified for MKN74.

BMP-2 is highly expressed in the chicken proventricular mesenchyme [12], and the receptors for BMP are expressed in the mouse embryonic stomach [13]. In addition, BMPs and their receptors are closely related to the respective TGF-β ligands and receptors. It is, therefore, possible that BMPs may play important roles in the control of gastric cell behavior. In the present study, we observed an antiproliferative effect of BMP-2 on OUMS37 and MKN74 cells, and both cell types showed the expression of receptors for BMP. It has been reported that Smad4 was expressed in MKN74 cells [33], thereby demonstrating that BMP receptors and the protein that mediates the BMP-2 signal to the nucleus were expressed in MKN74 cells. The susceptibility of OUMS37 and MKN74 cells to BMP-2 was supported by alterations in cell shape. Taken together, BMP signaling may participate in the regulation of gastric cell growth, which may be independent of the TGF-β pathway.

In other cell types, BMP-associated growth inhibitory responses were found to be transmitted, at least in part, by the CDK inhibitor p21/WAF1/CIP1. Inhibition of the cell growth of breast cancer cells and aortic smooth muscle cells by BMP-2 is mediated by p21/WAF1/CIP1 [19,22]. p21/WAF1/CIP1 binds to G_1 cyclin–CDK complexes, resulting in inhibition of CDK activity, and decreases phosphorylation of the retinoblastoma (RB) protein and then induces subsequent cell cycle arrest in the G_1-phase. In our study, BMP-2 up-regulated *p21/WAF1/CIP1* promoter activity and expression of the p21/WAF1/CIP1 protein in OUMS37 and MKN74 cells. Moreover, the BMP-2-treated cells exhibited cell cycle arrest in the G_1-phase. These data indicated that the growth inhibition by BMP-2 may be mediated by p21/WAF1/CIP1 in OUMS37 and MKN74 cells.

It was shown previously that p21/WAF1/CIP1 stimulates withdrawal from the cell cycle coupled to terminal differentiation [34]. In addition, epithelial–mesenchymal interactions are essential for normal development of the chicken proventriculus corresponding to the mammalian stomach [10]. *BMP-2*, one of the important genes expressed in the mesenchyme, contributes to proventricular gland formation and ECPg expression [12]. In the present study, rhBMP-2 increased the expression of pepsinogen II, a differentiation marker of stomach glandular cells, in MKN74 cells. Thus, BMP-2 may lead to differentiation of MKN74 cells. The inductive activation of cell differentiation by BMP-2 has been reported for several cell types including astrocytes, cardiomyocytes, and myoblast cells [5,35,36].

In conclusion, we revealed that BMP-2 caused cell cycle arrest in the G_1-phase in OUMS37 and MKN74 cells, and that this growth inhibitory action may be mediated by p21/WAF1/CIP1. We also showed that BMP-2 up-regulated pepsinogen II in MKN74 cells. Our findings indicate that the BMP pathway may play a pivotal role in modulating gastric epithelial cell behavior including that of gastric cancer cells. Further analyses of the effects of BMP-2 on gastric cells are necessary to better understand the roles of BMP-2 in gastric epithelial cell growth and differentiation.

Acknowledgments

We are grateful to Yamanouchi Pharmaceutical Co. for generously providing the rhBMP-2. We also thank Dr. Masayoshi Namba for the kind gift of OUMS37 cells.

References

[1] J.M. Wozney, V. Rosen, A.J. Celeste, L.M. Mitsock, M.J. Whitters, R.W. Kriz, R.M. Hewick, E.A. Wang, Novel regulators of bone formation: molecular clones and activities, Science 242 (1988) 1528–1534.
[2] B.L. Hogan, Bone morphogenetic proteins: multifunctional regulators of vertebrate development, Genes Dev. 10 (1996) 1580–1594.
[3] J.M. Wozney, The bone morphogenetic protein family and osteogenesis, Mol. Reprod. Dev. 32 (1992) 160–167.
[4] K. Miyazono, K. Kusanagi, H. Inoue, Divergence and convergence of TGF-beta/BMP signaling, J. Cell. Physiol. 187 (2001) 265–276.
[5] T. Katagiri, A. Yamaguchi, M. Komaki, E. Abe, N. Takahashi, T. Ikeda, V. Rosen, J.M. Wozney, A. Fujisawa-Sehara, T. Suda, Bone morphogenetic protein-2 converts the differentiation pathway of C2C12 myoblasts into the osteoblast lineage, J. Cell Biol. 127 (1994) 1755–1766.
[6] K.M. Lyons, R.W. Pelton, B.L. Hogan, Organogenesis and pattern formation in the mouse: RNA distribution patterns suggest a role for bone morphogenetic protein-2A (BMP-2A), Development 109 (1990) 4833–4844.
[7] M. Kretzschmar, F. Liu, A. Hata, J. Doody, J. Massague, The TGF-beta family mediator Smad1 is phosphorylated directly and activated functionally by the BMP receptor kinase, Genes Dev. 11 (1997) 984–995.
[8] C.H. Heldin, K. Miyazono, P. ten Dijke, TGF-beta signaling from cell membrane to nucleus through SMAD proteins, Nature 390 (1997) 465–471.
[9] F. Liu, A. Hata, J.C. Baker, J. Doody, J. Cárcamo, R.M. Harland, J. Massagué, A human Mad protein acting as a BMP-regulated transcriptional activator, Nature 381 (1996) 620–623.
[10] S. Yasugi, Role of epithelial–mesenchymal interactions in differentiation of epithelium of vertebrate digestive organs, Dev. Growth Differ. 35 (1993) 1–9.
[11] Y. Yuasa, Control of gut differentiation and intestinal-type gastric carcinogenesis, Nat. Rev. Cancer 3 (2003) 592–600.
[12] T. Narita, K. Saitoh, T. Kameda, A. Kuroiwa, M. Mizutani, C. Koike, H. Iba, S. Yasugi, BMPs are necessary for stomach gland formation in the chicken embryo: a study using virally induced BMP-2 and noggin expression, Development 127 (2000) 981–988.
[13] N. Dewulf, K. Verschueren, O. Lonnoy, A. Moren, S. Grimsby, K. Vande Spiegle, K. Miyazono, D. Huylebroeck, P. ten Dijke, Distinct spatial and temporal expression patterns of two type I receptors for bone morphogenetic proteins during mouse embryogenesis, Endocrinology 136 (1995) 2652–2663.
[14] H. Chang, D. Huylebroeck, K. Verschueren, Q. Guo, M.M. Matzuk, A. Zwijsen, Smad5 knockout mice die at mid-gestation due to multiple embryonic and extraembryonic defects, Development 126 (1999) 1631–1642.
[15] H. Jarvinen, K.O. Franssila, Familial juvenile polyposis coli: increased risk of colorectal cancer, Gut 25 (1984) 792–800.
[16] J.R. Howe, F.A. Mitros, R.W. Summers, The risk of gastrointestinal carcinoma in familial juvenile polyposis, Ann. Surg. Oncol. 5 (1998) 751–756.
[17] J.R. Howe, J.L. Bair, M.G. Sayed, M.E. Anderson, F.A. Mitros, G.M. Petersen, V.E. Velculescu, G. Traverso, B. Vogelstein, Germline mutations of the gene encoding bone morphogenetic protein receptor 1A in juvenile polyposis, Nat. Genet. 28 (2001) 184–187.
[18] M. Katoh, M. Terada, Overexpression of bone morphogenic protein (BMP)-4 mRNA in gastric cancer cell lines of poorly differentiated type, J. Gastroenterol. 31 (1996) 137–139.
[19] G.A. Wong, V. Tang, F. El-Sabeawy, R.H. Weiss, BMP-2 inhibits proliferation of human aortic smooth muscle cells via human p21cip1/waf1, Am. J. Physiol. Endocrinol. Metab. 284 (2003) 972–979.
[20] G. Ghosh-Choudhury, Y.S. Kim, M. Simon, J. Wozney, S. Harris, N. Ghosh-Choudhury, H.E. Abboud, Bone morphogenetic protein 2 inhibits platelet-derived growth factor-induced c-fos gene transcription and DNA synthesis in mesangial cells. Involvement of mitogen-activated protein kinase, J. Biol. Chem. 274 (1999) 10897–10902.
[21] H. Ide, T. Yoshida, N. Matsumoto, K. Aoki, Y. Osada, T. Sugimura, M. Terada, Growth regulation of human prostate cancer cells by bone morphogenetic protein-2, Cancer Res. 57 (1997) 5022–5027.
[22] F. Pouliot, C. Labrie, Role of Smad1 and Smad4 proteins in the induction of p21/WAF1/CIP1 during bone morphogenetic protein-induced growth arrest in human breast cancer cells, J. Endocrinol. 172 (2002) 187–198.
[23] M. Ito, W. Yasui, E. Kyo, H. Yokozaki, H. Nakayama, H. Ito, E. Tahara, Growth inhibition of transforming growth factor beta on human gastric carcinoma cells: receptor and postreceptor signaling, Cancer Res. 52 (1992) 295–300.
[24] H. Yokozaki, Molecular characteristic of eight gastric cancer cell lines established in Japan, Pathol. Int. 50 (2000) 767–777.
[25] H. Pu, C. Gao, T. Yuasa, M. Namba, A. Kondo, K. Inada, M. Sakaguchi, Establishment and characterization of a rat

pepsin-producing gastric cell line (OUMS37), In Vitro Cell Dev. Biol. Anim. 35 (1999) 488–490.
[26] Y.Q. Bai, Y. Akiyama, H. Nagasaki, O.K. Yagi, Y. Kikuchi, N. Saito, K. Takeshita, T. Iwai, Y. Yuasa, Distinct expression of CDX2 and GATA4/5, development-related genes, in human gastric cancer cell lines, Mol. Carcinog. 28 (2000) 184–188.
[27] M. Irwin, M.C. Marin, A.C. Philips, R.S. Seelan, D.I. Smith, W. Liu, E.R. Flores, K.Y. Tsai, T. Jacks, K.H. Vousden, W.G. Kaelin Jr., Role for the p53 homologue p73 in E2F-1-induced apoptosis, Nature 407 (2000) 645–648.
[28] C.J. Sherr, J.M Roberts, CDK inhibitors: positive and negative regulators of G1-phase progression, Genes Dev. 13 (1999) 1501–1512.
[29] K. Park, S.J. Kim, Y.J. Bang, J.G. Park, N.K. Kim, A.B. Roberts, M.B. Sporn, Genetic changes in the transforming growth factor beta (TGF-beta) type II receptor gene in human gastric cancer cells: correlation with sensitivity to growth inhibition by TGF-beta, Proc. Natl. Acad. Sci. USA 91 (1994) 8772–8776.
[30] B. Renault, D. Calistri, G. Buonsanti, O. Nanni, D. Amadori, G.N. Ranzani, Microsatellite instability and mutations of p53 and TGF-beta RII genes in gastric cancer, Hum. Genet. 98 (1996) 601–607.
[31] F. Vincent, M. Nagashima, S. Takenoshita, M.A. Khan, A. Gemma, K. Hagiwara, W.P. Bennett, Mutation analysis of the transforming growth factor-beta type II receptor in human cell lines resistant to growth inhibition by transforming growth factor-beta, Oncogene 15 (1997) 117–122.
[32] Y. Shitara, H. Yokozaki, W. Yasui, S. Takenoshita, Y. Nagamachi, E. Tahara, Mutation of the transforming growth factor-beta type II receptor gene in human sporadic gastric carcinomas, Int. J. Oncol. 12 (1998) 1061–1065.
[33] H. Ijichi, T. Ikenoue, N. Kato, Y. Mitsuno, G. Togo, J. Kato, F. Kanai, Y. Shiratori, M. Omata, Systematic analysis of the TGF-β–Smad signaling pathway in gastrointestinal cancer cells, Biochem. Biophys. Res. Commun. 289 (2001) 350–357.
[34] O. Halevy, B.G. Novitch, D.B. Spicer, S.X. Skapek, J. Rhee, G.J. Hannon, D. Beach, A.B. Lassar, Correlation of terminal cell cycle arrest of skeletal muscle with induction of p21 by MyoD, Science 267 (1995) 1018–1021.
[35] K. Nakashima, M. Yanagisawa, H. Arakawa, T. Taga, Astrocyte differentiation mediated by LIF in cooperation with BMP-2, FEBS Lett. 457 (1999) 43–46.
[36] K. Monzen, I. Shiojima, Y. Hiroi, S. Kudoh, T. Oka, E. Takimoto, D. Hayashi, T. Hosoda, A. Habara-Ohkubo, T. Nakaoka, T. Fujita, Y. Yazaki, I. Komuro, Bone morphogenetic proteins induce cardiomyocyte differentiation through the mitogen-activated protein kinase kinase kinase TAK1 and cardiac transcription factors Csx/Nkx-2.5 and GATA-4, Mol. Cell. Biol. 19 (1999) 7096–7105.

Developmental Biology 245, 291–303 (2002)
doi:10.1006/dbio.2002.0637, available online at http://www.idealibrary.com on IDEAL®

Significance of Bone Morphogenetic Protein-4 Function in the Initial Myofibrillogenesis of Chick Cardiogenesis

Yuji Nakajima,*,†,[1] Toshiyuki Yamagishi,† Katsumi Ando,† and Hiroaki Nakamura†

**Department of Anatomy, Graduate School of Medicine, Osaka City University, 1-4-3 Asahimachi, Abenoku, Osaka 545-8585 Japan; and †Department of Anatomy, Saitama Medical School, 38 Morohongo, Moroyamacho, Irumagun, Saitama 350-0495 Japan*

The heart is the first organ to form and function during vertebrate embryogenesis. Using a secreted protein, noggin, which specifically antagonizes bone morphogenetic protein (BMP)-2 and -4, we examined the role played by BMP during the initial myofibrillogenesis in chick cultured precardiac mesoendoderm (mesoderm + endoderm; ME). Conditioned medium from COS7 cells transfected with *Xenopus* noggin cDNA inhibited the expression of sarcomeric proteins (such as sarcomeric α-actinin, Z-line titin, and sarcomeric myosin), and so myofibrillogenesis was perturbed in cultured stage 4 precardiac ME; however, it did not inhibit the expression of smooth muscle α-actin (the first isoform of α-actin expressed during cardiogenesis). In cultured stage 5 precardiac ME, noggin did not inhibit either the formation of I-Z-I components or the expression of sarcomeric myosin, but it did inhibit the formation of A-bands. Although BMP4 was required to induce expressions of sarcomeric α-actinin, titin, and sarcomeric myosin in cultured stage 6 posterolateral mesoderm (noncardiogenic mesoderm), smooth muscle α-actin was expressed without the addition of BMP4. Interestingly, in cultured stage 6 posterolateral mesoderm, BMP2 induced the expressions of sarcomeric α-actinin and titin, but not of sarcomeric myosin. These results suggest that (1) BMP4 function lies upstream of the initial formation of I-Z-I components and A-bands separately in a stage-dependent manner, and (2) at least two signaling pathways are involved in the initial cardiac myofibrillogenesis: one is an unknown pathway responsible for the expression of smooth muscle α-actin; the other is BMP signaling, which is involved in the expression of sarcomeric α-actinin, titin, and sarcomeric myosin. © 2002 Elsevier Science (USA)

Key Words: **myofibrillogenesis; heart development; noggin; BMP (bone morphogenetic protein); chick embryo.**

INTRODUCTION

The heart is the first organ to form and function during vertebrate embryogenesis. In the pregastrula chick embryo, cells that contribute to the heart are found within the posterior half of the epiblast (Rawles, 1943; Hatada and Stern, 1994). During early gastrulation (stage 3; Hamburger and Hamilton, 1951), cardiac precursor cells migrate and are located within a region of the primitive streak caudal to Hensen's node. Thereafter, they migrate into the mesoderm and spread anterolaterally, resulting in the formation of right and left precardiac mesoderms (Rosenquist and DeHann, 1966; Garcia-Martinez and Schoenwolf, 1993). The anterior endoderm originates from cells within the node itself (Selleck and Stern, 1991). Consequently, prospective cardiac regions, containing precardiac mesoderm and anterior endoderm, have been completed by stage 4–5. In avian embryos, heart specification occurs in stage 3 primitive streak, and determination occurs during late gastrulation and is completed by stage 7–8 (Sater and Jacobson, 1989; Schultheiss and Lassar, 1999; Lough and Sugi, 2000).

During gastrulation, presumptive heart cells become committed to the cardiac-muscle lineage; at this time, the anterior endoderm subjacent to the precardiac mesoderm expresses bone morphogenetic protein (BMP)-2 and -4, members of the transforming growth factor (TGF)-β superfamily (Hogan, 1996; Schultheiss *et al.*, 1997). It has been

[1] To whom correspondence should be addressed at: Department of Anatomy, Graduate School of Medicine, Osaka City University, 1-4-3 Asahimachi, Abenoku, Osaka 545-8585 Japan. Fax: +81-6-6646-3603. E-mail: yuji@med.osaka-cu.ac.jp.

0012-1606/02 $35.00

reported that tissue from the avian midgastrula posterior primitive streak—which normally gives rise to extraembryonic mesoderm, including blood islands—will differentiate into cardiac muscle when cocultured with anterior endoderm (Schultheiss *et al.*, 1995). Another experiment showed that ectopic implantation of BMP-soaked beads into noncardiogenic mesoderm induces the cardiac-specific marker gene *Nkx-2.5*, which is a homologue of the *Drosophila tinman* gene (Schultheiss *et al.*, 1997). In *Drosophila*, *tinman* is expressed by Dpp signaling—Dpp being a member of the BMP family—and is required for heart formation (Frasch, 1995; Harvey, 1996). It has also been found that when noncardiogenic mesoderm from a chick stage 5–6 embryo is cultured in the presence of BMP2 plus FGF4, it can differentiate to a beating tissue (Lough *et al.*, 1996, Ladd *et al.*, 1998, Barron *et al.*, 2000). *BMP2*-knockout mutant embryos show abnormal heart development, ranging from complete absence to ectopic heart formation (Zhang and Bradley, 1996). *BMP4*-null mutants or *type I BMP receptor*-null mutants die before gastrulation, and thus cardiogenesis in these two mutants has not been examined (Winnier *et al.*, 1995; Mishima *et al.*, 1995). On the other hand, *Nkx-2.5*-null mutant mice die at around 9–10 days, but a beating heart tube still develops even though cardiac looping is disrupted (Lyons *et al.*, 1995). In these *Nkx-2.5*-null mutant hearts, several genes encoding myofibrillar proteins are normally expressed, although that encoding ventricular myosin light chain-2 is not (Lyons *et al.*, 1995). Recent experiments have implied that BMP, which is secreted by the endoderm of the presumptive heart field, is essential but not sufficient for the induction of cardiac muscle differentiation from a field of competent cells in the anterolateral mesoderm (Schultheiss *et al.*, 1997; Ladd *et al.*, 1998). However, still unclear is what kind of myofibrillar proteins lie downstream of BMP function in the initial myofibrillogenesis that occurs soon after the heart determination is completed.

Soon after heart determination has taken place, proteins for myofibrillar components are synthesized in the chick embryonic heart (at stage 6–7, just 10 h before spontaneous beating begins) (Ruzicka and Schwartz, 1988; Han *et al.*, 1992; Sugi and Lough, 1992). The assembly of these myofibrillar proteins into a functional unit, the sarcomere, must therefore be a rapid and well-coordinated process in early cardiogenesis. Indeed, there are biochemical data indicating coordinated synthesis of actin, myosin, and α-actinin during vertebrate myogenesis (Devlin and Emerson, 1978). To try to explain the processes involved in myofibrillogenesis, numerous studies have been performed and several models have been proposed. In one model in cultured cardiomyocytes, the first step involves a stress fiber-like structure acting as a scaffold (Dlugosz *et al.*, 1984); then, I-Z-I proteins (the Z-disk components being sarcomeric α-actinin, α-actin, and titin) and thick filaments (consisting mainly of myosin) are assembled independently, to later become incorporated into striated myofibrils (Wang *et al.*, 1988; Schultheiss *et al.*, 1990; Lu *et al.*, 1992; Lin *et al.*, 1994; Holtzer *et al.*, 1997). A different model is the premyofibril model proposed by Sanger's group (Rhee *et al.*, 1994; LoRusso *et al.*, 1997; Turnacioglu *et al.*, 1997). The premyofibril, a primordium of the mature myofibril, consists of minisarcomeres containing thin filaments, α-actinin, and nonmuscle myosin IIb. Later, the distance between the dense materials of the minisarcomere increases, the N-terminal region of titin is incorporated into the Z-band of the nascent myofibril, and nonmuscle myosin is replaced by muscle-specific myosin. Confocal microscopic *in situ* analysis of myofibrillogenesis in the chick embryonic heart by Ehler *et al.* (1999) has shown that thin and thick filaments are assembled in an independent manner, and that I-Z-I proteins are organized as a dense body-like structure in nascent cardiomyocytes.

In the present study, using a secreted protein, noggin—which antagonizes BMP activity and interacts specifically with BMP2 and -4, but not with other TGF family members (Re'em-Kalma *et al.*, 1995; Zimmerman *et al.*, 1996)—we investigated the role of BMP signaling in the initial heart myofibrillogenesis. Our results show that, in cultured stage 4 precardiac mesoendoderm (mesoderm + endoderm; ME), noggin inhibited the expression of sarcomeric α-actinin, titin, and sarcomeric myosin, thus perturbing the formation of sarcomeres, but it did not suppress the expression of the first isoform of α-actin, smooth muscle α-actin. In stage 5 precardiac ME, noggin did not inhibit either the formation of I-Z-I components or the expression of sarcomeric myosin, but it did inhibit the formation of the thick filaments of sarcomeric myosin (A-bands). Further, recombinant BMP4 induced expressions of sarcomeric α-actinin, titin, and sarcomeric myosin in cultured stage 6 noncardiogenic mesoderm, in which smooth muscle α-actin was expressed spontaneously even without the addition of BMP protein. These results suggest that (1) during the initial myofibrillogenesis, BMP4 functions upstream of the formation of I-Z-I components and A-bands, on which it acts separately, and that its role the initial myofibrillogenesis is stage dependent, and (2) at least two signaling pathways take part in the initial myofibrillogenesis [viz. BMP signaling(s) (involved in the expression of sarcomeric α-actinin, titin, and sarcomeric myosin) and another unknown type of signaling(s) (responsible for the expression of smooth muscle α-actin)].

MATERIALS AND METHODS

Culture Procedures

Stage 4 or 5 chick embryos (Hamburger and Hamilton, 1951) were collected on ice-cooled phosphate-buffered saline (PBS), and precardiac ME was cultured as previously described (Sugi *et al.*, 1993). Precardiac regions containing three germ layers were excised and separated in 0.25% trypsin (GIBCO). The ME layers were explanted onto bovine fibronectin-coated (GIBCO) chamber slides (Nunc) and cultured with (1) DMEM supplemented with 10% FBS, (2) conditioned medium from COS7 cells transfected with vector alone (Mock), or (3) conditioned medium from COS7 cells trans-

fected with *Xenopus* noggin cDNA. Stage 6 posterolateral mesoderm was resected and cultured with or without recombinant BMP4 (R&D Systems) in 10% FBS/DMEM. Identical regions were cultured with or without recombinant BMP4 or −2 (R&D Systems) in defined medium (75% DMEM, 25% McCoy's medium, supplemented with 10^{-7} M dexamethasone and penicillin-streptomycin; Ladd *et al.*, 1998).

COS 7 Cell Transfection

COS 7 cell transfection was performed as previously described (Tonegawa and Takahashi, 1998). COS7 cells were cultured in DMEM/10% FBS. Cells grown until 70–80% confluent were transfected with 1 μg of pCDM8-derived COS-expression vector, which contains an elongation factor promoter and *Xenopus* noggin cDNA (a gift from Dr. Takahashi, Nara, Japan), with lipofectamine (GIBCO) being used according to the manufacturer's recommendations. Conditioned medium was harvested after 48 h, and used as a source of noggin.

Reverse Transcription (RT)-PCR

Explants were collected and RNA extracted as described by Yamagishi *et al.* (1999). cDNAs were synthesized from 0.2 mg total RNA, and PCR was carried out in 10 μl of reaction buffer (0.2 mM dNTPs, 1 mM primers, 0.05 U Taq DNA polymerase). The sequences of the primers have been described elsewhere [Nkx-2.5 (Schultheiss *et al.*, 1995), GATA4 (Schultheiss *et al.*, 1997), MyoD (pair "a"; Lin-Jones and Hauschka, 1996), GAPDH (Yamagishi *et al.*, 1999)]. The primers for sarcomeric α-actinin were 5′-GCCATCAGAGGGAAAAATGG and 5′-ACGGACTTCTGTCAGAGATG (Accession No. X13874; Arimura *et al.*, 1988). Samples were cycled at 93°C for 30 s, at annealing temperature (sarcomeric α-actinin, 57°C; Nkx-2.5, 57°C; GATA4, 57°C; MyoD, 55°C; GAPDH, 45°C) for 30 s, and at 72°C for 90 s, with a final extension at 72°C for 10 min. The cycle numbers for the various primers were as follows: sarcomeric α-actinin, 26 cycles; Nkx-2.5, 30; GATA4, 26; MyoD, 28; and GAPDH, 28. PCR products were electrophoresed, then stained with ethidium bromide.

In Situ Hybridization

Digoxigenin-labeled single-strand RNA probes were prepared by using a DIG-RNA labeling kit (Roche Diagnostics). A 747-bp fragment of chick Nkx-2.5 cDNA (base pairs 76–823 in Accession No. X91838; Schultheiss *et al.*, 1995) or a 738-bp fragment of chick GATA4 cDNA (base pairs 106–843 in Accession No. U11887; Laverriere *et al.*, 1994) was subcloned into pGem3Z and pBluescript II KS (−). Antisense Nkx-2.5 and antisense GATA4 were produced by using *Eco*RI/SP6 RNA polymerase and *Eco*RI/T7 RNA polymerase, respectively. Explants were fixed with 4% paraformaldehyde in PBS for 30 min, washed in 0.1% DEPC/PBS, and equilibrated with 5× SSC for 15 min. They were then prehybridized in hybridization solution (50% formamide, 5× SSC, 40 mg/ml salmon sperm DNA) at 65°C for 2 h and hybridized for 12 h at 65°C. After the hybridization, samples were washed in 2× SSC for 30 min at room temperature, in 2× SSC for 1 h at 65°C, then in 0.1× SSC for 1 h at 65°C. After rinsing with Tris-buffered saline, samples were incubated with alkaline phosphatase-conjugated anti-digoxigenin antibody (diluted 1:5000 in 0.5% blocking reagent; Roche Diagnostics) for 2 h, and the hybridization was detected by BCIP/NBT.

Antibodies

The monoclonal antibodies anti-Z-line titin (anti-titin, clone 9D10, IgM and anti-zeugmatin, clone mab20, IgG2a; Maher *et al.*, 1985; Turnacioglu *et al.*, 1997) and anti-sarcomeric myosin heavy chain (clone MF20, IgG2b; Bader *et al.*, 1982) were obtained from the Developmental Studies Hybridoma Bank (Iowa City, IA). The monoclonal antibodies anti-smooth muscle α-actin (clone 1A4, IgG2a; Skalli *et al.*, 1986), anti-sarcomeric α-actin (clone 5C5, IgM), and anti-sarcomeric α-actinin (clone EA53, IgG1) were purchased from Sigma. The polyclonal anti-pan-actinin (rabbit IgG) was kindly donated by Dr. Imanaka (Mie, Japan; Imanaka, 1988). For double immunohistochemistry, we used FITC-conjugated goat anti-mouse IgG2a, RITC-conjugated goat anti-mouse IgG2a, FITC-conjugated goat anti-mouse IgG1, FITC-conjugated goat anti-mouse IgG2b, and RITC-conjugated goat anti-mouse IgM (Southern Biotechnology Associates Co.) as secondary antibodies. Affinity-purified RITC-conjugated goat anti-rabbit IgG was purchased from Cappel.

Indirect Immunofluorescence Microscopy

Immunohistochemistry was performed as described by Nakajima *et al.* (1997). Cultures were drained of medium, rinsed with PBS, fixed with 4% paraformaldehyde/PBS for 30 min at room temperature, then rinsed with PBS. Specimens were blocked for 1 h with 1% BSA/PBS containing 0.1% Triton X-100, incubated with primary antibody (or primary antibody mixture) at 4°C overnight, rinsed with PBS, then incubated with FITC- or RITC-conjugated secondary antibody (or secondary antibody mixture) for 1 h at room temperature. Some specimens were stained with FITC- or RITC-phalloidin (Sigma). Samples were observed under the fluorescence microscope by using narrow-band mirror units (U-MNIBA and U-MNG; Olympus).

RESULTS

Conditioned Medium from noggin-Transfected COS7 Cells Inhibits Cardiogenesis in Cultured Stage 4 Precardiac ME

In the present paper, we used a conditioned medium obtained from COS7 cells transfected with *Xenopus* noggin cDNA as a source of noggin protein (Tonegawa and Takahashi, 1998). Therefore, it was necessary first to examine whether the noggin-conditioned medium had the physiological ability to inhibit BMP signaling during cardiogenesis in culture. When stage 4 precardiac ME was cultured in DMEM containing 10% FBS or in conditioned medium from COS7 cells transfected with vector alone (Mock), the central region of the explant became circumscribed by a defined border within which cardiac myocytes beat rhythmically after 48 h in culture (87% and 86% in stage 4 explants cultured in DMEM/10%FBS and Mock, respectively; Fig 1). In contrast, explants cultured in noggin showed a flat and epithelial-like structure, and only 6% of explants from stage 4 embryos generated beating tissues. This inhibitory effect was reversed by the addition of recombinant BMP4 to the conditioned medium containing noggin (Fig. 1).

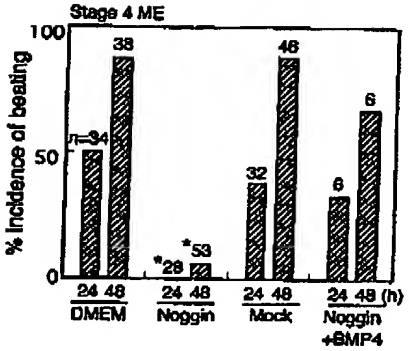

FIG. 1. Inhibition by noggin of the formation of a beating explant in precardiac ME. Stage 4 precardiac ME was cultured in DMEM/10% FBS, in conditioned medium from COS7 cells transfected with vector alone (Mock), or in conditioned medium from COS7 cells transfected with *Xenopus* noggin cDNA (Noggin). After 48 h, almost all precardiac ME cultured in DMEM or Mock generated beating tissue. On the other hand, only 6% of explants generated beating tissue when cultured in noggin. When explants were cultured in noggin plus 500 ng/ml BMP4 (Noggin + BMP4), the percentage generating beating tissue was similar to that seen when explants were cultured in DMEM (no statistical difference). An asterisk (*) indicates a value significantly different from other culture conditions ($P < 0.01$, Fisher's exact test). *n*, number of explants tested.

Next, we used *in situ* hybridization and examined whether or not the explants expressed the cardiac-specific marker genes, Nkx-2.5 and GATA4, because it has been reported that the expression of these genes is induced by BMP and inhibited by noggin in cultured precardiac ME (Schultheiss *et al.*, 1997). As shown in Fig. 2, 100% of stage 4 precardiac ME explants cultured in DMEM or Mock expressed both Nkx-2.5 and GATA4 after 48 h of incubation. On the other hand, explants treated with noggin did not express Nkx-2.5 to any appreciable extent (19% of explants exhibited a weak signal for Nkx-2.5), and GATA4 expression was completely suppressed (Fig. 2). These results (Figs. 1 and 2) indicated that conditioned medium obtained from COS7 cells that had been transfected with *Xenopus* noggin cDNA did indeed neutralize BMP2/4 signaling during chick cardiogenesis in culture.

Early Myofibrillogenesis Is Completed by 48 h in Cultured Stage 4 Precardiac ME

Before investigating the effect of noggin on the initial cardiac myofibrillogenesis, we carried out an immunohistochemical analysis of sarcomeric proteins in cultured stage 4 precardiac ME. Presumptive heart-forming ME was resected from stage 4 chick embryos and cultured in medium containing 10% FBS on plastic, with the resulting explant being fixed and double-stained with monoclonal antibodies against sarcomeric α-actinin (clone EA53), Z-line titin (clone 9D10 or mab20), smooth muscle α-actin (clone 1A4), and sarcomeric myosin (clone MF20). After 6–8 h in culture, there was no detectable staining for these sarcomeric proteins (data not shown). After 20 h in culture, tiny bead-like depositions of sarcomeric α-actinin were observed along the rhodamine-phalloidin-reactive F-actin, terminating at the epithelial-like cell borders (Fig. 3A). Sarcomeric α-actinin and F-actin were also present around the circumference at the cell–cell interfaces. At this time, no apparent sarcomeric structure was detected by using rhodamine-phalloidin staining. The N terminus domain of titin (Z-line

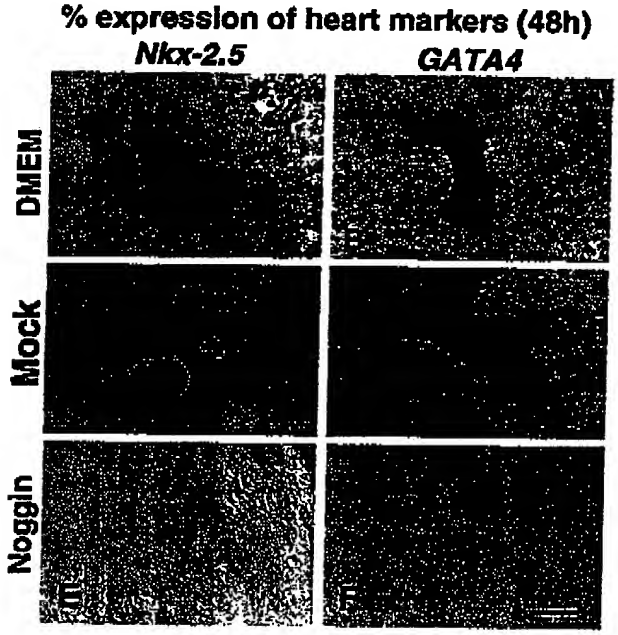

Culture conditions	% expression of heart markers (48h)	
	Nkx-2.5	*GATA4*
DMEM	100% (n=34)	100% (29)
Mock	100% (n=15)	100% (17)
Noggin	19% (16)*	0% (10)

FIG. 2. Stage 4 precardiac ME treated with noggin did not express heart marker genes. Stage 4 precardiac ME was cultured in DMEM/10% FBS with or without noggin. After 48 h, cultures were fixed and subjected to whole-mount *in situ* hybridization for Nkx-2.5 and GATA4. Among explants cultured in DMEM or Mock, 100% expressed Nkx-2.5 and GATA4 (arrowheads in A–D). Explants treated with noggin did not show heart marker genes to any appreciable extent (E, F). *, 19% of explants treated with noggin showed a weak signal for Nkx-2.5, slightly above sense control (not shown). Bar, 250 μm.

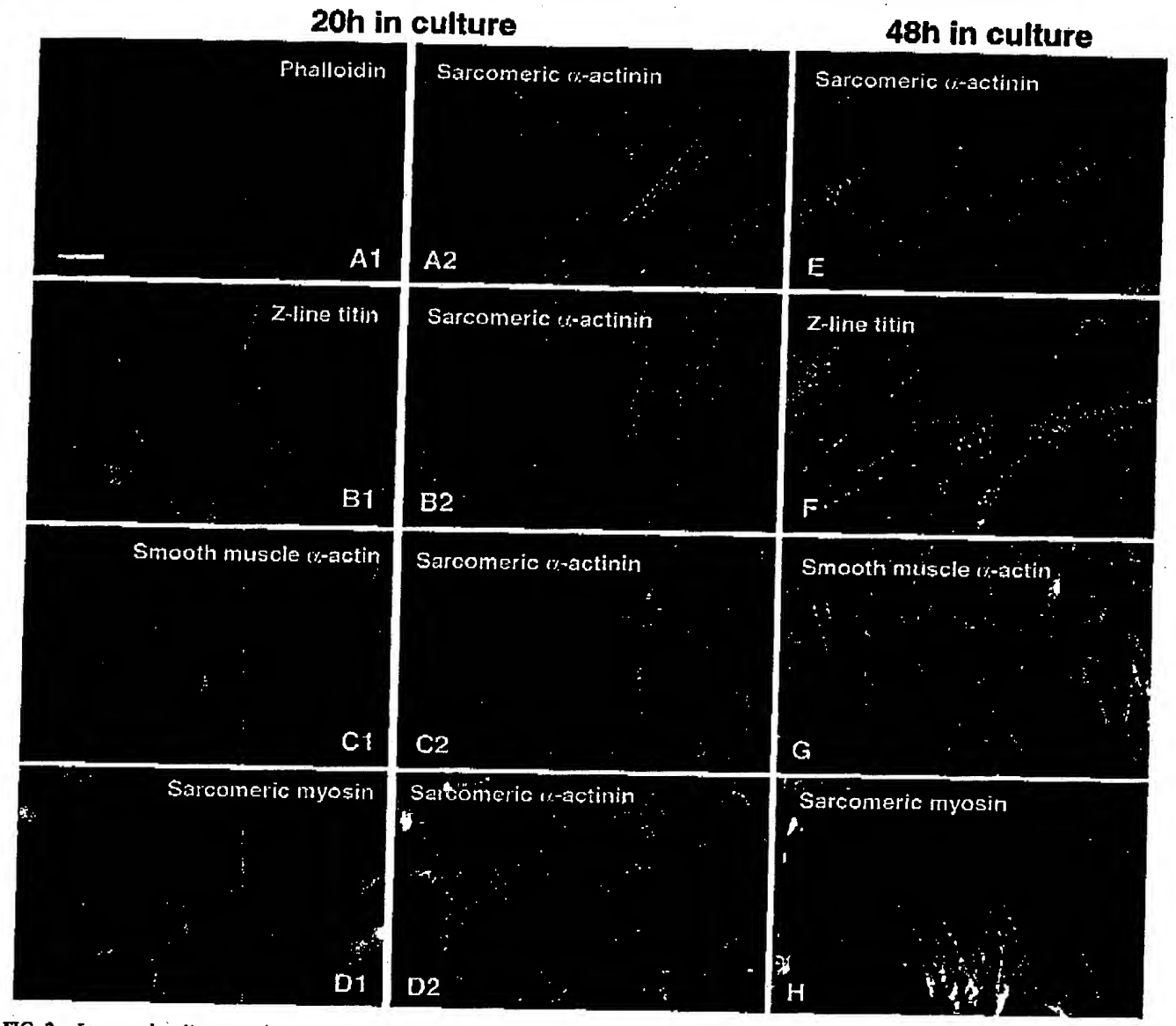

FIG. 3. Immunolocalization of sarcomeric proteins during initial myofibrillogenesis in cultured stage 4 precardiac ME. Precardiac ME of stage 4 embryos was cultured in DMEM/10% FBS and stained with antibodies against sarcomeric proteins. After 20 h in culture, tiny bead-like deposits of sarcomeric α-actinin were seen arranged linearly along F-actin (A), and were colocalized with titin (B). Smooth muscle α-actin was distributed as a stress-fiber-like structure, and was associated with sarcomeric α-actinin (C). Sarcomeric myosin was observed as cytoplasmic diffuse staining, and it was distributed independently of sarcomeric α-actinin (D). After 48 h in culture, the sarcomeric proteins we examined were incorporated into mature myofibrils exhibiting sarcomeres (E–H). Bar, 10 μm.

titin) was colocalized with the bead-like depositions of sarcomeric α-actinin (Fig. 3B). Smooth muscle α-actin was distributed as a stress fiber-like structure, and it was colocalized with sarcomeric α-actinin (Fig. 3C). Indeed, the cellular distribution of smooth muscle α-actin was coincident with that of phalloidin-reactive F-actin (not shown). The migrating mesenchymal cells surrounding the explant also expressed smooth muscle α-actin (not shown, presumably endocardial cushion mesenchymal cells; Nakajima *et al.*, 1997). Interestingly, there was no detectable staining for

sarcomeric α-actin (clone 5C5) in cultured stage 4 precardiac regions at around 20 h in incubation (not shown). Sarcomeric myosin (MF20) was distributed as a diffuse staining pattern in those cells within which bead-like sarcomeric α-actinin was observed (Fig. 3D). After 48 h in culture, although more than 80% of sarcomeric α-actinin, titin, and smooth muscle α-actin were incorporated into mature striated myofibrils, 52% of sarcomeric myosin was found as a sarcomeric pattern (Figs. 3E–3H; see Fig. 5). This immunohistochemical analysis of sarcomeric proteins in the cultured precardiac region made clear that an initial I-Z-I structure consisting of sarcomeric α-actinin, titin, and smooth muscle α-actin was generated by 20 h in culture and completed at around 48 h, and it appeared to be assembled independently of the diffusely distributed sarcomeric myosin at the onset of myofibrillogenesis. These results indicated that the antibodies against sarcomeric proteins we used can be expected to be reliable markers for the examination of early myofibrillogenesis in cultured precardiac ME.

Noggin Inhibits the Formation of Initial Myofibrillogenesis in Cultured Precardiac ME

To examine the role of BMP in the initial myofibrillogenesis of the developing chick heart, fluorescent immunohistochemical staining of the aforementioned sarcomeric proteins was performed against cultured stage 4 or 5 precardiac ME that had been incubated in noggin. When stage 4 precardiac ME was cultured in noggin, only 6% of explants had started to beat after 48 h in culture. In such explants, the expressions of sarcomeric α-actinin and titin were inhibited significantly (by comparison with those in explants cultured in DMEM/10% FBS or Mock) (Figs. 4 and 5). Tiny bead-like depositions of anti-panactinin immunoreactivity were observed in all cell types grown in explants treated with noggin (not shown). Most explants treated with noggin plus recombinant BMP4 protein (500 ng/ml) behaved in a manner similar to those cultured in DMEM/10% FBS (Fisher's exact test; data not shown): i.e., they beat spontaneously (Fig. 1) and expressed sarcomeric α-actinin assembled into Z-lines (not shown). In contrast, smooth muscle α-actin was expressed in 92% of explants treated with noggin; however, only 17% of these explants showed sarcomeric staining for smooth muscle α-actin (Figs. 4 and 5). Sarcomeric myosin was not detectable in explants treated with noggin (Figs. 4 and 5). Stage 5 precardiac ME treated with noggin generated an I-Z-I structure (consisting of sarcomeric α-actinin, titin, and smooth muscle α-actin) of a type similar to that seen in control cultures after 48 h. Although stage 5 explants treated with noggin expressed sarcomeric myosin with an incidence of 93%, only 22% of explants incorporated the sarcomeric myosin into A-bands in this culture condition (Figs. 4 and 5). These results indicate that, in stage 4 precardiac ME, noggin inhibited the expression of sarcomeric α-actinin, titin, and sarcomeric myosin, but not that of smooth muscle α-actin, thus perturbing the initial myofibrillogenesis. On this basis, it is hypothesized that at least two signaling pathways are involved in the initial myofibrillogenesis. In stage 5 precardiac ME, noggin inhibited the formation of A-bands even though sarcomeric myosin was expressed, but it did not inhibit the formation of the I-Z-I components, suggesting that BMP induces formation of A-bands and I-Z-I components differentially, in a stage-dependent manner.

Recombinant BMP4 Induces Expressions of Sarcomeric α-Actinin, Titin, and Sarcomeric Myosin in Stage 6 Noncardiogenic Mesoderm

To try to find support for the above hypothesis, we next examined whether BMP induces an expression of sarcomeric proteins in noncardiogenic mesoderm obtained from stage 6 posterolateral mesoderm, which gives rise to blood cells *in vivo*. We cultured stage 6 posterolateral mesoderm explants with or without recombinant BMP (BMP4 or -2) for 48 h, and stained them with antibodies against sarcomeric proteins. When posterolateral mesoderm was cultured without BMP, but with supplementary FBS, no apparent staining for sarcomeric α-actinin, titin, or sarcomeric myosin was observed, but smooth muscle α-actin was expressed (Fig. 6; Table 1). On the other hand, when it was cultured in DMEM + FBS supplemented with 500 ng/ml of recombinant BMP4 (Table 1) or in serum-free defined medium supplemented with a similar amount of recombinant BMP4, some cells did express sarcomeric α-actinin, titin, and sarcomeric myosin (Fig. 6; Table 1). Sarcomeric α-actinin and titin were deposited as tiny beads, and there was no apparent striation, at around 48 h in culture (Fig. 6), while sarcomeric myosin was distributed as a diffuse staining, and never showed striation (Fig. 6). Smooth muscle α-actin was expressed extensively and was coincident with F-actin in explants cultured with or without BMP (Fig. 6; Table 1). There was no detectable staining of sarcomeric α-actin after 48 h in culture (not shown). After an additional 24 h (total, 72 h in culture), some cells in the posterolateral mesoderm treated with BMP4 generated mature myofibrils with striations (not shown). Surprisingly, when similar posterolateral mesoderm was cultured in defined medium supplemented with BMP2, some 30–40% of explants expressed sarcomeric α-actinin and Z-line titin, but sarcomeric myosin was not expressed after 48 h in culture (Table 1).

We next examined whether such BMP4-treated noncardiogenic mesoderm expressed cardiac-specific marker genes. PCR amplification showed that explants treated with BMP4 expressed the cardiac muscle-related genes, sarcomeric α-actinin, Nkx-2.5, and GATA4, but not MyoD (Fig. 7). In contrast, explants cultured in DMEM/10% FBS without BMP4 did not express sarcomeric α-actinin, GATA4, or MyoD; however, they expressed Nkx-2.5 (Fig. 7). The expression of Nkx-2.5 in explants cultured without BMP is not entirely surprising, because several nonmuscle tissues express Nkx-2.5 at the mRNA and protein levels

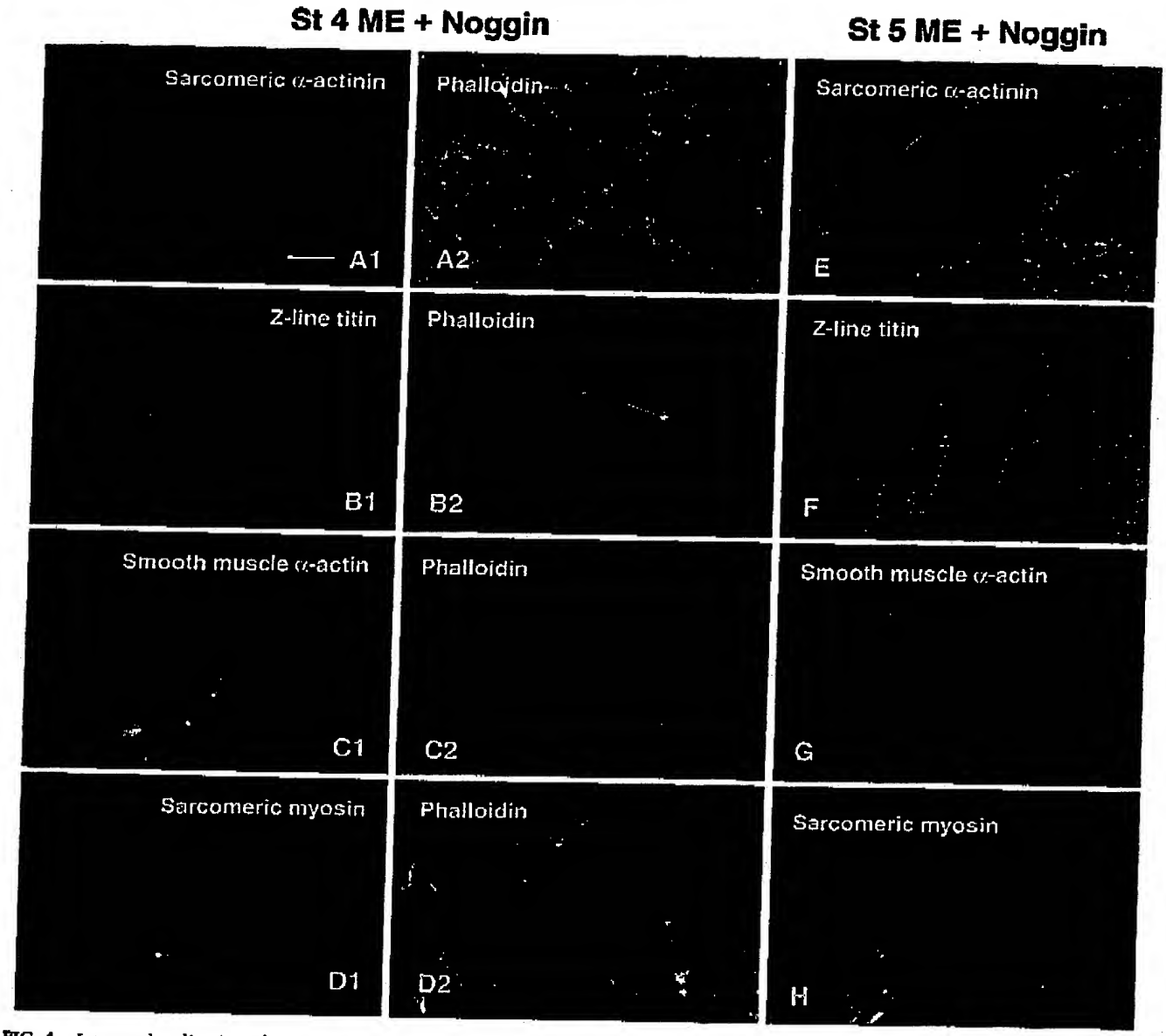

FIG. 4. Immunolocalization of sarcomeric proteins in cultured precardiac ME with or without noggin. When stage 4 precardiac ME were cultured in noggin, no detectable staining for sarcomeric α-actinin, titin, or sarcomeric myosin was observed after 48 h in culture (A, B, D). On the other hand, smooth muscle α-actin was expressed even if the explants were treated with noggin (C). While stage 5 ME explants treated with noggin generated I-Z-I components (E–G), sarcomeric myosin was expressed without the formation of A-bands after 48 h in culture (H). Note that the percentage incidence at which expression of sarcomeric proteins was detected is given in Fig. 5. Bar: (A), 50 μm; (B, C, E–G), 10 μm; (D, H), 25 μm.

during development (Kasahara *et al.*, 1998). The above results indicate that while BMP4 induces expressions of cardiac-specific genes in cultured noncardiogenic mesoderm, smooth muscle α-actin (the isoform of α-actin initially expressed in early cardiogenesis) is expressed independently of BMP. Thus, these results support the hypothesis that at least two signaling pathways are involved in the initial myofibrillogenesis in the heart: one is an unknown

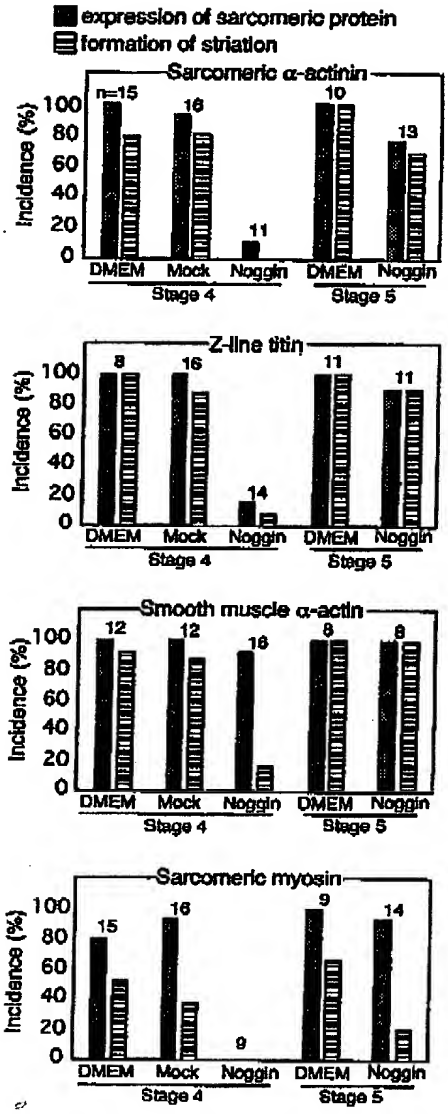

FIG. 5. Percentage incidence obtained for the expression of sarcomeric proteins and the formation of striation in cultured precardiac ME with or without noggin. In stage 4 precardiac ME, noggin inhibited the expressions of sarcomeric α-actinin, Z-line titin, and sarcomeric myosin, but not that of smooth muscle α-actin. In stage 5 precardiac ME, noggin did not inhibit the formation of I-Z-I components, but it did inhibit the formation of A-bands, even though there was a positive expression of sarcomeric myosin.

type of signaling responsible for the expression of smooth muscle α-actin, the other is the BMP signaling involved in the expression of sarcomeric α-actinin, titin, and sarcomeric myosin.

DISCUSSION

Heart Specification and Determination Occur during Gastrulation in Chick

During organogenesis, at least two levels of developmental commitment have been identified, viz. specification and determination (Slack, 1991). The timing of cardiac myocyte specification has been investigated in both amphibians and birds. In urodeles, cardiac specification occurs at around the neurula to tail-bud stage (Jacobson and Duncan, 1968), while in *Xenopus*, specification is highly committed by the end of gastrulation (Jacobson, 1961; Sater and Jacobson, 1989). In the chick, precardiac tissue is not yet specified in the epiblast or in the stage 3 primitive streak (Holtzer *et al.*, 1990; Inagaki *et al.*, 1993; Yatskievych *et al.*, 1997). Later, in the primitive streak of the stage 3–4 chick embryo, presumptive heart cells are specified at the tissue level (Gonzalez-Sanchez and Bader, 1990; Holtzer, *et al.*, 1990; Montgomomery, *et al.*, 1994), but they are not highly specified at the individual cell level (Montgomery *et al.*, 1994; Schultheiss and Lassar, 1999). Thereafter, precardiac cells originating from the primitive streak migrate into the anterior lateral region, and during this process they become highly specified to a heart lineage by stage 4+ (Antin *et al.*, 1994; Montogomery *et al.*, 1994; Gannon and Bader, 1995). In our experiments, cultured stage 4 precardiac ME that had differentiated to cardiomyocytes expressing the early cardiac marker genes, Nkx-2.5 and GATA4, were associated with sarcomeres after 48 h in culture. In contrast, stage 4 precardiac ME cultured in noggin did not express early cardiac marker genes, and they never generated sarcomeres. In addition, stage 5 precardiac ME treated with noggin generated I-Z-I components and expressed sarcomeric myosin, but it did not generate A-band. It has been reported that newly gastrulated cardiac progenitors (stage 4–6) were blocked in their differentiation by bromodeoxyuridine (BrdU), whereas later-staged progenitors (stage 7–8) were not (Montgomery *et al.*, 1994). Taken together, the progenitor cells of chick cardiac myocytes might be specified during gastrulation and then determined by stage 7–8.

BMP Acts Not Only Instructively, but Also Permissively in Early Chick Cardiogenesis

In cultured stage 4 precardiac ME, noggin inhibited not only the expression of early heart markers, but also the expression of sarcomeric proteins, and so it perturbed the initial myofibrillogenesis. In stage 5 precardiac ME, noggin did not inhibit the formation of I-Z-I components, but it did inhibit the formation of A-bands, even though there was a positive expression of sarcomeric myosin. It has been reported in the stage 6 chick embryo that implantation of BMP2-soaked beads into the anterior medial mesoderm (noncardiogenic region) can induce ectopic expressions of Nkx-2.5 and GATA4, and that similar regions cultured with BMP2 or -4 can undergo full cardiac differentiation (Schultheiss *et al.*, 1997; Andree *et al.*, 1998). We further

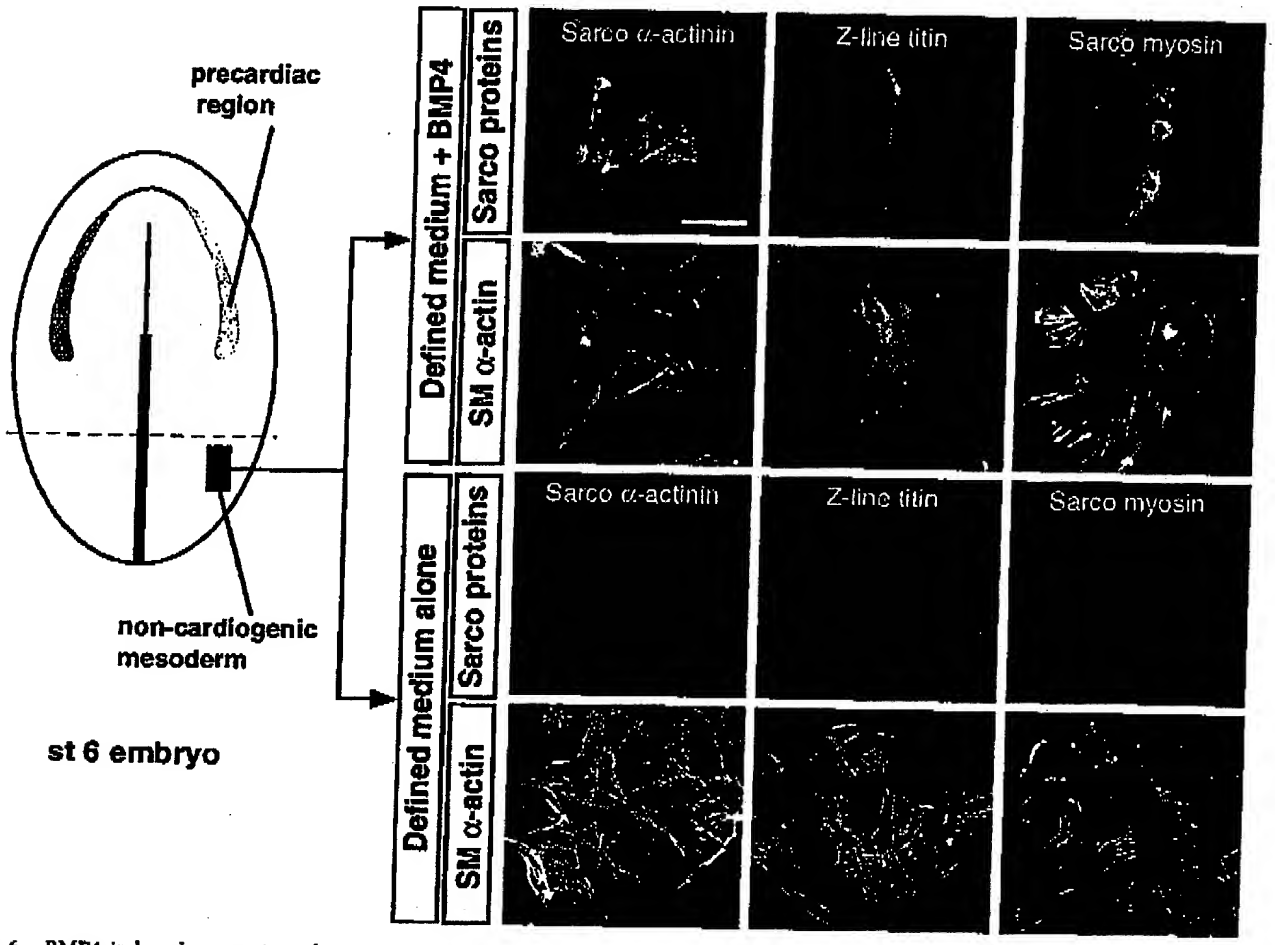

FIG. 6. BMP4 induced expression of sarcomeric proteins in cultured posterolateral mesoderm (noncardiogenic mesoderm). Noncardiogenic mesoderm was prepared from posterolateral mesoderm of stage 6 embryo was cultured in serum-free defined medium supplemented or not supplemented with BMP4. When noncardiogenic mesoderm was cultured in defined medium supplemented with BMP4 (500 ng/ml), sarcomeric (sarco) α-actinin, Z-line titin, and sarcomeric myosin were expressed after 48 h in culture; however, no apparent striation was observed by 48 h. On the other hand, noncardiogenic mesoderm cultured in serum-free defined medium alone never expressed sarcomeric α-actinin, Z-line titin, and sarcomeric myosin. Smooth muscle (SM) α-actin was expressed in noncardiogenic mesoderm cultured in defined medium with or without BMP4. Note that the percentage incidence obtained for the expression of sarcomeric proteins is given in Table 1. Bar, 25 μm.

showed that recombinant BMP4 was capable of committing stage 6 posterolateral mesoderm (noncardiac mesoderm) to a cardiomyocyte lineage, mature myofibrils associated with sarcomeres being assembled by 72 h in culture. Despite the significance of BMP signaling in cardiac myofibrillogenesis, BMP alone or BMP in combination with FGF4 fail to induce myogenesis in the cultured pregastrula chick epiblast (Ladd *et al.*, 1998), and isolated precardiac mesoderm from stage 4+−5 embryos gives rise to beating myocytes without the addition of BMP protein (Gonzalez-Sanchez and Bader, 1990; Antin *et al.*, 1994; our unpublished observations). In *Xenopus* cardiogenesis, BMPs are required for terminal myocyte differentiation as well as maintaining early transcriptional regulations of cardiac fate (Walters *et al.*, 2001). Consideration of the above evidences, taken together, suggested strongly to us that a transient exposure to BMP signals during gastrulation may be necessary to induce cardiac differentiation in competent tissue (Ladd *et al.*, 1998), and that the inducing ability of the BMP signal is probably not only "instructive" (influencing lineage decisions in the responding tissue), but also "permissive" (promoting differentiation of already committed precardiac

TABLE 1

Significance of Bone Morphogenetic Protein-4 Function in the Initial Myofibrillogenesis of Chick Cardiogenesis

Culture conditions	% expression of sarcomeric proteins (after 48 h)			
	Sarco α-actinin	Z-line titin	SM α-actin	Sarco myosin
DMEM/10% FBS	0 (n = 10)	0 (10)	100 (8)	0 (10)
DMEM/10% FBS + BMP4 (500 ng/ml)	82 (11)	100 (12)	100 (11)	91 (11)
Defined medium	0 (10)	0 (11)	100 (10)	0 (11)
Defined medium + BMP4 (500 ng/ml)	44 (16)	54 (11)	100 (16)	29 (17)
Defined medium + BMP2 (500 ng/ml)	30 (20)	40 (10)	100 (19)	0 (19)

Note. Percentage incidence at which expression of sarcomeric proteins was detected in stage 6 posterolateral mesoderm (noncardiogenic mesoderm) cultured with or without BMP protein. Note that when the explants were cultured in defined medium supplemented with BMP4 (500 ng/ml) + FGF4 (200 ng/ml), 93% (14/15) of explants expressed sarcomeric α-actinin and 88% (7/8) expressed sarcomeric α-actin; however, explants treated with BMP4 alone did not express sarcomeric α-actin. *n*, number of explants tested; sarco, sarcomeric; SM, smooth muscle

myocytes). In other words, BMP signaling lies upstream of both the expression of early heart marker genes and the initial myofibrillogenesis that takes place immediately after the gastrula stage.

BMP Regulates the Formation of I-Z-I Components and A-Bands Separately, in a Stage-Dependent Manner

As already mentioned, our results showed that initial heart myofibrillogenesis was inhibited by exogenously applied noggin protein. In cultured stage 4 precardiac ME, noggin inhibited the formation of I-Z-I components (consisting of sarcomeric α-actinin, Z-line titin, and smooth muscle α-actin) and of A-bands (thick filaments of sarcomeric myosin). However, in cultured stage 5 precardiac ME, noggin perturbed the formation only of A-bands, even though a positive expression of sarcomeric myosin was present at this stage. Furthermore, when stage 6 posterolateral mesoderm (noncardiogenic mesoderm) was cultured with BMP4, the cells expressed sarcomeric α-actinin, Z-line titin, and sarcomeric myosin. In contrast, when similarly prepared posterolateral mesoderm were cultured in BMP2, an expression of sarcomeric myosin was not induced, even though the I-Z-I components were expressed in a manner similar to that seen in explants cultured in BMP4. In the cardiac myofibrillogenesis we observed in cultured stage 4 precardiac ME, the I-Z-I components of the nascent myofibrils consisted of periodic tiny bead-like deposits of sarcomeric α-actinin/titin and thin filaments of smooth muscle α-actin, whereas the sarcomeric myosin was still distributed diffusely throughout the cell. This suggests that isolated I-Z-I components and thick filaments of sarcomeric myosin are organized independently, and then assembled at a later stage (Hill *et al.*, 1986; Tokuyasu and Maher, 1987; Furst *et al.*, 1989; Schultheiss *et al.*, 1990; Lu *et al.*, 1992; Ehler *et al.*, 1999). Taking our present results together with those published by others leads us to conclude that BMP functions upstream of the initial myofibrillogenesis in early cardiogenesis, and that they regulate the formation of I-Z-I components and A-bands separately, in a stage-dependent manner. Our results also suggest that, in cardiac myofibrillogenesis, the BMP4 function is more powerful than that of BMP2, as BMP4 induced an expression of sarcomeric myosin as well as an expression of I-Z-I components in posterolateral mesoderm (whereas BMP2 failed to induce sarcomeric myosin). One possibility is that at the onset of myofibrillogenesis *in vivo*, BMP4 and -2 act synergistically to induce the formation of I-Z-I components, and then

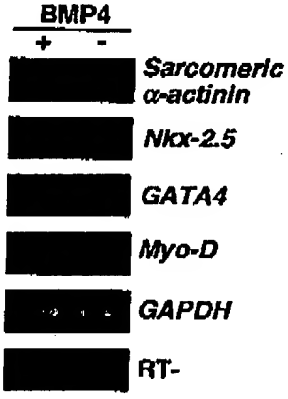

FIG. 7. BMP4 induced expression of cardiac marker genes in cultured posterolateral mesoderm (noncardiogenic mesoderm). Stage 6 posterolateral mesoderm was cultured in DMEM/FBS with or without BMP4. After 48 h in culture, cultures were subjected to PCR amplification (see Materials and Methods). PCR amplification showed that explants treated with BMP4 expressed sarcomeric α-actinin, Nkx-2.5, and GATA4, but not the skeletal muscle gene MyoD. Cells cultured in DMEM/10% FBS without BMP expressed only Nkx-2.5. GAPDH, the normalization control, was expressed equally under all culture conditions. GAPDH was not detected in any sample in the absence of reverse transcriptase (RT−).

BMP4 stimulates/maintains the expression of both I-Z-I components and A-bands.

At Least Two Signaling Pathways Lie Upstream of Initial Myofibrillogenesis

In cultured stage 4 precardiac ME, noggin inhibited the expressions of sarcomeric α-actinin, titin, and sarcomeric myosin, but not that of the earliest α-actin isoform, smooth muscle α-actin. Furthermore, recombinant BMP4 induced expressions of sarcomeric α-actinin, titin, and sarcomeric myosin in cultured stage 6 posterolateral mesoderm, while BMP2 induced the expressions of sarcomeric α-actinin and titin, but not of sarcomeric myosin in similarly prepared noncardiogenic mesoderm. In contrast, smooth muscle α-actin was expressed spontaneously, without the addition of BMP4. It has been reported that BMP2 plus FGF4 is needed to induce full cardiac differentiation (a beating heart with expression of sarcomeric α-actin) in cultured stage 6 posterolateral mesoderm (Lough *et al.*, 1996). Our results do not contradict this data, because 93% of stage 6 posterolateral mesoderm explants cultured with BMP4 plus FGF4 expressed sarcomeric α-actinin and 88% expressed sacomeric α-actin after 48 h in culture (data not shown) (when the similar regions were cultured with BMP4 alone, 44% of the explants expressed sarcomeric α-actinin but they did not express sacomeric α-actin). To judge from these two sets of results (1) BMP appear to commit the noncardiogenic mesoderm to a cardiac lineage and induce cariomyocyte differentiation (Walters *et al.*, 2001), while FGF4 stimulates its proliferation or makes its terminal differentiation occur more rapidly (Sugi *et al.*, 1993, Sugi and Lough, 1995), and (2) BMP4 appears to be a more powerful inducer for cardiac myofibrillogenesis than BMP2. Schultheiss *et al.* (1995, 1997) reported that while anterior endoderm induces the generation of a heart from the posterior primitive streak (noncardiogenic region), BMP cannot induce cardiogenesis in this region. They therefore proposed two signals for heart induction: unknown signals from the anterior endoderm seem to need to combine with BMP signaling to commit the presumptive heart-forming mesoderm to differentiate into a heart. Marvin *et al.* (2000) reported that inhibition of Wnt signaling promotes heart formation in the anterior lateral mesoderm, whereas active signaling in the posterior lateral mesoderm promotes blood development. Therefore, they proposed a model in which two orthogonal gradients, one of Wnt activity along the anterior–posterior axis and the other of BMP signals along the dorsal–ventral axis, intersect in the heart-forming region to induce cardiogenesis in a region of high BMP and low Wnt activity. Our explant-culture experiments followed by immunostaining for sarcomeric proteins suggest that at least two signaling pathways are required for the initiation of myofibrillogenesis in competent mesodermal cells during gastrulation: one is BMP-related signaling (involved in the expression of sarcomeric α-actinin, titin, and sarcomeric myosin), and the other is an unknown signaling that lies upstream of smooth muscle α-actin. A realistic candidate molecule for the unknown signal may be activin/TGFβ because (1) it has been reported that BMP signaling lies downstream of an activin/TGFβ signal in the cardiac myogenesis pathway (Ladd *et al.*, 1998) and (2) XTC/MIF (activin) has been found to induce the ventrolateral mesoderm to express smooth muscle α-actin in a *Xenopus* animal cap assay (Saint-Jeannet *et al.*, 1992). In addition, two discrete signaling interactions regulating cardiomyogenesis have been proposed in the early avian embryo: one is derived from the hypoblast and acts on the epiblast, while the other is secreted by the anterior endoderm and acts on the anterior lateral mesoderm. These signaling interactions are mimicked by activin/TGFβ and BMP, respectively (Lough *et al.*, 1996; Schultheiss *et al.*, 1997; Ladd *et al.*, 1998). Further experiments will be necessary to identify the unknown signaling molecule(s) that up-regulate the expression of smooth muscle α-actin and act synergistically with BMP to trigger the initial myofibrillogenesis.

In summary, we cultured precardiac ME with or without noggin followed by immunostaining for sarcomeric proteins, and revealed that (1) heart specification and determination occur during gastrulation in the chick embryo, (2) BMP acts not only instructively, but also permissively in early chick cardiogenesis, (3) the BMP function lies upstream of the initial myofibrillogenesis, and it regulates the formation of I-Z-I components and A-bands separately, in a stage-dependent manner, and (4) in addition to BMP, another unknown signaling pathway(s) responsible for the expression of smooth muscle α-actin is involved in the initial heart myofibrillogenesis.

ACKNOWLEDGMENTS

We thank Dr. Y. Takahashi for providing noggin-expression vector, Dr. K. Imanaka-Yoshida for anti-panactinin, and Ms. K. Yoneyama for technical assistance. The monoclonal antibodies were obtained from the Developmental Studies Hybridoma Bank developed under the auspices of the NICHD, and maintained by The University of Iowa, Department of Biological Sciences (Iowa City, IA). This work was supported by a Grant-in-Aid from the Ministry of Education, Science and Culture of Japan (No. 10670027 to Y.N.) and a grant from Welfide Medical Research Foundation 1999 (Y.N.).

REFERENCES

Andree, B., Duprez, D., Vorbusch, B., Arnold, H.-H., and Brand, T. (1998). BMP-2 induces ectopic expression of cardiac lineage markers and interferes with somite formation in chick embryos. *Mech. Dev.* 70, 119–131.

Antin, P. B., Taylor, R. G., and Yatskievych, T. (1994). Precardiac mesoderm is specified during gastrulation in quail. *Dev. Dyn.* 200, 144–154.

Arimura, C., Suzuki, T., Yanagisawa, M., Imamura, M., Hamada, Y., and Masaki, T. (1988). Primary structure of chicken skeletal muscle and fibroblast α-actinins deduced from cDNA sequences. *Eur. J. Biochem.* 177, 649–655.

Bader, D., Masaki, T., and Fischman, D. A. (1982). Immunochemical analysis of myosin heavy chain during avian myogenesis in vivo and in vitro. *J. Cell Biol.* 95, 763–770.

Barron, M., Gao, M., and Lough, J. (2000). Requirement for BMP and FGF signaling during cardiogenic induction in non-precardiac mesoderm is specific, transient, and cooperative. *Dev. Dyn.* 218, 383–393.

Devlin, R. B., and Emerson C. P. (1978). Coordinate regulation of contractile proteins during myoblast differentiation. *Cell* 13, 599–611.

Dlugosz, A. A., Antin, P. B., Nachmias, V. T., and Holtzer, H. (1984). The relationship between stress fiber-like structure and nascent myofibrils in cultured cardiac myocytes. *J. Cell Biol.* 99, 2268–2278.

Ehler, E., Rothen, B. M., Hammerle, S. P., Komiyama, M., and Perriard J.-C. (1999). Myofibrillogenesis in the developing chicken heart: assembly of Z-disk, M-line and thick filaments. *J. Cell Sci.* 112, 1529–1539.

Frasch, M. (1995). Induction of visceral and cardiac mesoderm by ectodermal DPP in the early Drosophila embryo. *Nature* 374, 464–467.

Furst, D., Osborn, M., and Weber, K. (1989). Myogenesis in the mouse embryo: Differential onset of expression of myogenic proteins and the involvement of titin in myofibril assembly. *J. Cell Biol.* 109, 517–527.

Gannon, M., and Bader, D. (1995). Initiation of cardiac differentiation occurs in the absence of anterior endoderm. *Development* 121, 2439–2450.

Garcia-Martinez, V., and Schoenwolf, G. C. (1993). Primitive-streak origin of cardiovascular system in avian embryos. *Dev. Biol.* 159, 706–719.

Gonzalez-Sanchez, A., and Bader, D. (1990). In vitro analysis of cardiac progenitor cell differentiation. *Dev. Biol.* 139, 197–209.

Hamburger, V., and Hamilton, H. L. (1951). A series of normal stages in the development of the chick embryo. *J. Morphol.* 88, 49–92.

Han, Y., Dennis, J. E., Cohen-Gould, L., Bader, D. M., and Fischman, D. A. (1992). Expression of sarcomeric myosin in the presumptive myocardium of chicken embryos occurs within 6 hours of myocyte commitment. *Dev. Dyn.* 193, 275–265.

Harvey, R. P. (1996). NK-2 homeobox genes and heart development. *Dev. Biol.* 178, 203–216.

Hatada, Y., and Stern, C. D. (1994). A fate map of the epiblast of the early chick embryo. *Development* 120, 2879–2899.

Hill, C. S., Duran, S., Lin, Z., Weber, K., and Holtzer, H. (1986). Titin and myosin, but not desmin are linked during myofibrillogenesis in postmitotic monomicleated myoblasts. *J. Cell Biol.* 101, 1413–1421.

Hogan, B. L. M. (1996). Bone morphogenetic proteins: Multifunctional regulators of vertebrate development. *Genes Dev.* 10, 1580–1594.

Holtzer, H., Schultheiss, T., Dilullo, C., Choi, J., Costa, M., Lu, M., and Holtzer, S. (1990). Autonomous expression of the differentiation programs of cells in the cardiac and skeletal myogenic lineages. *Ann. N.Y. Acad. Sci.* 599, 158–169.

Holtzer, H., Hijikata, T., Lin, Z. X., Zhang, Z. Q., Holtzer, S., Protasi, F., Franzini-Armstrong, C., and Sweeney, H. L. (1997). Independent assembly of 1.6 μm long bipolar MHC filaments and I-Z-I bodies. *Cell Struct. Funct.* 22, 83–93.

Imanaka, K. (1988). Rearrangement of myofibrils and intermediate filaments in cultured ventricular cardiomyocytes of the adult rat. *Mie Med. J.* 38, 223–241.

Inagaki, T., Garcia-Martinez, V., and Schoenwolf G. C. (1993). Regulative ability of the prospective cardiogenic and vasculogenic areas of the primitive streak during avian gastrulation. *Dev. Dyn.* 197, 57–68.

Jacobson, A. G. (1961). Heart determination in the newt. *J. Exp. Zool.* 146, 139–152.

Jacobson, A. G., and Sater, A. K. (1988). Features of embryonic induction. *Development* 104, 341–359.

Jacobson, A. G., and Duncan, J. T. (1968). Heart induction in salamanders. *J. Exp. Zool.* 167, 79–103.

Kasahara, H., Bartunkova, S., Schinke, M., Tanaka, M., and Izumo, S. (1998). Cardiac and extracardiac expression of Csx/Nkx2.5 homeodomain protein. *Circ. Res.* 82, 936–946.

Ladd, A. N., Yatskievych, T. A., and Antin, P. B. (1998). Regulation of avian cardiac myogenesis by activin/TGFβ and bone morphogenetic proteins. *Dev. Biol.* 204, 407–419.

Laverriere, A. C., MacNeill, C., Mueller, C., Poelmann, R. E., Burch, J. B. E., and Evans, T. (1994). GATA-4/5/6, a subfamily of three transcription factors transcribed in developing heart and gut. *J. Biol. Chem.* 269, 23177–23184.

Lin, Z., Lu, M.-H., Schultheiss, T., Choi, J., Holtzer, S., DiLullo, C., Fischman, D. A., and Holtzer, H. (1994). Sequential appearance of muscle-specific proteins in myoblasts as a function of time after cell division: Evidence for a conserved myoblast differentiation program in skeletal muscle. *Cell Motil. Cytoskeleton* 29, 1–19.

Lin-Jones, J., and Hauschka, S. D. (1996). Myogenic determination factor expression in the developing avian limb bud: An RT-PCR analysis. *Dev. Biol.* 174, 407–422.

LoRusso, S. M., Rhee, D., Sanger, J. M., and Sanger, J. W. (1997). Premyofibrils in spreading adult cardiomyocytes in tissue culture: Evidence for reexpression of the embryonic program for myofibrillogenesis in adult cells. *Cell Motil. Cytoskeleton* 37, 183–198.

Lough, J., Barron, M., Brogley, M., Sugi, Y., Bolender, D. L., and Zhu, X. (1996). Combined BMP-2 and FGF-4, but neither factor alone, induces cardiogenesis in non-precardiac embryonic mesoderm. *Dev. Biol.* 178, 198–202.

Lough, J., and Sugi, Y. (2000). Endoderm and heart development. *Dev. Dyn.* 217, 327–342.

Lu, M.-H., DiLullo, C., Schultheiss, T., Holtzer, S., Murray, J. M., Choi, J., Fischman, D. A., and Holtzer, H. (1992). The vinculin/sarcomeric-α-actinin/α-actinin nexus in cultured cardiac myocytes. *J. Cell Biol.* 117, 1007–1022.

Lyons, I., Parsons, L. M., Hartley, L., Li, R., Andrews, J. E., Robb, L., and Harvey, R. P. (1995). Myogenic and morphogenetic defects in the heart tubes of murine embryos lacking the homeo box gene Nkx2–5. *Genes Dev.* 9, 1654–1666.

Maher, P., Cox, G. F., and Singer, S. J. (1985). Zeugmatin: A new high molecular weight protein associated with Z-lines in adult and early embryonic striated muscle. *J. Cell Biol.* 101, 1871–1883.

Marvin, M. J., Rocco, G. D., Gardiner, A., Bush, S. M., and Lassar, A. B. (2000). Inhibition of Wnt activity induces heart formation from posterior mesoderm. *Genes Dev.* 15, 316–327.

Mishima, Y., Suzuki, A., Ueno, N., and Behringer, R. R. (1995). Bmpr encodes a type I bone morphogenetic protein receptor that is essential for gastrulation during mouse embryogenesis. *Genes Dev.* 9, 3027–3037.

Montgomery, M. O., Litvin, J., Gonzalez-Sanchez, A., and Bader, A. (1994). Staging of commitment and differentiation of avian cardiac myocytes. *Dev. Biol.* 164, 63–71.

Nakajima, Y., Mironov, V., Yamagishi, T., Nakamura, H., and Markwald, R. R. (1997). Expression of smooth muscle alph-actin in mesenchymal cells during formation of avian endocardial cushion tissue: a role for transforming growth factor β3. *Dev. Dyn.* 208, 296–309.

Rawles, M. E. (1943). The heart-forming regions of the early chick blastoderm. *Physiol. Zool.* 16, 22–42.

Re'em-Kalma, Y., Lamb, T., and Frank, D. (1995). Competition between noggin and bone morphogenetic protein 4 activities may regulate dorsalization during Xenopus development. *Proc. Natl. Acad. Sci. USA* 92, 12141–12145.

Rhee, D., Sanger, J. M., and Sanger, J. W. (1994). The premyofibril: Evidence for its role in myofibrillogenesis. *Cell Motil. Cytoskeleton* 28, 1–24.

Rosenquist, G. C., and DeHaan, R. L. (1966). Migration of precardiac cells in the chick embryo: A radiographic study. *Contrib. Embryol.* 38, 111–121.

Ruzicka, D. L., and Schwartz, R. J. (1988). Sequential activation of α-actin genes during avian cardiogenesis: Vascular smooth muscle α-actin gene transcripts mark the onset of cardiomyocyte differentiation. *J. Cell Biol.* 107, 2575–2586.

Saint-Jeannet, J.-P., Levi, G., Cirault, J.-M., Koteliansky, V., and Thiery, J.-P. (1992). Ventrolateral regionalization of *Xenopus laevis* mesoderm is characterized by the expression of α-smooth muscle actin. *Development* 115, 1165–1173.

Sater, A. K., and Jacobson, A. G. (1989). The specification of heart mesoderm occurs during gastrulation in *Xenopus laevis*. *Development* 105, 821–830.

Schultheiss, T. M., Lin, Z., Murray, J., Fischman, D., Weber, K., Masaki, T., Imamura, T., and Holtzer, H. (1990). Differential distribution of subsets of myofibrillar proteins in cardiac nonstriated and striated myofibrils. *J. Cell Biol.* 110, 1159–1172.

Schultheiss, T. M., Xydas, S., and Lassar, A. B. (1995). Induction of avian cardiac myogenesis by anterior endoderm. *Development* 121, 4203–4214.

Schultheiss, T. M., Burch, J. B. E., and Lassar, A. B. (1997). A role for bone morphogenetic proteins in the induction of cardiac myogenesis. *Genes Dev.* 11, 451–462.

Schultheiss, T. M., and Lassar, A. B. (1999). Vertebrate heart induction. In "Heart Development" (R. P. Harvey and N. Rosenthal, Eds.), pp. 51–62. Academic Press, San Diego.

Selleck, M. A., and Stern, C. D. (1991). Fate mapping and cell lineage analysis of Hensen's node in the chick embryo. *Development* 112, 615–626.

Skalli, O., Ropraz, P., Trzeciak, A., Benzonana, G., Gillessen, D., and Gabbiani, G. (1986). A monoclonal antibody against α-smooth muscle actin: A new probe for smooth muscle differentiation. *J. Cell Biol.* 103, 2787–2796.

Slack, J. M. W. (1991). The concepts of experimental embryology. In "Regional Specification in Early Development," pp. 9–33. Cambridge Univ. Press, Cambridge, UK.

Sugi, Y., and Lough, J. (1992). Onset of expression and regional deposition of alpha-smooth and sarcomeric actin during avian heart development. *Dev. Dyn.* 193, 116–124.

Sugi, Y., Sasse, J., and Lough, J. (1993). Inhibition of precardiac mesoderm cell proliferation by antisense oligodeoxynucleotide complimentary to fibroblast growth factor-2 (FGF-2). *Dev. Biol.* 157, 19–27.

Sugi, Y., and Lough, J. (1995). Activin-A and FGF-2 mimics the inductive effects of anterior endoderm on terminal cardiac myogenesis. *Dev. Biol.* 169, 567–574.

Tokuyasu, K. T., and Maher, P. A. (1987). Immunocytochemical studies of cardiac myofibrillogenesis in early chick embryos. II. Generation of α-actinin dots within titin spots at the time of the first myofibril formation. *J. Cell Biol.* 105, 2795–2801.

Tonegawa, A., and Takahashi, Y. (1998). Somitogenesis controlled by noggin. *Dev. Biol.* 202, 172–182.

Turnacioglu, K. K., Mittal, B., Dabiri, G. A., Sanger, J. M., and Sanger, J. W. (1997). Zeugmatin is part of the Z-band targeting region of titin. *Cell Struct. Funct.* 22, 73–82.

Walters, M. J., Wayman, G. A., and Christian J. L. (2001). Bone morphogenetic protein function is required for terminal differentiation of the heart tube but not for early expression of cardiac marker genes. *Mech. Dev.* 100, 263–273.

Wang, S. M., Greaser, M. L., Schultz, E., Bulinski, J. C., Lin, J. J., and Lessard, J. L. (1988). Studies on cardiac myofibrillogenesis with antibodies to titin, actin, tropomyosin and myosin. *J. Cell. Biol.* 107, 1075–1083.

Winnier, G., Blessing M., Labosky, P. A., and Hogan, B. L. M. (1995). Bone morphogenetic protein-4 is required for mesoderm formation and patterning in the mouse. *Genes Dev.* 9, 2105–2116.

Yamagishi, T., Nakajima, Y., Miyazono, K., and Nakamura, H. (1999). Bone morphogenetic protein-2 acts synergistically with transforming growth factor-b3 during endothelial-mesenchymal transformation in the developing chick heart. *J. Cell Physiol.* 180, 35–45.

Yatskievych, T. A., Ladd, A. N., and Antin, P. B. (1997). Induction of cardiac myogenesis in avian pregastrula epiblast: The role of the hypoblast and activin. *Development* 124, 2561–2170.

Zhang, H., and Bradley, A. (1996). Mice deficient for BMP2 are nonviable and have defects in amnion/chorion and cardiac development. *Development* 122, 2977–2986.

Zimmerman, L. B., Jesus-Escobar, J. D., and Harland, R. M. (1996). The Spemann organizer signal noggin binds and inactivates bone morphogenetic protein-4. *Cell* 86, 599–606.

Received for publication July 17, 2000
Revised February 26, 2002
Accepted February 26, 2002
Published online April 16, 2002

CORRECTED 4 JUNE 2004; SEE LAST PAGE

De Novo Crypt Formation and Juvenile Polyposis on BMP Inhibition in Mouse Intestine

Anna-Pavlina G. Haramis,[1] Harry Begthel,[1] Maaike van den Born,[1] Johan van Es,[1] Suzanne Jonkheer,[1] G. Johan A. Offerhaus,[2] Hans Clevers[1]*

Little is known about the signaling mechanisms that determine the highly regular patterning of the intestinal epithelium into crypts and villi. With the use of mouse models, we show that bone morphogenetic protein (BMP)–4 expression occurs exclusively in the intravillus mesenchyme. Villus epithelial cells respond to the BMP signal. Inhibition of BMP signaling by transgenic expression of noggin results in the formation of numerous ectopic crypt units perpendicular to the crypt-villus axis. These changes phenocopy the intestinal histopathology of patients with the cancer predisposition syndrome juvenile polyposis (JP), including the frequent occurrence of intraepithelial neoplasia. Many JP cases are known to harbor mutations in BMP pathway genes. These data indicate that intestinal BMP signaling represses de novo crypt formation and polyp growth.

Juvenile polyposis (JP) is an autosomal-dominant, gastrointestinal polyposis syndrome (*1*). Germline mutations in *SMAD4* (homolog of the *Drosophila* gene *mothers against decapentaplegic*) have been found in a subset of JP patients (*2*, *3*). Smad4 is an intracellular signal transducing transcription factor shared by the transforming growth factor β, activin and BMP pathways (*4*). More recently, mutations in the gene encoding the BMP receptor type IA (BMPRIA) have been found in some JP patients who were wild-type for *SMAD4* (*5*), implying a role for the BMP pathway in the pathogenesis of JP and, by inference, in the physiology of the intestine. Targeted disruption of BMP2, BMP4, and BMPR types IA and II in mice all lead to embryonic lethality (*6*–*9*). Similarly, mice deficient for the soluble BMP inhibitors noggin and gremlin die at birth (*10*–*12*).

To address the role of BMP signaling during intestine development and function, we first determined expression of *bmp4* message and protein during development. It has been reported that, in the early developing mouse intestine, *bmp4* message is expressed uniformly in the mesenchymal layer before folding of the epithelium (*13*). We examined *bmp4* expression at embryonic days (E15.5 to E18.5) when villus formation is underway and found that *bmp4* message is expressed at high levels in the intravillus mesenchyme of nascent villi but not in the mesenchyme underlying the proliferative intervillus epithelial pockets, which are the precursors of the crypts of Lieberkühn (*14*). At postnatal day 28 (P28) when the crypts have reached their mature form, BMP4 protein expression was strong in the intravillus mesenchyme (Fig. 1A). Phosphorylation and nuclear translocation of BMP-associated Smads 1, 5, and 8 [the hallmark of active BMP signaling (*15*, *16*)] was observed predominantly in differentiated villus epithelial cells (Fig. 1C), indicating that paracrine BMP signaling occurs specifically in the villus from the mesenchyme to the adjacent epithelium.

To investigate the role of BMP signaling in intestinal homeostasis, we generated transgenic mice expressing a *Xenopus* cDNA encoding the BMP inhibitor noggin (*X-noggin*) (*17*) under control of the mouse villin gene promoter. This promoter drives expression throughout the intestinal epithelium and becomes fully active during late gestation (*18*). In situ hybridization with a transgene-specific riboprobe revealed that *X-noggin* (*19*) was indeed expressed in the intestinal epithelium of adult transgenic mice (Fig. 1B). Immunoreactivity to phosphorylated Smad 1, 5, and 8 was almost entirely absent in *X-noggin*–transgenic intestines (Fig. 1D), demonstrating the effectiveness of the inhibition of BMP signaling by exogenous noggin.

At 3 months of age, transgenic animals of all three generated lines displayed identical architectural abnormalities throughout the small intestine with complete penetrance. One line was further characterized. No morphological alterations were detected in the intestines of newborns and animals up to 3 weeks old (*14*). We first noticed subtle abnormalities in the small intestine of 4-week-old animals, when the shallow proliferative intervillus pockets are being replaced by adult crypts of Lieberkühn, which extend downward toward the muscularis mucosae of the intestine. The villi in the transgenics were broad-based with blunted tips. Abnormal epithelial invaginations were seen alongside the villi that contained proliferative Ki-67-positive cells (Fig. 2B) and expressed crypt-specific genes such as the Wnt signaling targets

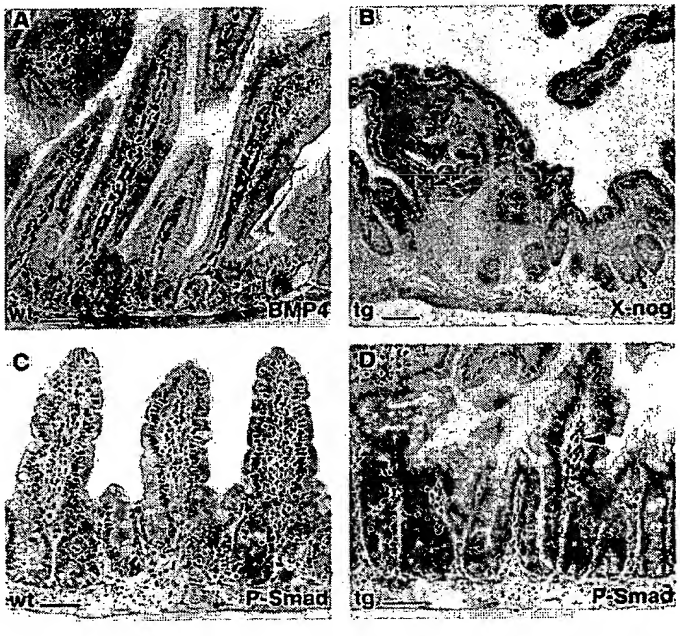

Fig. 1. Villus epithelial cells in the mouse intestine respond to mesenchymal BMP signaling. (**A**) Expression of BMP4 protein is detected in the intravillus mesenchyme of adult wild-type (wt) mice. (**B**) Transgenic expression of *Xenopus* noggin (X-nog) inhibits BMP signaling. In situ hybridization with a transgene-specific riboprobe reveals that the *Xenopus* noggin mRNA is expressed by intestinal epithelial cells in adult mice. (**C**) Immunoreactivity to phosphorylated Smad1, 5, and 8 proteins (P-Smad) reveals nuclear staining in wt villus epithelial cells. (**D**) In noggin-transgenic intestines, immunoreactivity to phospho-Smad1, 5, and 8 is almost absent in epithelial cells. Arrowhead indicates a positive mesenchymal cell. tg, noggin-transgenic. Scale bars indicate 0.1 mm in (A) and (B) and 25 μm in (C) and (D).

[1]Hubrecht Laboratory, Netherlands Institute for Developmental Biology, Uppsalalaan 8, 3584 CT Utrecht, Netherlands. [2]Department of Pathology, Academic Medical Center, University of Amsterdam, PB 22660, 1100 DD Amsterdam, Netherlands.

*To whom correspondence should be addressed. E-mail: clevers@niob.knaw.nl

c-myc (*20*), (fig. S1B) and EphB3 (see below). These invaginations appeared to be capable of developing into complete ectopic crypt-villus units that established polarity and a new crypt-villus axis, which was often perpendicular to the original axis. The aberrant units comprised a defined proliferative compartment as revealed by Ki67 immunostaining (Fig. 2E) and contained differentiated Paneth cells at their base as evidenced by staining for the receptor tyrosine kinase EphB3 (*21*) and lysozyme (fig. S1, C to F). Epithelial differentiation in the ectopic crypt-villus units appeared grossly normal, because goblet cells, enterocytes, and enteroendocrine cells were present in near-normal numbers (*14*).

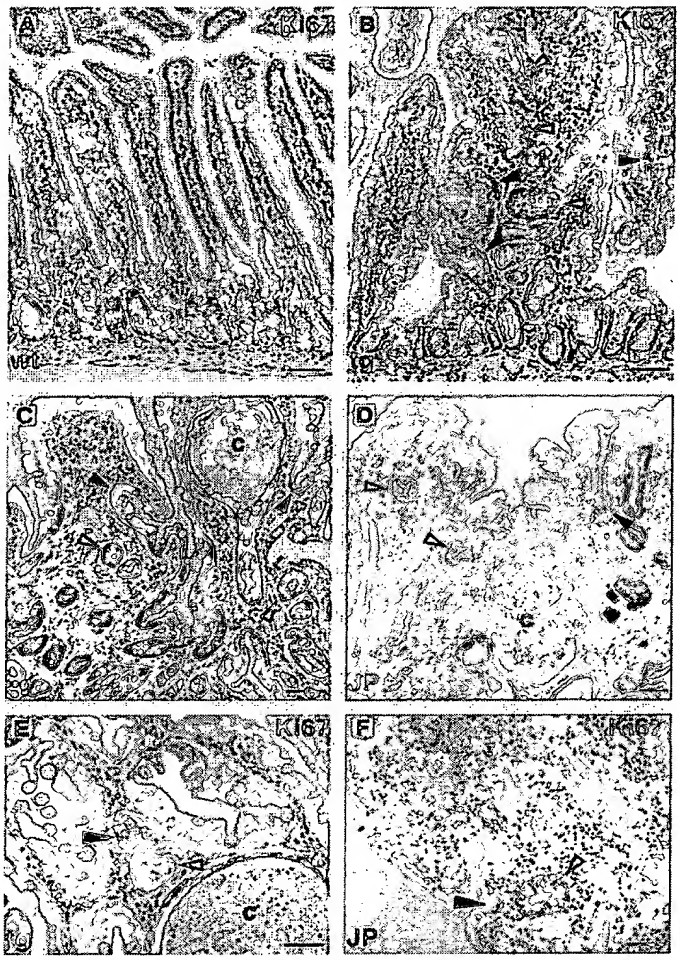

Fig. 2. The intestinal histopathology of noggin-transgenic mice resembles that of humans with JP. **(A)** Section of wt mouse intestine stained with Ki67. Ki67-positive epithelial cells are confined to the proliferative compartment of the crypts. **(B)** Section of noggin-transgenic intestine stained with Ki67. Ectopic epithelial invaginations contain proliferative cells and give rise to ectopic crypt villus units. **(C)** Section of the small intestine of a noggin-transgenic mouse stained with hematoxylin and eosin (H&E), showing the presence of abnormal crypt-villus units, cystic dilated crypts (c), and numerous crypts dispersed in the stroma. **(D)** Excision of an intestinal polyp from a human JP patient stained with H&E, showing the branching and budding of the intestinal epithelium and the dilated cysts (c). **(E)** Ki67 staining of a noggin-transgenic intestine showing an ectopic crypt-villus unit with a proliferative compartment. The epithelium lining the cyst contains proliferating cells. **(F)** Ki67 staining of a human JP polyp. Abnormally positioned crypts contain proliferating cells. Black arrowheads in (B) to (F) indicate ectopic epithelial invaginations; white arrowheads indicate dispersed crypts in the stroma. Scale bar, 0.1 mm in (A) to (D) and 25 μm in (E) and (F).

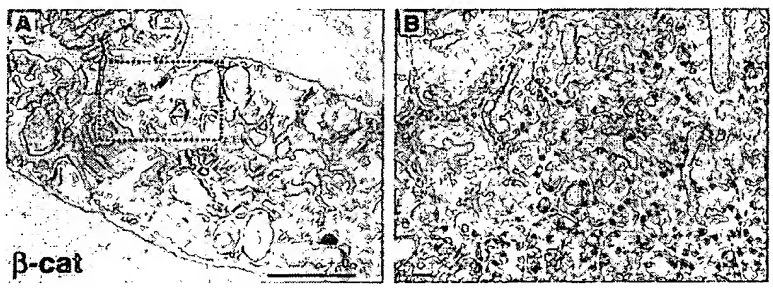

Fig. 3. Foci of dysplastic epithelium and adenomatous changes in polyps of 7-month-old noggin-transgenic mice. **(A)** β-catenin (β-cat) staining of an intestinal adenoma of a 7-month-old transgenic mouse. **(B)** Enlargement of the boxed area in (A). High levels of cytoplasmic and nuclear β-catenin are observed in the adenoma. Scale bar, 1 mm in (A) and 20 μm in (B).

At later stages, invaginations and ramifications of the intestinal epithelium extended from these proliferative foci deep into the villi, resulting in a complex architecture of branching villi with dilated cysts as the characteristic feature of the polyps observed in 3-month-old mice. The cystically dilated crypts were often filled with inspissated mucin and remnants of shed cells and lined by flattened epithelium. Lymphoid aggregates were sometimes present inside villi, and an increase in inflammatory cells was observed (Fig. 2C). These features are also seen in humans with JP (Fig. 2, D and F). The branching and budding of the intestinal epithelium, combined with the dilated cysts and reactive inflammatory changes, are particularly typical of the polyps in JP and discriminate them from the histopathological changes seen in familial adenomatous polyposis (FAP) and Peutz-Jeghers syndrome (*22*).

JP patients have an elevated risk of developing gastrointestinal cancers later in life (*23*). To study neoplastic changes in our mouse model, we examined the intestines of 7- and 8-month-old transgenic mice. In four of seven aged mice analyzed, we observed one or more foci of dysplastic epithelium and adenomatous change, in which the cells were abnormally arranged with an increased nuclear cytoplasmic ratio and pseudostratification of the cells. Most cells in these adenomatous foci were proliferating, as assessed by Ki67 staining (fig. S2, A and B). The overwhelming majority of colorectal cancers in humans initiate with activating mutations of the Wnt signaling cascade, typically targeting the tumor suppressor protein adenomatous polyposis coli (APC) (*24*). The hallmark of this mutational transformation is the stabilization and accumulation of β-catenin. Indeed, all adenomatous foci in aged *X-noggin* transgenics displayed high levels of cytoplasmic and nuclear β-catenin (Fig. 3). The cells in the adenomas also expressed CD44 (fig. S2, C and D), a target gene of the Wnt signaling cascade that is up-regulated in intestinal adenomas upon loss of APC (*25*).

Thus, the *X-noggin*–transgenic mice displayed a JP-like phenotype at a relatively young age (2 to 3 months), whereas adenomatous polyps frequently developed at a later stage (6 to 8 months), recapitulating the syndrome in humans. *Smad4*$^{+/-}$ mice were previously reported to develop polypous lesions, though not as juveniles and without some of the pathologic features described above (*26*).

It was originally proposed that JP polyps develop because of defects in the stroma ("landscaper" defects) (*27*). An early study of

juvenile polyps gave support to this notion, because deletions of the tumor suppressor locus 10q22-24 were found in the lamina propria and not the epithelium (*28*). However, in a more recent study, homozygous *SMAD4* deletions were found specifically in the epithelium of JP polyps (*29*). Similarly, loss of the wild-type *Smad4* allele was observed in the epithelium of the inflammatory polyps in *Smad4*$^{+/-}$ mice (*26*). In contrast to these studies, no consistent loss of heterezygosity of the *BMPRIA* gene was observed in the stroma or epithelial cells of the JP polyps (*5*), which would argue against a tumor-suppressor mechanism.

We propose that inactivating mutations in BMP pathway components primarily affect the perception of mesenchymal BMP signals by epithelial cells. BMP signaling delimits ectopic crypt induction once the orthotopic structures have been specified. With loss of these inhibitory signals, the epithelial cells proceed to establish ectopic crypts, ultimately leading to the growth of juvenile polyps and to neoplasia. Thus, the "landscaper" defect would reflect the disruption of mesenchymal-epithelial communication. It is likely that JP patients with wild-type *SMAD4* and *BMPRIA* genes (*2*, *30*) harbor mutations in other components of the BMP pathway.

References and Notes

1. M. M. Entius *et al.*, *Hepatogastroenterology* **46**, 661 (1999).
2. R. Houlston *et al.*, *Hum. Mol. Genet.* **7**, 1907 (1998).
3. J. R. Howe *et al.*, *Science* **280**, 1086 (1998).
4. G. Lagna, A. Hata, A. Hemmati-Brivanlou, J. Massagué, *Nature* **383**, 832 (1996).
5. J. R. Howe *et al.*, *Nat. Genet.* **28**, 184 (2001).
6. H. Beppu *et al.*, *Dev. Biol.* **221**, 249 (2000).
7. K. A. Lawson *et al.*, *Genes Dev.* **13**, 424 (1999).
8. Y. Mishina, A. Suzuki, N. Ueno, R. R. Behringer, *Genes Dev.* **9**, 3027 (1995).
9. H. Zhang, A. Bradley, *Development* **122**, 2977 (1996).
10. L. J. Brunet, J. A. McMahon, A. P. McMahon, R. M. Harland, *Science* **280**, 1455 (1998).
11. M. K. Khokha, D. Hsu, L. J. Brunet, M. S. Dionne, R. M. Harland, *Nat. Genet.* **34**, 303 (2003).
12. J. A. McMahon *et al.*, *Genes Dev.* **12**, 1438 (1998).
13. M. J. Bitgood, A. P. McMahon, *Dev. Biol.* **172**, 126 (1995).
14. A. P. G. Haramis, H. C. Clevers, unpublished data.
15. M. Kretzschmar, F. Liu, A. Hata, J. Doody, J. Massague, *Genes Dev.* **11**, 984 (1997).
16. F. Liu *et al.*, *Nature* **381**, 620 (1996).
17. Materials and methods are available as supporting material on *Science* Online.
18. D. Pinto, S. Robine, F. Jaisser, F. E. El Marjou, D. Louvard, *J. Biol. Chem.* **274**, 6476 (1999).
19. W. C. Smith, R. M. Harland, *Cell* **70**, 829 (1992).
20. T.-C. He *et al.*, *Science* **281**, 1509 (1998).
21. E. Batlle *et al.*, *Cell* **111**, 251 (2002).
22. L. A. Aaltonen *et al.*, In *WHO Classification of Tumours*, S. R. Hamilton, L. A. Aaltonen, Eds. (World Health Organization, Oxford Univ. Press, Cary, NC, 2000), pp. 130–132.
23. F. M. Giardiello, J. G. Offerhaus, *Eur. J. Cancer* **31A**, 1085 (1995).
24. M. Bienz, H. Clevers, *Cell* **103**, 311 (2000).
25. V. J. Wielenga *et al.*, *Am. J. Pathol.* **154**, 515 (1999).
26. K. Takaku *et al.*, *Cancer Res.* **59**, 6113 (1999).
27. K. W. Kinzler, B. Vogelstein, *Science* **280**, 1036 (1998).
28. R. F. Jacoby *et al.*, *Gastroenterology* **112**, 1398 (1997).
29. K. Woodford-Richens *et al.*, *Cancer Res.* **60**, 2477 (2000).
30. X. P. Zhou *et al.*, *Am. J. Hum. Genet.* **69**, 704 (2001).

31. We thank R. Harland for *Xenopus* noggin cDNA, H. Kulessa for sharing unpublished results, M. van de Wetering for advice, and members of the Clevers lab for helpful discussions.

Supporting Online Material
www.sciencemag.org/cgi/content/full/303/5664/1684/DC1
Materials and Methods
Figs. S1 and S2

12 November 2003; accepted 30 January 2004

ERRATUM

post date 4 June 2004

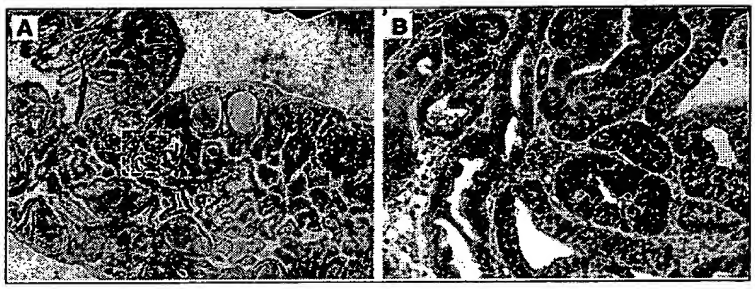

REPORTS: "De novo crypt formation and juvenile polyposis on BMP inhibition in mouse intestine" by A.-P. G. Haramis *et al.* (12 Mar. 2004, p. 1684). There was an error in Fig. 3. Fig. 3B should be an enlargement of the area boxed in Fig. 3A. The corrected figure is shown here.